

# Intimate Molecular Interactions of *P. falciparum* Merozoite Proteins Involved in Invasion of Red Blood Cells and Their Implications for Vaccine Design

Luis Eduardo Rodriguez,<sup>†,‡,||</sup> Hernando Curtidor,<sup>†,‡,||</sup> Mauricio Urquiza,<sup>†</sup> Gladys Cifuentes,<sup>†</sup> Claudia Reyes,<sup>†</sup> and Manuel Elkin Patarroyo<sup>\*,†,§</sup>

Fundación Instituto de Inmunología de Colombia, Carrera 50 No. 26-00, Bogotá, Colombia

Received December 13, 2006

## Contents

1. Introduction	3656	4.1.4. Erythrocyte Binding-like-1 (EBL-1)	3685
1.1. Merozoite's Structure	3658	4.2. Apical Membrane Antigen-1 (AMA-1)	3686
1.1.1. Rhoptries	3658	4.3. MAEBL	3687
1.1.2. Micronemes	3660	4.4. <i>Plasmodium</i> Thrombospondin-Related Apical Merozoite Protein (PTRAMP)	3687
1.1.3. Dense Granules	3660	5. Rhoptry Proteins	3688
1.2. <i>P. falciparum</i> Infection-Induced RBC Structures (Maurer's Clefts)	3660	5.1. Reticulocyte Binding-like Protein Family (RBL)	3688
1.3. Merozoite Proteins Involved in RBC Invasion	3660	5.1.1. <i>Plasmodium falciparum</i> Normocyte Binding Protein-1 (PfNBP-1) or <i>Plasmodium falciparum</i> Reticulocyte Binding Protein-Homologue-1 (PfrBP-H1)	3688
2. Defining Target Molecules for Triggering a Protection-Inducing Immune Response	3660	5.1.2. Reticulocyte Binding Protein-2 Homologues a and b (PfrBP-2Ha and -2Hb)	3689
2.1. Synthetic Peptides Used for Acquiring Knowledge about Merozoite Protein RBC Binding Regions	3661	5.2. Rhoptry-Associated Protein-1 (RAP-1)	3689
2.2. Rationale for High-Activity Binding Peptide Recognition	3661	5.3. Rhoptry-Associated Protein-2 (RAP-2)	3690
3. Merozoite Surface Protein (MSP) Family	3662	5.4. Rhoptry-Associated Protein-3 (RAP-3)	3690
3.1. Merozoite Surface Protein-1 (MSP-1)	3664	5.5. Rhoptry-Associated Membrane Antigen (RAMA)	3690
3.2. Merozoite Surface Protein-2 (MSP-2)	3675	5.6. RhopH3	3691
3.3. Merozoite Surface Protein-3 (MSP-3)	3677	5.7. Cytoadherence-Linked Asexual Gene (RhopH-1/CLAG 3.2)	3692
3.4. Merozoite Surface Protein-4 (MSP-4)	3677	6. Infected RBC (iRBC) Membrane-Associated <i>P. falciparum</i> Proteins and Transportome-Associated Proteins	3692
3.5. Merozoite Surface Protein-5 (MSP-5)	3678	6.1. Ring-Infected Erythrocyte Surface Antigen (RESA)-155	3692
3.6. Merozoite Surface Protein-6 (MSP-6)	3678	6.2. RESA-like Protein	3693
3.7. Merozoite Surface Protein-7 (MSP-7)	3678	6.3. Histidine-Rich Proteins	3693
3.8. Merozoite Surface Protein-8 (MSP-8)	3679	6.4. <i>P. falciparum</i> Erythrocyte Membrane Protein-1 (PfEMP-1)	3694
3.9. Merozoite Surface Protein-9 (MSP-9) or Acid Basic Repeat Antigen (ABRA)	3679	7. Supporting Background for the Subunit-based Synthetic Vaccine Concept	3695
3.10. Merozoite Surface Protein-10 (MSP-10)	3680	7.1. Conserved HABP Structural Characteristics	3695
3.11. Glycophorin Binding Protein-130 (GBP-130)	3681	7.1.1. Functional and Structural Compartmentalization of Merozoite Proteins Involved in RBC Invasion	3695
3.12. Serine Repeat Antigen-5 (SERA-5)	3681	7.1.2. Minimal Subunit-based Synthetic Peptide Vaccine Concept is Correct	3697
3.13. Lipid Raft-Associated <i>Plasmodium falciparum</i> Cys6 Peptide Family	3682	8. Implications for Vaccine Design and Perspectives	3698
4. Microneme Proteins	3683	9. Acknowledgments	3699
4.1. Erythrocyte Binding-like (EBL) Family	3683	10. References	3699
4.1.1. Erythrocyte Binding Antigen-175 (EBA-175)	3683		
4.1.2. Erythrocyte Binding Antigen-181 (EBA-181) or JESEBL	3684		
4.1.3. Erythrocyte Binding Antigen-140 (EBA-140) or BAEBL	3685		

\* To whom correspondence should be addressed. Tel.: +57-1-3244672, +57-1-4815219. Fax: +57-1-4815269. E-mail: mepatarr@gmail.com, mepatarr@fidic.org.co.

<sup>†</sup> Fundación Instituto de Inmunología de Colombia (FIDIC).

<sup>‡</sup> Universidad del Rosario.

<sup>||</sup> These authors contributed equally to this work.

<sup>§</sup> Universidad Nacional de Colombia.

## 1. Introduction

Malaria continues to be one of the main public health problems for mankind; it is the transmissible disease with the greatest morbidity and mortality around the world. It kills



Luis E. Rodriguez graduated in chemistry at the Universidad Nacional de Colombia in 1991. He is candidate for a Dr. Sc. degree in chemistry at the Universidad Nacional de Colombia and is currently working as a researcher in the Virology department at the Fundación Instituto de Inmunología de Colombia. The main focus of his research is the host–parasite interaction in *P. falciparum* and *P. vivax* malaria infection, cervical carcinoma caused by Human Papilloma Virus, and lymphoma associated with Epstein–Barr virus infections.



Mauricio Urquiza graduated in chemistry at the Universidad Nacional de Colombia in 1991. He is currently working as a researcher in the Virology department at the Fundación Instituto de Inmunología de Colombia and is candidate for a Dr. Sc. degree in chemistry at the Universidad Nacional de Colombia. The main focus of his research is the study of the host–parasite interactions, using as model *P. falciparum*, *P. vivax*, Human Papilloma virus, and Epstein–Barr virus. He is also working in the development of a Human Papilloma virus detection test.



Hernando Curtidor received his B.Sc. degree in chemistry at the Universidad Nacional de Colombia in 1991. The principal focus of his research at the Fundación Instituto de Inmunología de Colombia is the molecular characterization of receptor–ligand interactions between pathogenic proteins involved in invasion and their corresponding host cell receptors, mainly for *P. falciparum* and *M. tuberculosis*. He is currently candidate for a Dr. Sc. degree in chemistry at the Universidad Nacional de Colombia.

more than 2 million people annually, mainly African children aged less than 5, while ~500 million more become infected each year.<sup>1</sup> Human malaria is caused by four species of parasites from the *Plasmodium* genus: *Plasmodium falciparum*, *P. vivax*, *P. ovale*, and *P. malariae*, with *P. falciparum* being the most aggressive one and developing the greatest resistance to antimalarial drugs.<sup>1</sup>

A completely effective vaccine has not yet been developed against this disease, mainly due to the incomplete knowledge of the intimate molecular interactions between parasite proteins and their specific host cell membrane receptor(s) during invasion. There is also a lack of complete information regarding the structural and immunological properties of antigens able to activate the very complex mechanisms of protection-inducing immunity.

A thorough analysis of the intimate molecular interactions of the molecules involved in the parasite's invasion of red blood cells (RBCs), including secondary and three-dimensional (3D) structure determination of some of them, was, therefore, carried out as a first step in the development of a



Gladys Cifuentes graduated in chemistry at the Universidad Nacional de Colombia in 1994 and is a member of the Nuclear Magnetic Resonance and Molecular Design section of the Three-Dimensional Structure Department at the Fundación Instituto de Inmunología de Colombia. Her research interests include 3D-structure and molecular design of peptides and proteins with shown biological and chemical relevance in host–parasite interactions.

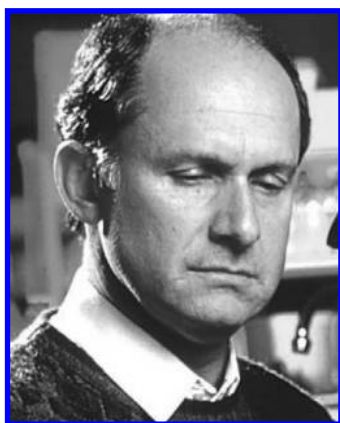
logical and rational methodology for obtaining vaccines against this threatening disease. This led to the suggestion that blocking such interactions could be specifically induced by activating the immune system with these molecules, thus forming the present work's *raison d'être*.

Provided below is a very brief description of the *P. falciparum* life cycle (Figure 1A). It begins when an infected female *Anopheles* mosquito injects the larvae-like parasite (sporozoite) into the skin while biting the human host. These sporozoites travel via the bloodstream (Figure 1A1) until reaching the liver, where they recognize hepatic cells<sup>2</sup> through specific molecular interactions so as to infect them; such infection takes no more than 60 min for *P. vivax* or *P. falciparum*.

Sporozoites can directly invade hepatocytes or pass through the Kupffer cells prior to invasion of hepatocytes, and the exoerythrocytic schizogony (as this stage is called) takes a characteristic course in each species, with minimum maturation time being 5.5 days in *P. falciparum* and 15 days in *P. malariae*. The parasite can reproduce itself and change



Claudia A. Reyes is Chemical Engineer at the Fundación Universidad de América (Colombia, 1997) and Environmental Engineering Specialist at the Universidad Industrial de Santander (2007). Her career has been mainly focused on the synthesis of synthetic peptides as vaccine candidates against several diseases, using different strategies. She is working at the Fundación Instituto de Inmunología de Colombia in studies involving circular dichroism and scaling up of peptides production.



Professor Manuel E. Patarroyo (1946) received his M.D. degree from the Universidad Nacional de Colombia in 1971 where he is Full Professor of Molecular Pathology. He conducted post-doctoral studies at the Rockefeller University, U.S.A., with Professor Henry Kunkel and on Tumor Immunology at Karolinska Institute, Sweden, with Professor George Klein. In 1976, he founded the Instituto de Inmunología at the San Juan de Dios Hospital, devoted to the development of chemically synthesized vaccines, among them the antimalarial vaccine, with the advice of Professor Bruce Merrifield (Rockefeller University) and Professor Richard Lerner (Scripps Research Institute). The first chemically synthesized vaccine against this scourging disease was published in 1987 followed by a large series of clinical and field trials in different parts of the world that allowed the conclusion of the feasibility of chemically synthesized vaccines. He has received numerous awards including the Third World Academy of Science (TWAS) in 1998, the Prince of Asturias Award in Science and Technology (Spain) in 1994, the Robert Koch Award (Germany) in 1994, the Medecin de l'annee Award (France) in 1995, the Edinburgh Medal (England) in 1995, the National Science Award (Colombia) in 1986, 1984, 1982, and 1978, and 26 Honoris Causa Doctor degrees from different universities throughout the world. He is founder and current director of the Fundación Instituto de Inmunología de Colombia since 2001.

its morphology inside these cells during a proliferation-differentiation process<sup>3–5</sup> (Figure 1A).

The hepatocytes rupture, releasing parasites having dramatic morphological, functional, and biochemical differences from sporozoites that reach the blood stream via the hepatic sinusoids (Figure 1A2). These parasites, which have now adopted a pear-shaped (merozoite) structure, come into contact with RBCs, invade them, and thus start a new cellular cycle called RBC schizogony (Figure 1B); both invaded

RBCs and the invading parasite suffer dramatic structural changes during invasion (see parts B and C of Figure 1 for a structural example and our immunofluorescence studies of infected RBCs in Figure 1E). The merozoite grows following RBC invagination. A large, round vacuole named the parasitophorous vacuole (PV) appears in RBC cytoplasm, and a ringlike structure (ring stage) starts appearing inside it (Figure 1C2, 1E1, and 1E2). A mature form called a trophozoite then develops (Figure 1C3 and 1E3). Later on its nucleus divides to form mature schizonts that burst (Figure 1C4, 1E7, and 1E8), releasing new merozoites; each one invades a new RBC as part of a cycle, thereby producing host cell death<sup>6,7</sup> (Figure 1A3). The merozoite can also change its morphology to produce male and female gametocytes in a cycle called gametogenesis (Figure 1A4). A mosquito biting a malaria-infected human receives gametocyte-infected RBCs (iRBCs), thereby initiating the reproductive sexual cycle in the mosquito's midgut<sup>4,6,8</sup> (Figure 1A5), making it infective and beginning the process once again.

## 1.1. Merozoite's Structure

Receptor–ligand high-affinity interactions between merozoite proteins and molecules located on the RBC surface lead to merozoite binding and reorientation on RBC surface in less than 40 s. The merozoites become detained on the surface of some of these RBCs after rolling over several of them (Figure 1B1) to begin the binding process. The parasite becomes reorientated in such a way that the merozoite's apical extreme (juxtaposed to the RBC membrane) will anchor to the RBC membrane (Figure 1B2). Such merozoite reorientation is associated with RBC deformation, triggering the release of the merozoites' apical organelle content onto RBC membrane<sup>7,9</sup> (Figure 1B3). These specialized secretor organelles, located at the parasite's apical end (called micronemes, rhoptries, and dense granules), facilitate merozoite penetration and PV formation<sup>7,9</sup> (Figure 1B4).

Data obtained from *Toxoplasma gondii* (another apicomplexan parasite) has indicated that the micronemes release their content immediately before the rhoptries do so (Figures 1B4 and 1B5). Most dense granule secretions occur after the parasite has completed its entry into the RBCs (Figure 1B6). Apical localization and rhoptry and microneme content release (coincident with invasion) suggest that these organelles participate directly in invasion.<sup>9,10</sup>

Different studies have reported each organelle system's structural homology among most members of the phylum apicomplexa, suggesting that they share similar biological functions.<sup>10</sup> The micronemes and their molecular products are apparently used in recognizing and binding to the host cell, as well as possibly in mobility. It has been reported that the rhoptries are involved in PV formation and the dense granules are involved in remodelling the PV in an active metabolic compartment.<sup>11</sup> A brief description of these organelles as invasion mediators is therefore needed.

### 1.1.1. Rhoptries

The rhoptries are merozoite membrane-bound vesicles, having a pear-shaped structure during their mature stage (Figure 1D). Morphologically, electron microscopy has shown that each rhoptry is made up of two different segments: a rounded electron-dense basal bulb and a duct (somewhat less electron-dense or hidden) below the plasmatic membrane covering the apical prominence. The rhoptries are

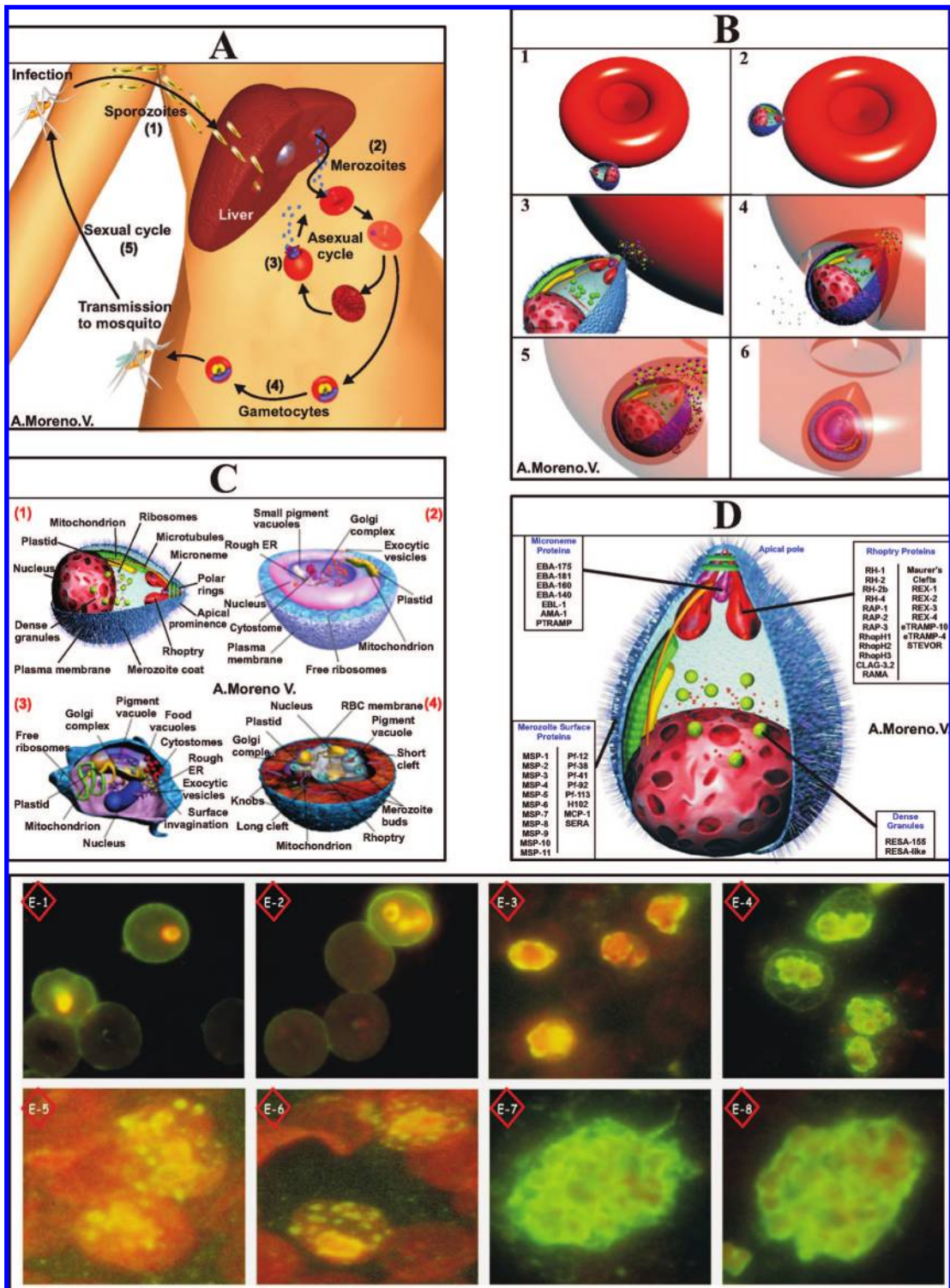


**Figure 1.** *P. falciparum* life-cycle. (A) Sporozoites inoculated during a mosquito bite migrate to liver cells via the blood stream (1) infecting the hepatocytes where they reproduce 30 000× in a week and transform into merozoites (2) that invade RBCs, reproducing 30–40× every 48 h to release new merozoites in an asexual cycle (3) causing clinical symptoms and, in some cases, the host's death. Some of them become male and female gametes (4) that are taken up by a mosquito during its blood meal to start its sexual cycle (5) and produce new sporozoites in the mosquito. (B) The sequence of *P. falciparum* merozoite invasion of RBCs. The merozoite rolls over the surface of some RBCs (1), becomes detained and reorientates itself toward its apical pole (2), releases micronemal proteins onto the RBC surface (3), starts to penetrate it, forms junctions between the merozoite and RBC membrane as well as releases rhoptry proteins that become cleaved by enzymes named shedases (4), releases new rhoptry proteins for PV formation (5), completes its invagination into the PV (6) to start differentiation into ring forms (Figures 1C2, 1E1, and 1E2), and multiplies. (C) Morphology throughout the blood-stage parasite's asexual life-cycle; the merozoite (1), ring (2), trophozoite (3), and schizont stages (4) (displaying each stage's main structures). (D) Morphology and localization of merozoite invasion-related proteins recognized to date that have been located on the membrane, micronemes, rhoptries, and dense granules. (E) Our immunofluorescence studies showing ring-infected erythrocyte surface antigen-like (RESA-like) in E1, E2 as green fluorescence on iRBC membrane with intracytoplasmic *P. falciparum* rings detected as orange fluorescence. Early trophozoites inside the PV in E3. Late trophozoites, early schizonts, and some soluble proteins inside iRBCs in E4. Maurer's clefts in E5 and E6 detected as fluorescent granules inside the iRBC. Late schizonts in E7 and E8 showing merozoite membrane separation just before rupture and release.

about 550 nm long and 250 nm at their widest point in *P. falciparum*. The base bulb is made up of 5 nm homogeneous, packed granules or short fibrils.<sup>9–11</sup>

### 1.1.2. Micronemes

The micronemes are smaller structures than the rhoptries, and variations in their form and number occur among the different species<sup>10</sup> (Figure 1D). They are fusiform sacs about 120 nm long in *P. falciparum*, bound at one end to the rhoptries' duct while fanning out at the other end with the merozoite's apical cytoplasm. The micronemes (which are bound by a typical cytoplasmic membrane and have a fine granular interior) disappear during invasion, probably as a consequence of their contents being released and/or the merging of membranes within the rhoptries' duct. Structural evidence suggests that micronemes are formed by vesicular budding triggered by the Golgi apparatus, in a similar way to that observed with other apical organelles.<sup>10,12</sup>

### 1.1.3. Dense Granules

These are spheroid membranous vesicles, about 100–150 nm in diameter in *P. knowlesi*, having a similar appearance to those of *P. falciparum* (Figure 1D). They are situated in between the rhoptries and the merozoite nucleus. These dense granules move toward the merozoite surface following invasion of RBCs. Here they produce an opening in the parasite's plasmic membrane, releasing their proteinaceous content into the PV, accompanied by the lengthening of this membrane, and thus forming finger-like profusions that extend around RBC cytoplasm.<sup>7,10,13</sup>

## 1.2. *P. falciparum* Infection-Induced RBC Structures (Maurer's Clefts)

*P. falciparum* significantly reforms its structure and, thereby, host-cell structure during its intraerythrocytic development, exporting a series of proteins beyond the limits of their own membrane. The parasites must install and adapt their own protein exportation system within the host RBCs to be able to export them either to the Maurer's clefts (MCs) or to the iRBC surface. MCs were discovered by Georg Maurer in 1902 and are parasite-derived membranous structures<sup>14,15</sup> (Figures 1E5 and 1E6).

Increasing evidence has suggested that MCs are secretor organelles, able to transport parasite proteins via host-cell cytoplasm to the RBC surface where they play a role in taking nutrients, adhering to other cells, and evading the immune response. It has been proposed that these clefts play a role in cellular signaling during merozoite release, phospholipid biosynthesis, and, possibly, in other biochemical routes, thereby making MCs a crucial component of this export machinery by classifying and transporting proteins outside the parasite.<sup>14,15</sup>

## 1.3. Merozoite Proteins Involved in RBC Invasion

As they are so critical for survival, multiple merozoite proteins are implicated in invasion of RBCs; some of them are situated on the merozoite surface while others are located in the rhoptries, micronemes, and dense granules. These proteins have been grouped into several families, according to their cellular localization or molecular characteristics.

The merozoite surface protein family (MSP-1 to MSP-10) represents a group of proteins situated on the merozoite

surface. Some of them such as MSP-1, MSP-2, MSP-4, MSP-5, MSP-8, and MSP-10 are anchored to the membrane via glycosylphosphatidylinositol (GPI) groups;<sup>16–18</sup> others like MSP-3, MSP-6, MSP-7, and MSP-9 are soluble and may be weakly bound to the merozoite surface or associated with other membrane proteins<sup>16,19</sup> (Figure 1D). Some MSP family molecules (MSP-1, MSP-4, MSP-8, and MSP-10) contain one or two epidermal growth factor (EGF) like-domains; it has been suggested that they are involved in merozoite invasion.<sup>16,19</sup>

Erythrocyte binding proteins (EBPs) (located in the micronemes) are able to bind to different receptors on RBC membrane and have been involved in RBC invasion. These display similar internal structural composition, having two Duffy-binding-like (DBL) domains located at the N-terminal, a cysteine-rich region at the C-terminal, a transmembrane region, and a small cytoplasmic tail. DBL domains have been involved in RBC binding activity.<sup>20–22</sup> These proteins have been grouped into the so-called DBL–EBP family which includes *P. falciparum* *eb1* gene family encoded products: erythrocyte binding antigen 175 or EBA-175, EBA-140, EBA-181, EBA-165, erythrocyte binding ligand (EBL), and MAEBL (the latter located in the rhoptries) and its homologues in *P. vivax* and *P. knowlesi*.<sup>16</sup>

Apical membrane antigen 1 (AMA-1) is a critical protein produced in the micronemes and present in the merozoites' apical pole. This protein becomes translocated to the merozoite membrane during invasion and is partly responsible for merozoite reorientation.<sup>23,24</sup>

Other rhoptry-associated protein families that could be playing an important role in RBC–merozoite interaction would include the following:

- The reticulocyte-binding-like (RBL) family, including normocyte binding proteins (NBP-1, -2a, -2b, -3, -4), also called reticulocyte binding protein homologues (RBP-H1, -2Ha, -2Hb, -H3, and -H4);<sup>25,26</sup>

- Rhoptry-associated protein families<sup>9,27</sup> having two protein complexes, the low molecular weight (LMW) complex consisting of rhoptry-associated proteins (RAP-1, -2, and -3)<sup>28</sup> and the high molecular weight (HMW) complex consisting of Rhop-H1/CLAG, Rhop-H2, and Rhop-H3;<sup>29</sup> and

- Other rhoptry-associated proteins such as rhoptry-associated membrane antigen (RAMA), MAEBL, and Rhop-148.<sup>9,30</sup>

All these proteins have been involved in merozoite binding to RBC surface allowing adhesion and host cell tropism.<sup>9,27,31</sup>

A large number of proteins present on merozoite membrane or secreted by the micronemes and rhoptries are thus involved in invasion of RBCs and must, therefore, be thoroughly analyzed at a molecular level to use them in further studies that include them as components of a multiantigen, multistage, subunit-based, synthetic antimalarial vaccine.

## 2. Defining Target Molecules for Triggering a Protection-Inducing Immune Response

Merozoite proteins implicated in binding to and invasion of host cells are attractive targets for developing antimalarial vaccines; an immune response directed against these proteins might, thus, be able to inhibit merozoite invasion of RBCs.

It has been found that antibodies recognizing merozoite protein regions involved in binding to RBCs induced protection against *in vitro* and *in vivo* blood-stage infection;

their presence has also been correlated with clinical immunity against malaria in human beings.<sup>32,33</sup> It has also been found that immunization with merozoite antigens has induced protection against *P. falciparum* experimental infection, this protection being partially mediated by antibodies. Passive transfer of immunoglobulin G (IgG) from semi-immune individuals has provided partial protection against infection and has been able to inhibit merozoite invasion.<sup>34</sup>

However, triggering such a protection-inducing immune response is not easy. The following are some of the more relevant difficulties involved in this task.

- The time available (~40 s) for antibody to bind to merozoite proteins is very short and limited, since merozoite molecules are exposed to the immune system for less than 1 min after leaving iRBCs and before invading new RBCs. High-concentration and/or high-affinity antibodies are, thus, required for blocking merozoite invasion of RBCs.<sup>35</sup> This also suggests that the number of copies of these molecules on the merozoite surface is critical for an efficient antibody-blocking effect.

- Merozoites display multiple alternative invasion mechanisms that are commonly used by field isolates.<sup>36–39</sup> This parasite strategy represents an advantage for evading the immune response against parasite ligands used in host-cell invasion and for overcoming host-cell receptor polymorphism or heterogeneity.<sup>40,41</sup> Some *P. falciparum* clones are, thus, able to use different invasion routes by switching the expression of parasite ligands that can bind to alternate receptors.<sup>39,40,42–47</sup> A fully effective antimalarial vaccine should, thus, contain antigens from all these proteins to induce an appropriate immune response capable of blocking all such alternative invasion routes.

- Genetic polymorphism in merozoite's RBC invasion proteins represents another great difficulty, due to these parasite molecules' tremendous genetic variability. Variable sequences are thereby involved in inducing a strain-specific immune response as a consequence of recognizing individual merozoite protein polymorphisms,<sup>42,48–50</sup> with this being one of the most commonly used mechanism for evading the immune response.

- Irrelevant, highly immunogenic, mostly tandem-repeat amino acid sequences are used during invasion to distract the immune response by acting as decoys or smokescreens.<sup>51,52</sup>

However, the worst difficulty lies in the conserved regions involved in merozoite invasion often being cryptic, poorly antigenic or nonantigenic, and nonimmunogenic,<sup>53–55</sup> mainly due to the following: (a) homology between parasite and host proteins allowing merozoites to escape immune recognition and develop chronic infection (the immune system down-regulates these potentially autoreactive responses) and (b) interference by immunodominant, nonrelevant sequences, thereby distracting immune system's attention from a protein's functionally active conserved regions.

The wide use of such mechanisms means that competition between a protection-inducing and a nonprotection-inducing immune response is one of the molecular strategies developed by the parasite to avoid its own destruction by the immune system. An example of this would be the antibodies directed against the MSP-1 EGF-like region that block the processing of inhibitory antibodies.<sup>56</sup>

Added to this (and thereby complicating vaccine development), there is an exquisite and perfect antigen-presentation mechanism that, when not functioning exactly as it should do, could induce an inappropriate immune response such as

short-lived antibody response,<sup>57</sup> long-lasting nonprotective antibody induction,<sup>58</sup> and cellular immune response.<sup>59</sup> Genetic control of the host's immune response adds more complexity to fully effective antimalarial vaccine development.

To overcome some of these difficulties, one must bear the following objectives in mind:

- A protection-conferring, antibody-mediated immune response must be directed against merozoite protein amino acid sequences involved in the invasion of RBCs. However, antibody levels and affinity constants must be greater than those between RBC receptors and their merozoite interacting sequences for efficiently inhibiting merozoite binding to RBCs and, therefore, preventing merozoite invasion.

- RBC receptor and merozoite binding amino acid sequence concentrations must also be considered. A large number of receptors plus a high concentration of high-affinity binding antibodies is required for these RBC binding proteins to overcome the physicochemical demands imposed by the short exposure time during which the merozoite is free (~40 s). Saul et al. have suggested that an antibody concentration lower than or equal to 10  $\mu\text{g/mL}$  is very unlikely to effectively inhibit merozoite invasion.<sup>35</sup>

Our analysis has strongly suggested that all highly conserved RBC binding amino acid sequences (for ALL invasion routes used by the merozoite) must be identified for inducing an appropriate immune response against them, thereby avoiding the trap of polymorphic, tandem-repeat, cryptic, silent or suppressor sequences by which the parasite can evade the immune response.

## 2.1. Synthetic Peptides Used for Acquiring Knowledge about Merozoite Protein RBC Binding Regions

A large number of merozoite proteins involved in invading RBCs have been identified to date. They contain antibody-inducing regions inhibiting in vitro merozoite invasion of RBCs and are recognized by merozoite immunocluster-eluted antibodies, indicating that they are exposed to the immune system.<sup>60,61</sup>

Several merozoite protein binding regions involved in the invasion of RBCs have been identified by using recombinant protein fragments or synthetic peptides corresponding to these proteins' amino acid sequences.<sup>43,62–64</sup>

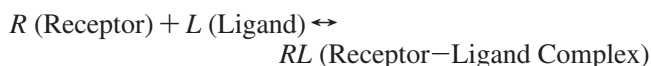
This review focuses on short (~20 mer long) merozoite protein-derived amino acid sequences involved in binding to RBCs. Such synthetic peptides present several advantages as they are chemically defined, their production is reproducible, they are easily available and cheap to synthesize, and an unlimited quantity can be rapidly produced. They can also be modified to produce analogues leading to a molecular definition of amino acids directly involved in binding, their stability facilitates their delivery to underdeveloped parts of the world, they are free of contaminants that can interfere with their biological function or induce undesired immune responses, and they are not infectious. These are, thus, some of the reasons why we chose synthetic peptide methodology as the ideal tool for dissecting *P. falciparum* merozoite proteins' intimate molecular interactions with RBCs.

## 2.2. Rationale for High-Activity Binding Peptide Recognition

On the basis of the above rationale, ~20 mer long peptides covering the whole length of known merozoite proteins

involved in RBC invasion have been synthesized in our institute and tested in RBC binding assays. Experimental binding assay conditions (defined from theoretical binding curves using a bimolecular interaction) were chosen for identifying high-affinity binding regions recognizing from 2 000 to 100 000 binding sites per cell. Specifically bound peptide's relationship to added peptide is directly proportional to the affinity constant and the number of peptide receptors on RBCs or host cell (binding ability) in these conditions.<sup>65,66</sup>

This can be defined as follows:



Renaming  $RL$  as  $b$  (bound ligand),  $R$  as  $r - b$  (unbound receptor), and  $L$  as  $l - b$  (free ligand) and replacing them in the above equation yields the following:

$$(r - b) + (l - b) \leftrightarrow b \quad (1)$$

In equilibrium, from eq 1, the affinity constant  $Ka$  is

$$Ka = \frac{[b]}{[r - l][l - b]} \quad (2)$$

In conditions where there is no ligand depletion and  $r \gg l$ , then  $(l - b) = l$  and  $(r - b) = r$ , eq 2 can thus be rewritten as follows:

$$Ka \cdot r = \frac{[b]}{[l]} \quad (3)$$

The  $[b]/[l]$  ratio is defined as being the binding activity; those peptides having binding activity greater than or equal to 0.02 (2% binding) are considered to have high binding activity and are named high-activity binding peptides (HABPs), indicating that there are more than 2 000 receptor sites per cell.<sup>54,64,67</sup>

Binding assay conditions have been completely standardized, taking factors that could affect merozoite invasion of RBCs into account, such as hematocrit, reaction time, and temperature.<sup>67</sup> It has been found that specific binding curves, which have been considered as selection and comparison criteria, present the best linear response at 20–60% hematocrite (Figure 2A1) 1 h after reaction (even when significant binding may have already been observed after 5 min) (Figure 2A2) when equilibrium has been reached at 18 °C (not significantly increasing at 37 °C) (Figure 2A3). Binding assays for this type of cells were developed in these conditions, providing a highly sensitive, specific, and robust methodology for this type of receptor–ligand interaction.

Lineal regression and statistical analysis of different proteins have revealed three types of binding peptides: high-activity binding peptides (HABPs) (Figure 2B1), nonbinding peptides (Figure 2B2), and nonspecific binding peptides (Figure 2B3).<sup>64,67</sup> Nonbinding and ordinary nonspecific binding peptides have obviously been discarded. Jumbled peptides having the same amino acid composition but different amino acid sequence to HABPs have systematically proven to be nonbinding peptides.

HABPs mainly bind to human and *Aotus* RBCs which can be invaded and infected by *P. falciparum* merozoites.<sup>68,69</sup> HABPs bind with less ability to rabbit RBCs, which *P. falciparum* merozoites can adhere to and infect but not reproduce themselves within.<sup>70</sup> However, HABPs do not bind to goat, horse, or chicken RBCs, which *P. falciparum* merozoites also do not bind to, or invade, showing the high

specificity of their reaction with receptor cell molecular structures.<sup>68,70</sup>

The vast majority of our studies have shown that most HABPs bind to human RBC surface molecules since  $\geq 60\%$  of HABP RBC binding ability can be removed by enzymatic treatment with neuraminidase, trypsin, or chymotrypsin.<sup>64,67,68,71</sup> This has suggested that there are at least six different RBC binding sites and that at least one of them is sialic-acid-dependent. Three of these could be glycoporphins, and at least three could be cryptic receptors.<sup>71–73</sup>

HABP binding constants have also been determined via saturation assays (Figure 2C) in which ligand concentration is kept constant in the presence of increasing concentrations of radioactively labeled ligand. HABP–RBC binding has simple interaction characteristics, with dissociation constants ( $K_d$ ) being in the nanomolar range, and involving  $\gg 2$  000 binding sites per cell. Hill plots have shown that most of these peptides present positive cooperativity, suggesting that once a first ligand had bound to its receptor site then this facilitates the next ligand's binding.<sup>65,66,71–73</sup>

Critical residues in HABP binding to receptor cells have been determined for a large number of these HABPs by competition assays between HABPs and glycine analogue scanning. Critical residues are those where peptide analogues show at least 50% reduced specific binding in their ability to compete with the original peptide (bold and underlined in Figure 2D and throughout the whole manuscript) at three different concentrations.<sup>67,68,74,75</sup>

From a biological viewpoint, these HABPs have shown three different types of behavior in invasion inhibition assays or during the parasite's intraerythrocytic development in *in vitro* cultures. Some of them have inhibited merozoites' invasion *in vitro* but not their development; others can inhibit merozoites' invasion and their development, while others have had no effect whatsoever.<sup>75–79</sup>

Immunogens containing part of a HABP, or a peptide sequence analogous to that of a HABP, have induced antibodies that have not only inhibited merozoite invasion but have also induced protection in an experimental animal model.<sup>80–82</sup>

However, HABPs that do not present genetic variability in their amino acid sequences in different isolates or strains from different parts of the world (here named conserved HABPs) are usually poor immunogens, and a different strategy has to be developed to trigger their immunogenicity and protection-inducing capacity.

HABPs identified by this methodology have displayed all the characteristics of specific receptor–ligand interactions involved in RBC invasion, such as

- saturability;
- binding inhibition induced by enzymatic treatment of susceptible cells;
- specific binding to cells to which *P. falciparum* also binds;
- glycine analogues' differential binding;
- absence of HABP jumbled peptide binding; and
- *in vitro* inhibition of new RBC invasion.

The above make this a highly sensitive, specific, and robust methodology for identifying RBC–HABPs.

### 3. Merozoite Surface Protein (MSP) Family

MSPs correspond to a family of membrane-associated proteins present on free merozoite surface and must be very important for invasion since antibodies directed against them

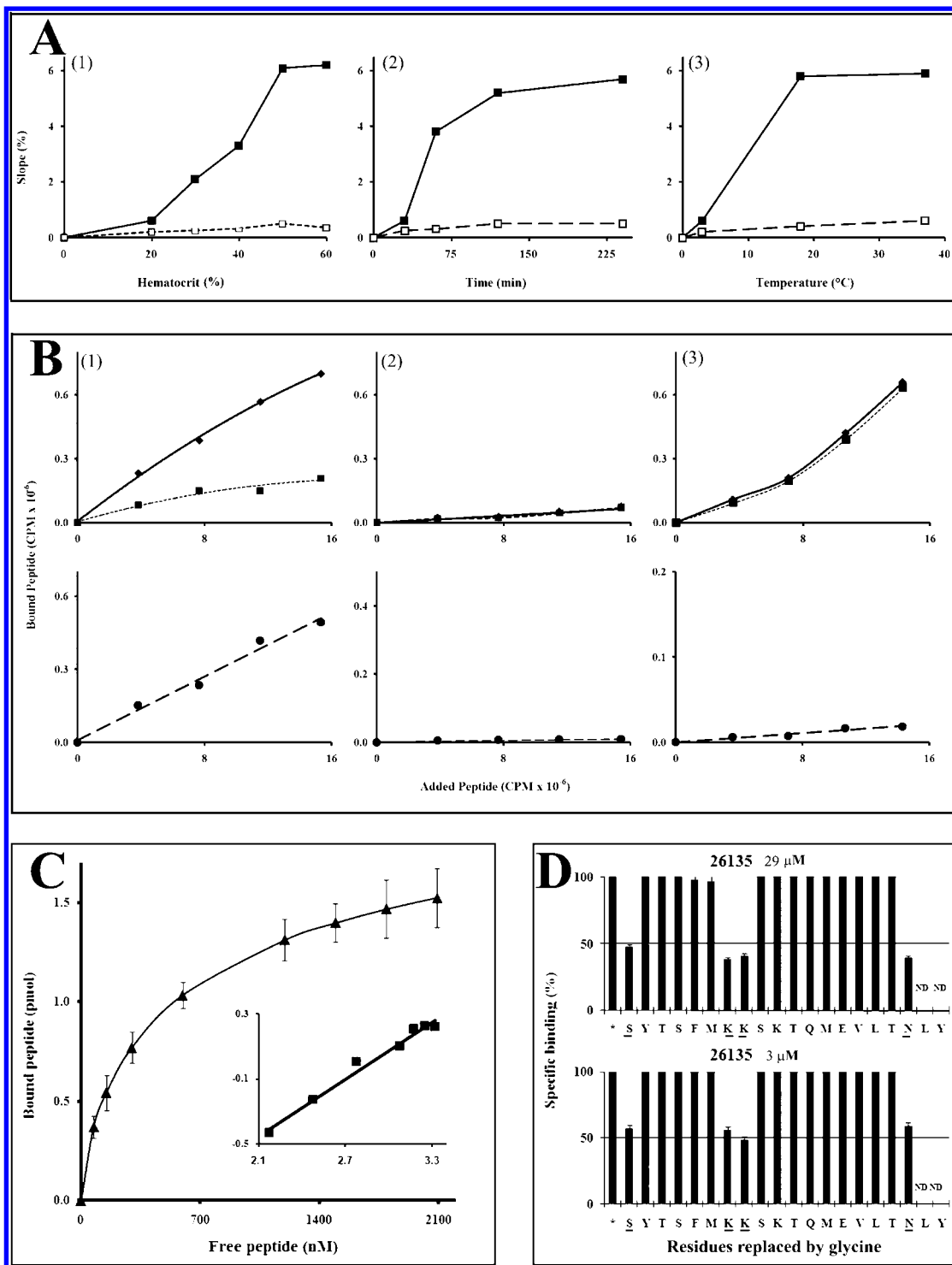


**Figure 2.** (A) Factors influencing binding assays for peptides with high binding activity (■) and low binding activity (□) to RBCs: (1) Specific binding curve slope values plotted against different hematocrit levels ( $T = 18\text{ }^{\circ}\text{C}$ , 90 min), (2) the effect of reaction time on specific binding curve slope values (50% hematocrit,  $18\text{ }^{\circ}\text{C}$ ), and (3) the effect of temperature on specific binding curve slope values (60% hematocrit, 60 min), adapted from Rodriguez et al.<sup>67</sup> (B) Binding to human RBCs. Figures in the top 1, 2, 3 panels show: (◆) total binding, obtained from samples with radio-labeled peptide alone, nonspecific binding (■) represents the residual radio-labeled peptide bound with the addition of  $400\times$  the concentration of identical unlabeled peptide. Figures in 1, 2, 3 at the bottom panels show specific binding (●) obtained by subtracting nonspecific binding from total binding. The three types of behavior observed for the studied peptides are shown in these graphs: (1) peptides that are specifically bound to RBC with high affinity (e.g., 30312); (2) low-binding peptides or nonbinding peptides (e.g., 30193); (3) peptides that are bound with high affinity but are nonspecific (e.g., 30190). Figure adapted from Ocampo et al.<sup>289</sup> (C) HABP–RBC saturation curve. The binding of EBA-140 protein peptide 26135, where the saturation curve led to its dissociation constant being calculated as 350 nM. Statistical treatment and Hill plot slope presented nH (Hill coefficient) equal to 1 (positive cooperativity) and 1 800 receptor sites per cell for this ligand, adapted from Rodriguez et al.<sup>259</sup> (D) Competition binding assays with analogue peptides. Original radio-labeled peptide binding was inhibited by glycine analogue peptides at 3 and 29  $\mu\text{M}$ . The y-axis shows the RBC specific binding activity of HABP 26135 and its analogues, 100% representing the original peptide’s specific binding activity (\*). The x-axis shows the amino acid replaced in the analogue peptide. Peptides that inhibited original peptide specific binding by at least 50% at all concentrations are underlined and called critical amino acids, adapted from Rodriguez et al.<sup>259</sup>

can block merozoite invasion of RBCs. A thorough analysis of each one is, thus, given below.

### 3.1. Merozoite Surface Protein-1 (MSP-1)

MSP-1 (PFI1475w, the first to be described) has provided the greatest bulk of information concerning parasite recognition and invasion of RBCs because of the elegant studies performed with this molecule.<sup>83–86</sup> This molecule is proteolytically cleaved into 83, 30, 38, and 42 kDa fragments on the merozoite surface during a first step, forming a noncovalently bound macromolecular complex<sup>85</sup> (Figures 3 and 9). The MSP-1<sub>42</sub> fragment undergoes a second Ca<sup>2+</sup>-dependent cleavage producing 33 and 19 kDa fragments, with the latter remaining anchored to the merozoite membrane via the GPI tail (Figures 3, 4, 7, and 13) and being the only fragment from this protein that enters the RBC.<sup>87,88</sup>

Seventeen blocks have been identified in the gene encoding this protein when comparing nucleotide sequences: five conserved, five semiconserved, and seven variable blocks. There are essentially two versions of each block (MAD20 and K1) according to representative isolates.<sup>89</sup> The main exception to this dimorphic rule is the variable block 2, which is a third version of a RO33 isolate. Such allele diversity is produced by intragenic recombination among representative sequences.

Please note that conserved regions are represented throughout this manuscript in green while variable regions (dimorphic, polymorphic, or tandem repeats) are shown in yellow in all figures representing merozoite protein-RBC binding profiles and HABP identification and localization. Immunization with intact constructs containing MSP-1 segments or synthetic peptides based on this protein's amino acid sequences could induce partial or complete protection in mice, monkeys and humans.<sup>90–93</sup>

Several expression systems (*Escherichia coli*, *Baculovirus*, *Pichia pastoris*, and *Saccharomyces cerevisiae*) have been extensively used for producing recombinant MSP-1 or its MSP-1<sub>42</sub> and MSP-1<sub>19</sub> fragments to induce a protection-inducing immune response.<sup>94–98</sup> All these expression systems theoretically give correctly folded, possibly immunogenic recombinant proteins, and antibodies induced by them have been analyzed by different methods such as ELISA, immunofluorescence, Western blot, in vitro inhibition of parasite growth, and parasitaemia reduction or absence after blood-stage *P. falciparum*-challenge in *Aotus* or *Saimiri* monkeys.<sup>95–98</sup>

The major epitopes recognized by these antibodies localize to conserved determinants of the MSP-1<sub>19</sub> domain derived from cleavage of the MSP-1<sub>42</sub> processing fragment.<sup>99</sup> Protective immunity in monkeys was correlated with antibody titer against this segment's MSP-1<sub>19</sub> EGF-like domain 2.<sup>95,97</sup>

Antigenicity studies have reported ~40 amino acid sequences (from 11 to 22 mer long) from MSP-1 protein as containing CD4<sup>+</sup> cell epitopes or T-helper lymphocyte activators. Some of them are located at the C-terminal end of MSP-1, most corresponding to dimorphic regions and differing in their immunogenicity at major histocompatibility complex (MHC) restriction level.<sup>99–101</sup> On the basis of this information, it has been suggested that the *P. falciparum* MSP-1<sub>19</sub> fragment is an ideal putative target for obtaining protection-inducing antibodies against blood-stage infection, since high antibodies titers against this MSP-1 C-terminal region are involved in protection against severe malaria and are correlated with clinical immunity.<sup>102–104</sup>

MSP-1<sub>19</sub> monoclonal antibodies inhibit *P. falciparum* merozoite invasion of RBC in vitro and direct immunization providing protection against challenge-induced infection.<sup>88,91,95,105,106</sup> The above has led to most efforts being focused on inducing a protection-inducing immune response by immunization with this fragment. However, great difficulties have been encountered in obtaining protection-inducing immunity with recombinant MSP-1 fragments due to the large number of dimorphic or polymorphic positions which they display, indicating that such diversity seems to be associated with the parasite evading the immune response.

Making this issue more complex, it has been found that the MSP-1<sub>19</sub> domain is also the target for antibodies able to increase merozoite invasion by inhibitory antibody-mediated blocking. Monoclonal antibodies such as MoAb 12.8 recognizing MSP-1<sub>19</sub> in residues 5–13 and 14–18 or MoAb 12.10 recognizing residues 5–7 and 15–18 have been able to block merozoite invasion of RBCs. However, MoAb 1E1 interferes with MoAbs 12.8 and 12.10 being able to block invasion.<sup>106</sup> It has been also described that the highly conserved MSP-1<sub>19</sub> domain is poorly antigenic and poorly immunogenic, perhaps due to resistance to this protein's processing, as a consequence of disulfide bonds in its EGF-like domains.<sup>56,107–109</sup>

MSP-1 tends to form dimers<sup>110</sup> and binds to MSP-6 and MSP-7.<sup>111–113</sup> It has been shown that MSP-1<sub>19</sub> contains two epidermal growth factor-like (EGF-like) domains probably binding together with MSP-1<sub>33</sub> to band 3 on the surface of human RBCs. These fragments, together with MSP-9 (ABRA) and other proteins currently being studied, form a macromolecular complex facilitating merozoite entry into RBCs.<sup>114–116</sup>

Our RBC binding assays, employing nonoverlapping 20 mer peptides, covering the entire MSP-1 protein sequence, have shown that nine HABPs bound with high affinity to RBCs. Please note that, throughout this manuscript, HABP numbers correspond to our institute's serial numbering and the superscripts above N and C terminal amino acid sequences correspond to their position on the molecule from which the amino acid sequence was derived for binding studies. Underlined residues shown in bold are critical binding residues.

HABPs 1513 (<sup>42</sup>GYSLFQ**KEK**MVLNEG**TSTA**<sup>62</sup>) and 1522 (<sup>202</sup>QIPFNL**KIRAN**ELD**VLKKLV**<sup>221</sup>) were located in the 83 kDa domain, and HABPs 1577 (<sup>1142</sup>FKVLSKLEGKLDN**LNLEKK**<sup>1161</sup>) and 1582 (<sup>1242</sup>AESNTITTSQNVDD**DDVI**<sup>1261</sup>) were located in the 38 kDa domain. HABPs 1585 (<sup>1302</sup>EVLYL**KPLAG**VYRSL**KKQLE**<sup>1321</sup>), 1589 (<sup>1382</sup>LSSYNYIKDSID**T**DINFAD<sup>1401</sup>), 1590 (<sup>1402</sup>VLGYYKILSEKYKSD**LDI**<sup>1421</sup>), and 1591 (<sup>1422</sup>KYINDKQGENEKYLPFLNNI<sup>1441</sup>) were found in the 33 kDa domain, and HABP 5501 (<sup>1542</sup>QGMLN**ISQHQCVK**QCP**QNS**<sup>1561</sup>) was found in the 19 kDa fragment<sup>64</sup> (Figures 3 and 9). HABP 1513, 1522, 1585, and 5501 amino acid sequences were highly conserved; critical amino acids involved in RBC binding were identified via glycine analogue scanning.

Part of the HABP 1513 sequence was included in the only synthetic vaccine produced so far against malaria (SPf66), which induced 30–50% protective efficacy in different field trials in people aged more than 1 year<sup>92,117–120</sup> for a period of up to 2 years.<sup>121–123</sup> HABP 1513 shares a sequence with reported T- and B-cell epitopes.<sup>108</sup> Cyclic peptides and pseudopeptides having HABP 1513 sequence have been

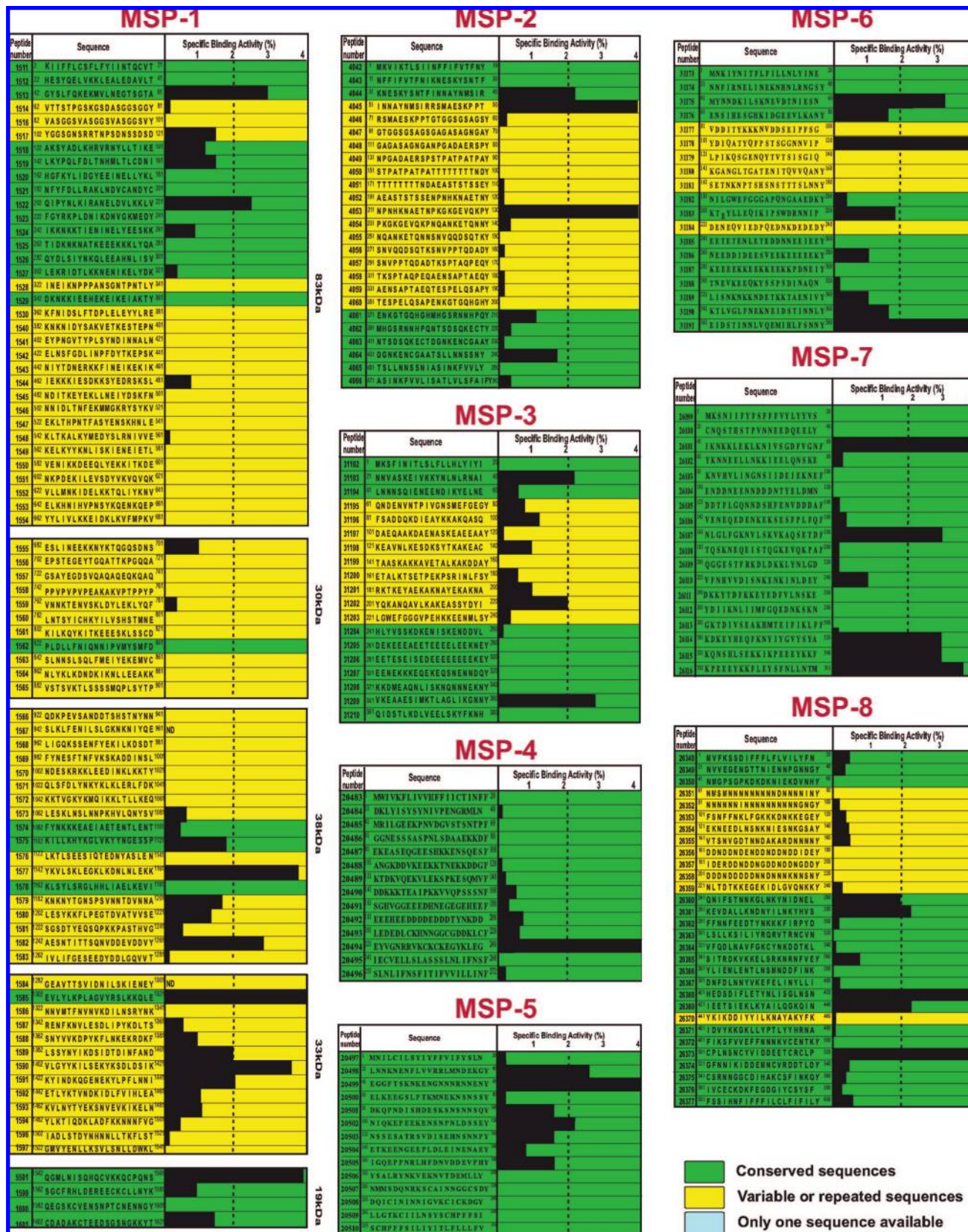


**Figure 3.** Peptide RBC binding activity, corresponding to some of the 35 merozoite invasion-related proteins presented in this manuscript. Peptide amino acid sequences are shown on the left, with our institute’s serial peptide numbers and small superscript numbers to indicate their position in the protein amino acid sequence. The black bars on the corresponding protein’s right-hand side show each peptide’s specific binding activity (the slope of the specific binding graph). The dotted line at 2% binding is the cutoff for selecting high-activity binding peptides (HABPs). Please note that conserved regions are represented throughout this manuscript in green while variable regions (dimorphic, polymorphic, or tandem repeats) are shown in yellow. Pale blue proteins or fragments are those for which only one sequence has been described. Fuchsia in Figures 4 and 6 represents regions for which specific RBC protein binding regions have been found, such as band 3 and spectrin. Colored bars on the right-hand side of the EBL proteins in Figures 5 and 6 correspond to a diagrammatic representation of the protein where the different domains have been assigned.

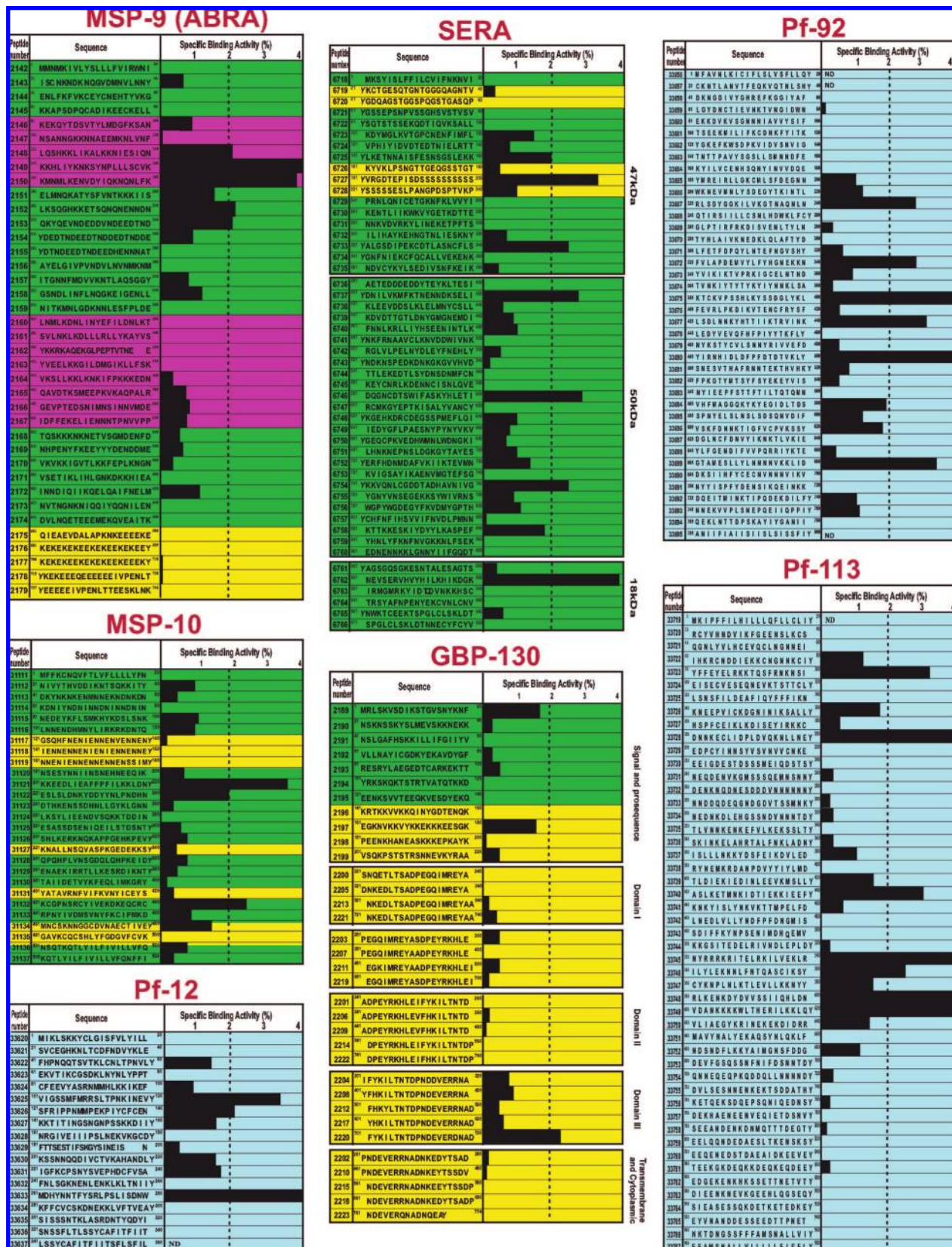


**Figure 4.** Peptide RBC binding activity, corresponding to some of the 35 merozoite invasion-related proteins presented in this manuscript. Peptide amino acid sequences are shown on the left, with our institute’s serial peptide numbers and small superscript numbers to indicate their position in the protein amino acid sequence. The black bars on the corresponding protein’s right-hand side show each peptide’s specific binding activity (the slope of the specific binding graph). The dotted line at 2% binding is the cutoff for selecting high-activity binding peptides (HABPs). Please note that conserved regions are represented throughout this manuscript in green while variable regions (dimorphic, polymorphic, or tandem repeats) are shown in yellow. Pale blue proteins or fragments are those for which only one sequence has been described. Fuchsia in Figures 4 and 6 represents regions for which specific RBC protein binding regions have been found, such as band 3 and spectrin. Colored bars on the right-hand side of the EBL proteins in Figures 5 and 6 correspond to a diagrammatic representation of the protein where the different domains have been assigned.

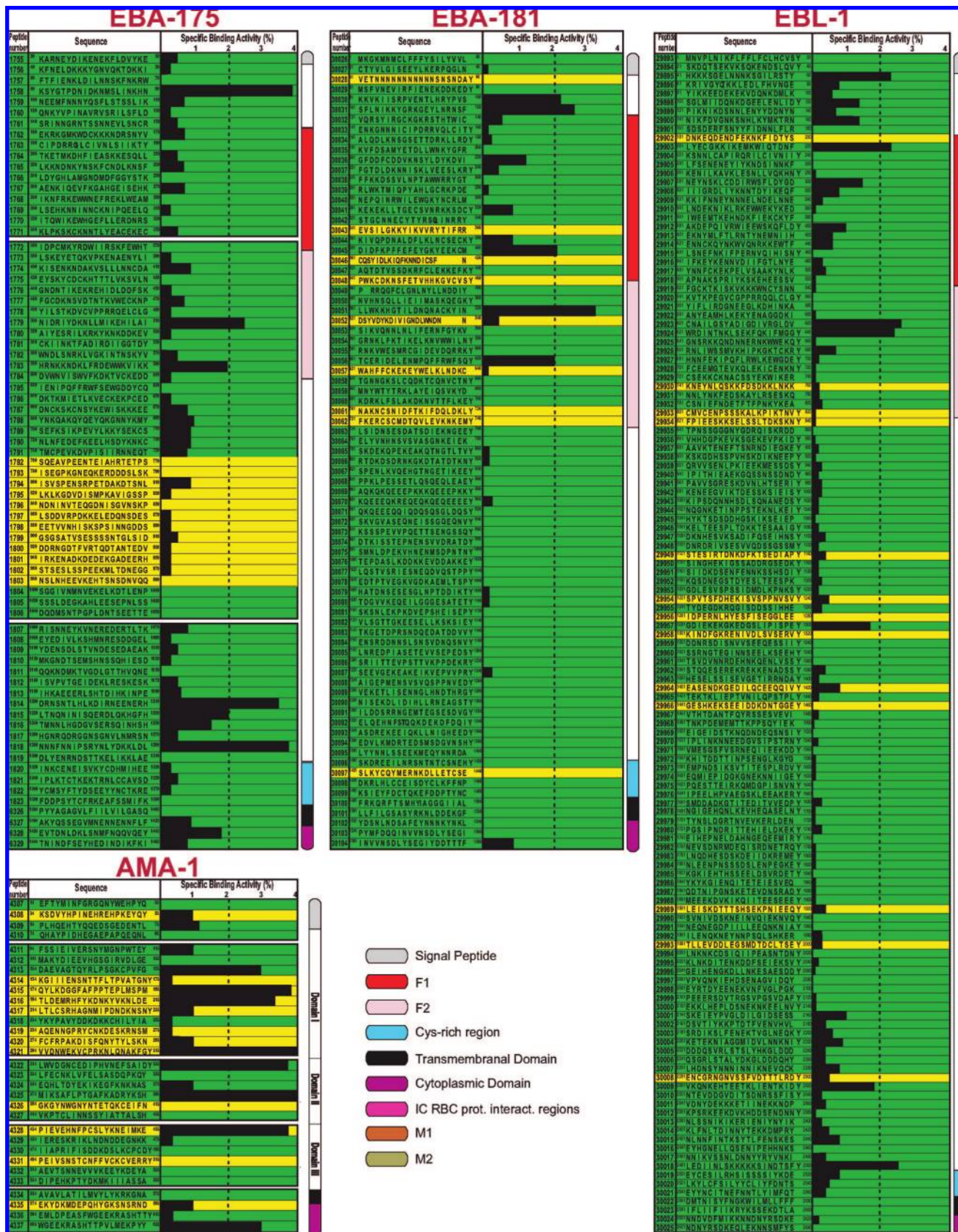


**Figure 5.** Peptide RBC binding activity, corresponding to some of the 35 merozoite invasion-related proteins presented in this manuscript. Peptide amino acid sequences are shown on the left, with our institute's serial peptide numbers and small superscript numbers to indicate their position in the protein amino acid sequence. The black bars on the corresponding protein's right-hand side show each peptide's specific binding activity (the slope of the specific binding graph). The dotted line at 2% binding is the cutoff for selecting high-activity binding peptides (HABPs). Please note that conserved regions are represented throughout this manuscript in green, while variable regions (dimorphic, polymorphic, or tandem repeats) are shown in yellow. Pale blue proteins or fragments are those for which only one sequence has been described. Colored bars on the right-hand side of the EBL proteins in Figures 5 and 6 correspond to a diagrammatic representation of the protein where the different domains have been assigned.

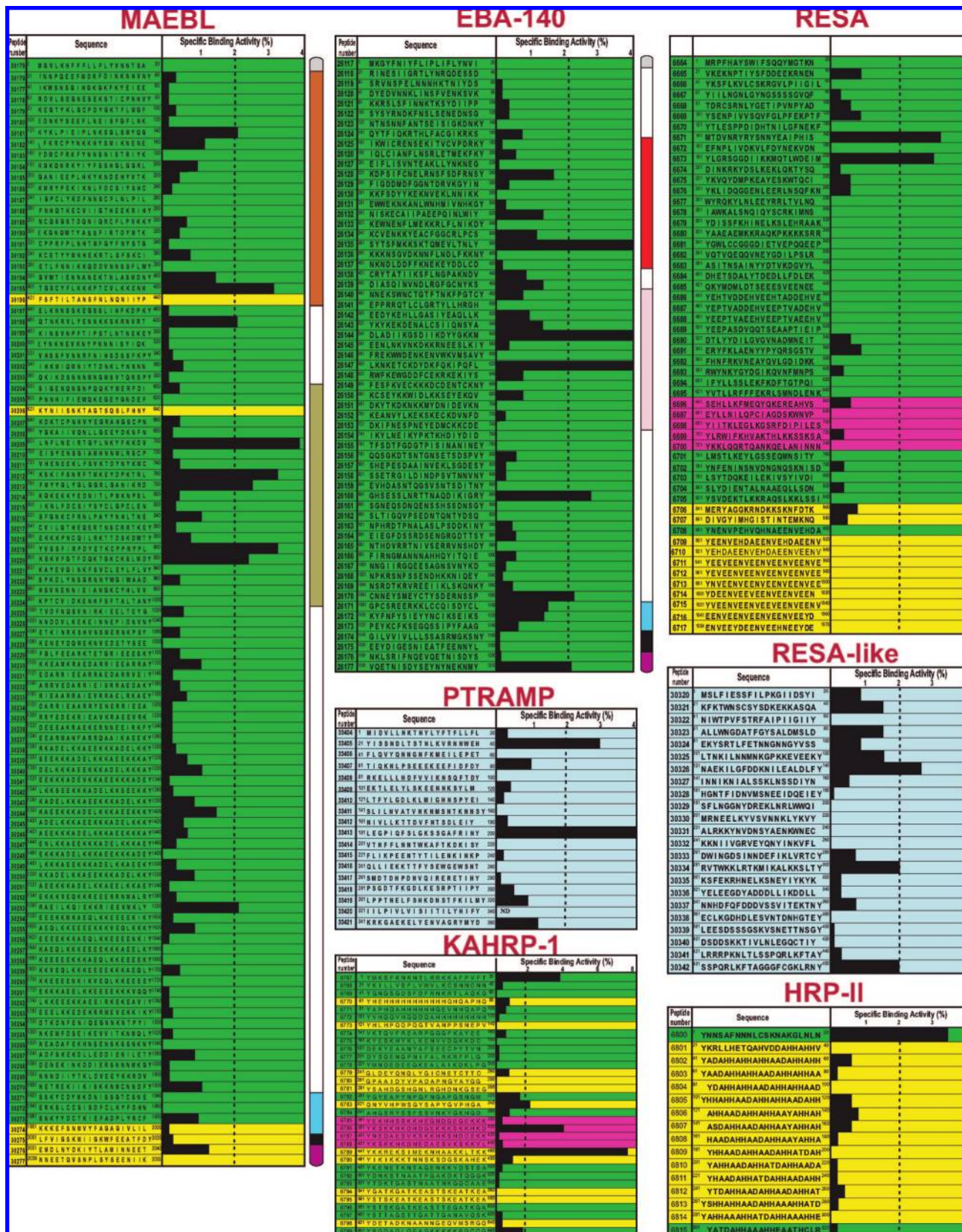


**Figure 6.** Peptide RBC binding activity, corresponding to some of the 35 merozoite invasion-related proteins presented in this manuscript. Peptide amino acid sequences are shown on the left, with our institute’s serial peptide numbers and small superscript numbers to indicate their position in the protein amino acid sequence. The black bars on the corresponding protein’s right-hand side show each peptide’s specific binding activity (the slope of the specific binding graph). The dotted line at 2% binding is the cutoff for selecting high-activity binding peptides (HABPs). Please note that conserved regions are represented throughout this manuscript in green, while variable regions (dimorphic, polymorphic, or tandem repeats) are shown in yellow. Pale blue proteins or fragments are those for which only one sequence has been described. Fuchsia in Figures 4 and 6 represents regions for which specific RBC protein binding regions have been found, such as band 3 and spectrin. Colored bars on the right-hand side of the EBL proteins in Figures 5 and 6 correspond to a diagrammatic representation of the protein where the different domains have been assigned.

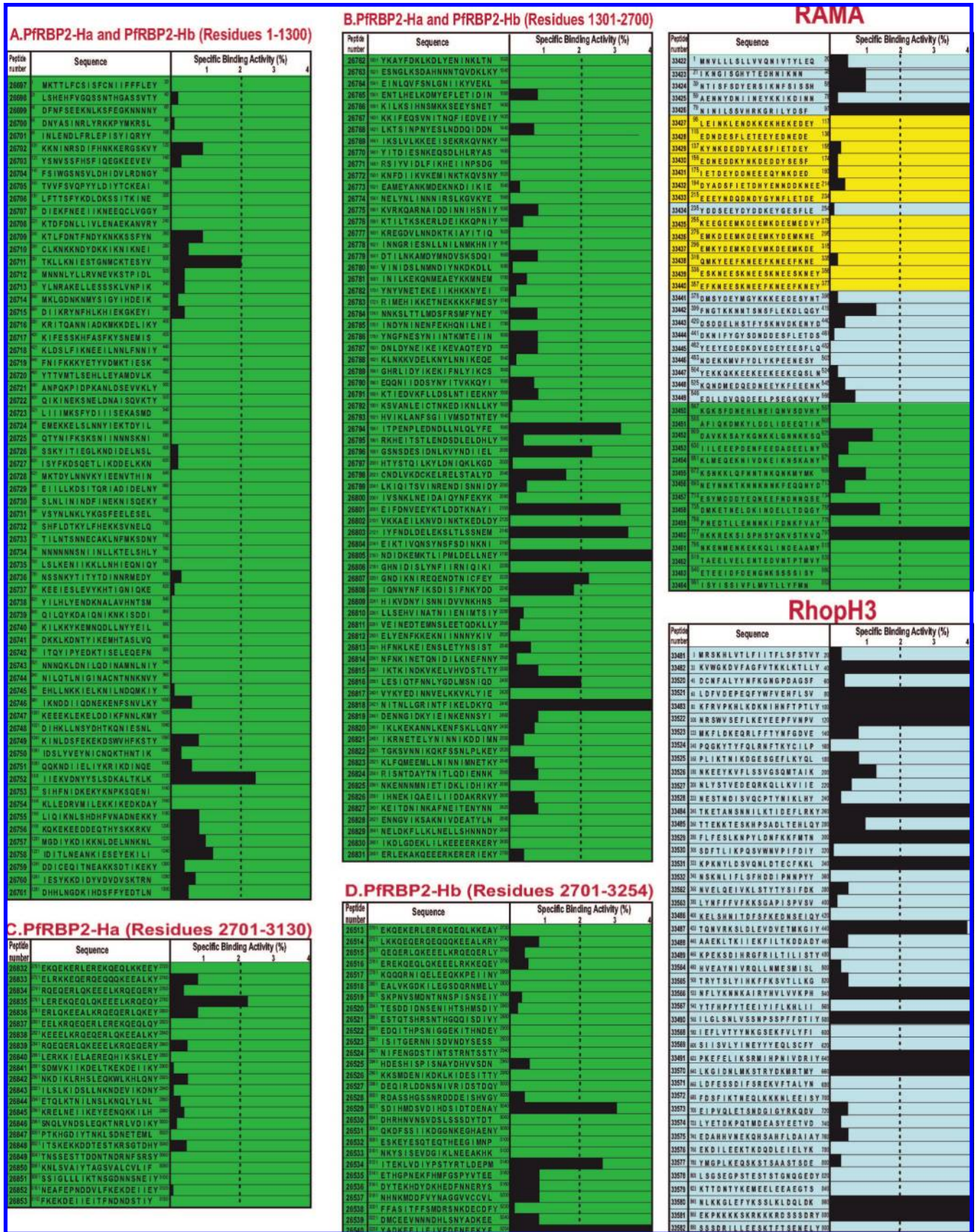


**Figure 7.** Peptide RBC binding activity, corresponding to some of the 35 merozoite invasion-related proteins presented in this manuscript. Peptide amino acid sequences are shown on the left, with our institute's serial peptide numbers and small superscript numbers to indicate their position in the protein amino acid sequence. The black bars on the corresponding protein's right-hand side show each peptide's specific binding activity (the slope of the specific binding graph). The dotted line at 2% binding is the cutoff for selecting high-activity binding peptides (HABPs). Please note that conserved regions are represented throughout this manuscript in green, while variable regions (dimorphic, polymorphic, or tandem repeats) are shown in yellow. Pale blue proteins or fragments are those for which only one sequence has been described.

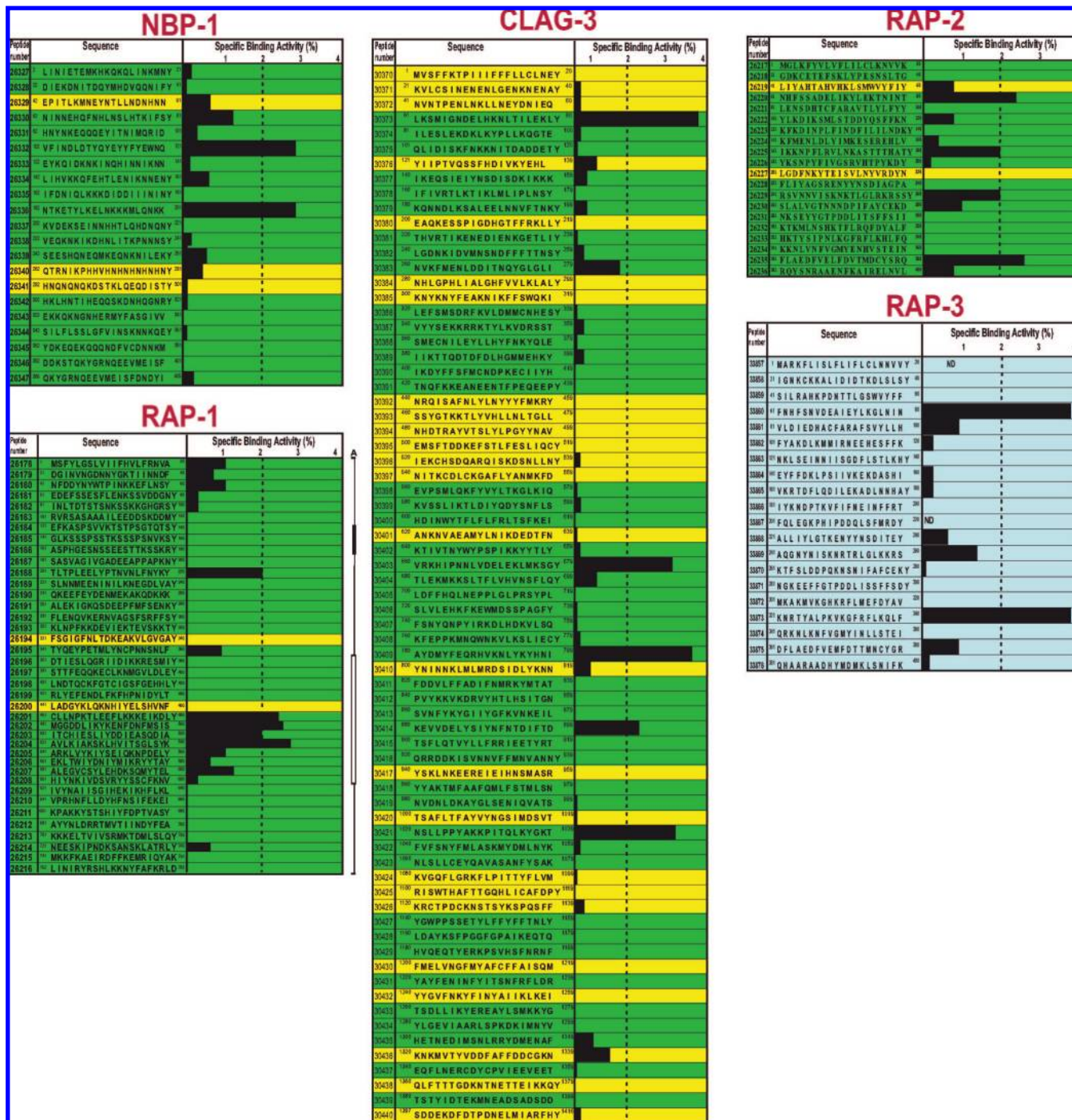


**Figure 8.** Peptide RBC binding activity, corresponding to some of the 35 merozoite invasion-related proteins presented in this manuscript. Peptide amino acid sequences are shown on the left, with our institute’s serial peptide numbers and small superscript numbers to indicate their position in the protein amino acid sequence. The black bars on the corresponding protein’s right-hand side show each peptide’s specific binding activity (the slope of the specific binding graph). The dotted line at 2% binding is the cutoff for selecting high binding activity peptides (HABPs). Please note that conserved regions are represented throughout this manuscript in green, while variable regions (dimorphic, polymorphic, or tandem repeats) are shown in yellow. Pale blue proteins or fragments are those for which only one sequence has been described.

seen to produce antibodies inhibiting in vitro merozoite invasion.<sup>124–126</sup>

HABP 1513 (characterized by limited genetic polymorphism) has presented at least one of the parasite mechanisms associated with evading the immune response, since antibodies against this antigen recognized minimum variations in its amino acid sequence<sup>48</sup>KEKMVL<sup>53</sup> with very different affinities.<sup>127</sup> However, only HABP 1513 induced exclusive T-cell clones against the variable sequence used in im-

munization assays, where dimorphic amino acids were potential TCR contact residues.<sup>128</sup> This data has shown the importance of designing peptides inducing a suitable fit into the TCR–peptide–MHC complex to induce an appropriate immune response. HABP 1522 is highly conserved, being nonantigenic and nonimmunogenic in all studies and displaying a classical  $\alpha$ -helical structure.

Conserved HABP 1585 shares almost the whole sequence (underlined) with T-cell epitope PL146 (<sup>137</sup>LKPLAGVYRSL-

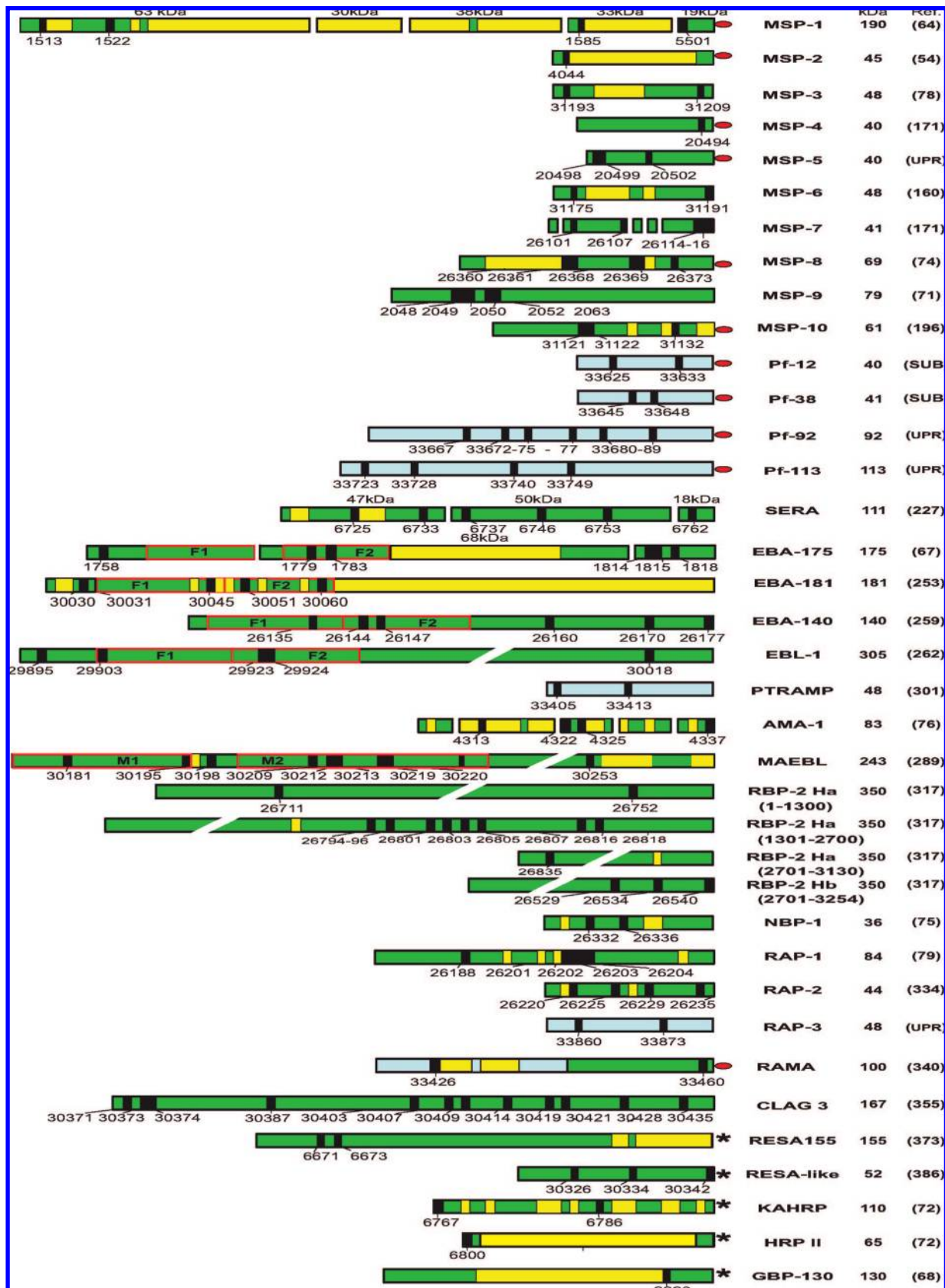


**Figure 9.** Schematic representation of 35 merozoite proteins involved in RBC invasion and approximate location of conserved HABPs in their amino acid sequences. Green corresponds to conserved regions, yellow shows variable regions, and pale blue represents proteins or their fragments for which only one amino acid sequence has been described to date (20/11/07). Some proteins have been cut down because of their large size. GPI anchored proteins (●) and those containing PEXEL motifs (\*) are also shown. The molecular mass is presented in kDa; ref = references.

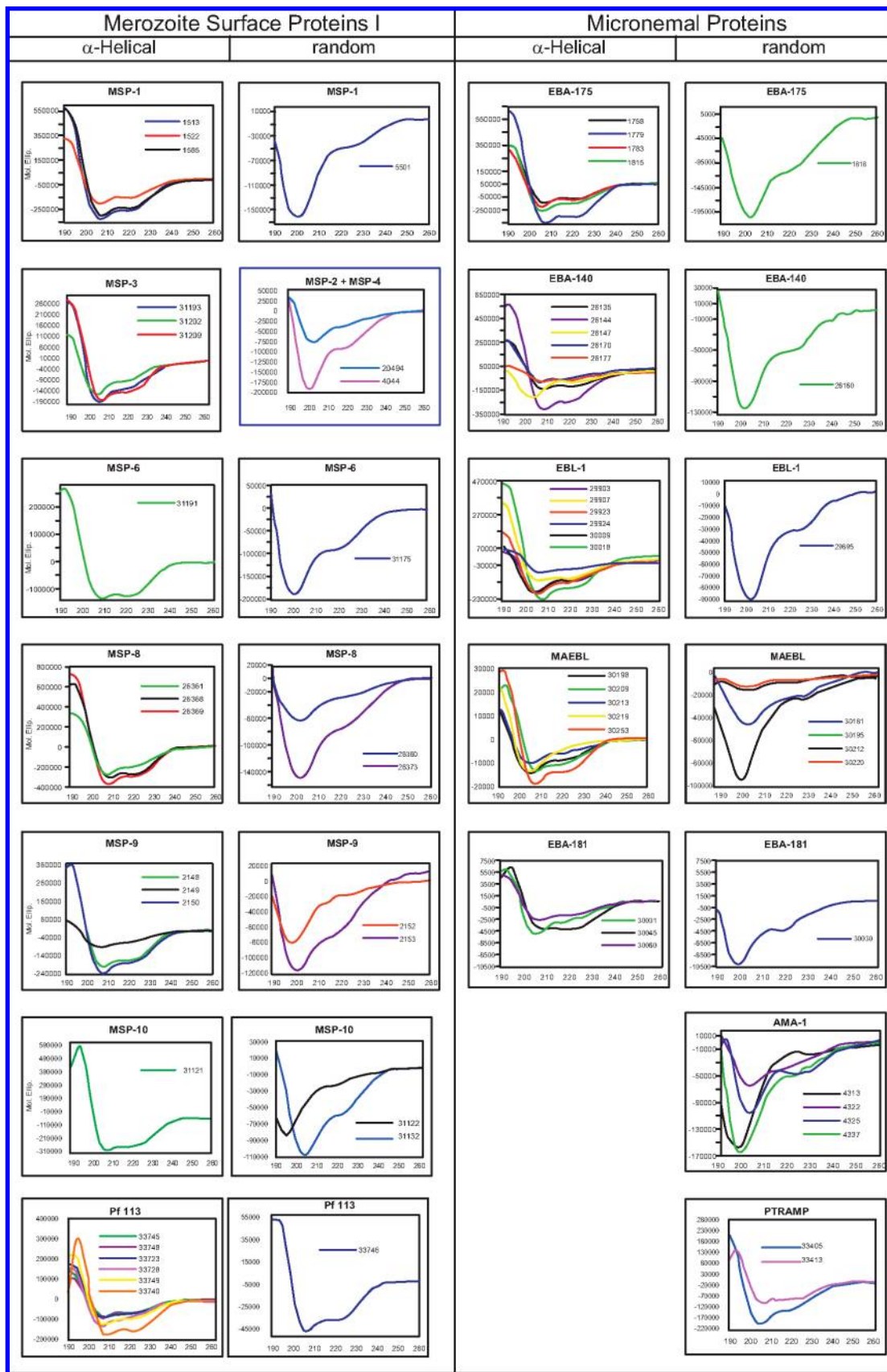


**Figure 10.** Structural features for HABPs corresponding to the 35 most relevant proteins involved in RBC invasion. CD assays were performed at room temperature on nitrogen flushed cells on a Jasco J 810 spectropolarimeter. Results are expressed as mean residue ellipticity. Deconvolution studies to determine the proportion of regular (r), distorted (d),  $\alpha$ -helical (h), or strand turns and unordered configurations for most peptides have been published elsewhere.<sup>132</sup> The figures show the CD spectra for 150 HABPs;  $\alpha$ -helical structural elements were determined according to 208 and 222 nm minimum values and 190 nm maximum ellipticity, whereas those HABPs displaying a random coil or  $\beta$ -turn structure presented a minimum at 200 nm below 0.

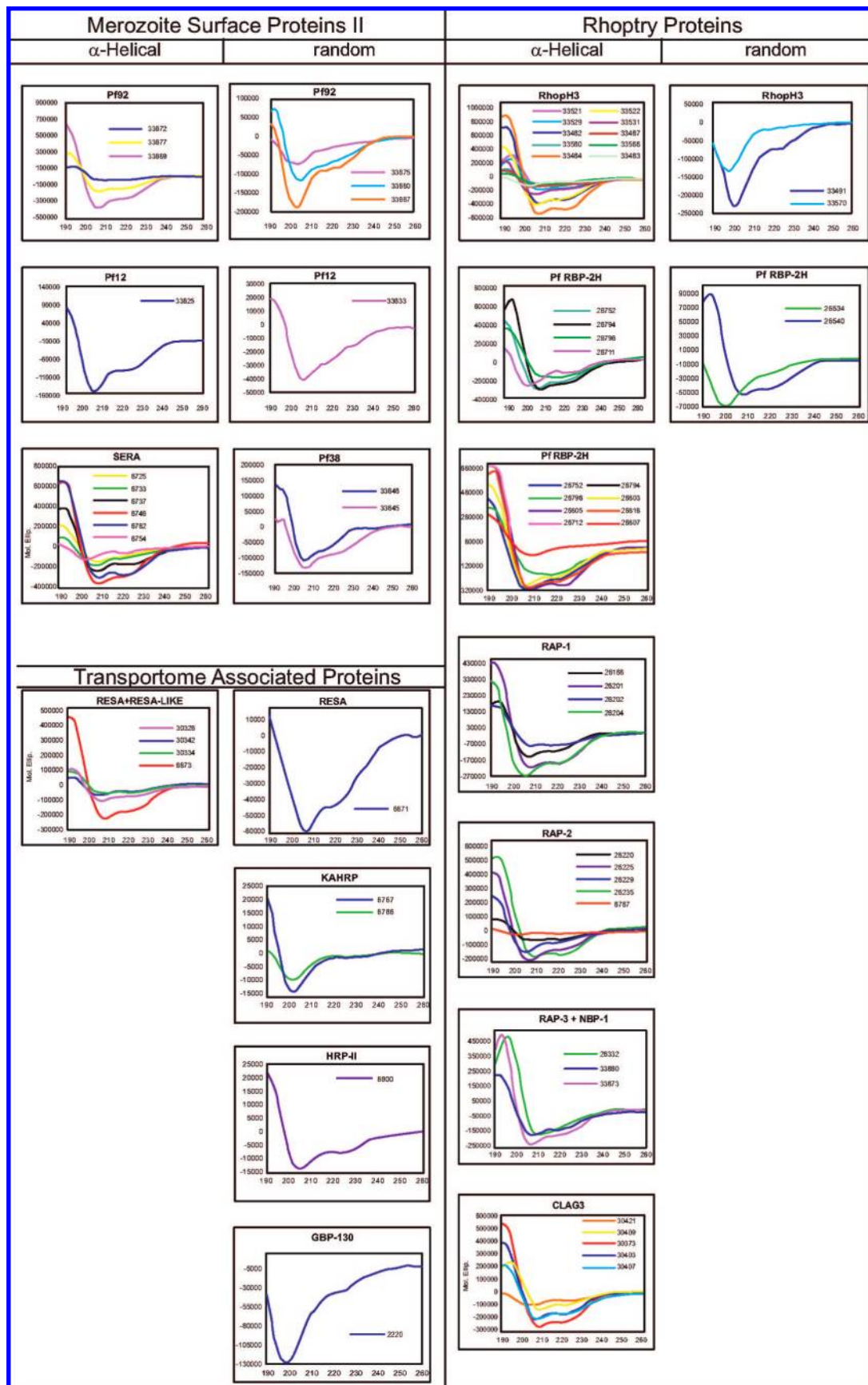


**Figure 11.** Structural features for HABPs corresponding to the 35 most relevant proteins involved in RBC invasion. CD assays were performed at room temperature on nitrogen flushed cells on a Jasco J 810 spectropolarimeter. Results are expressed as mean residue ellipticity. Deconvolution studies to determine the proportion of regular (r), distorted (d),  $\alpha$ -helical (h), or strand turns and unordered configurations for most peptides have been published elsewhere.<sup>132</sup> The figures show the CD spectra for 150 HABPs;  $\alpha$ -helical structural elements were determined according to 208 and 222 nm minimum values and 190 nm maximum ellipticity, whereas those HABPs displaying a random coil or  $\beta$ -turn structure presented a minimum at 200 nm below 0.

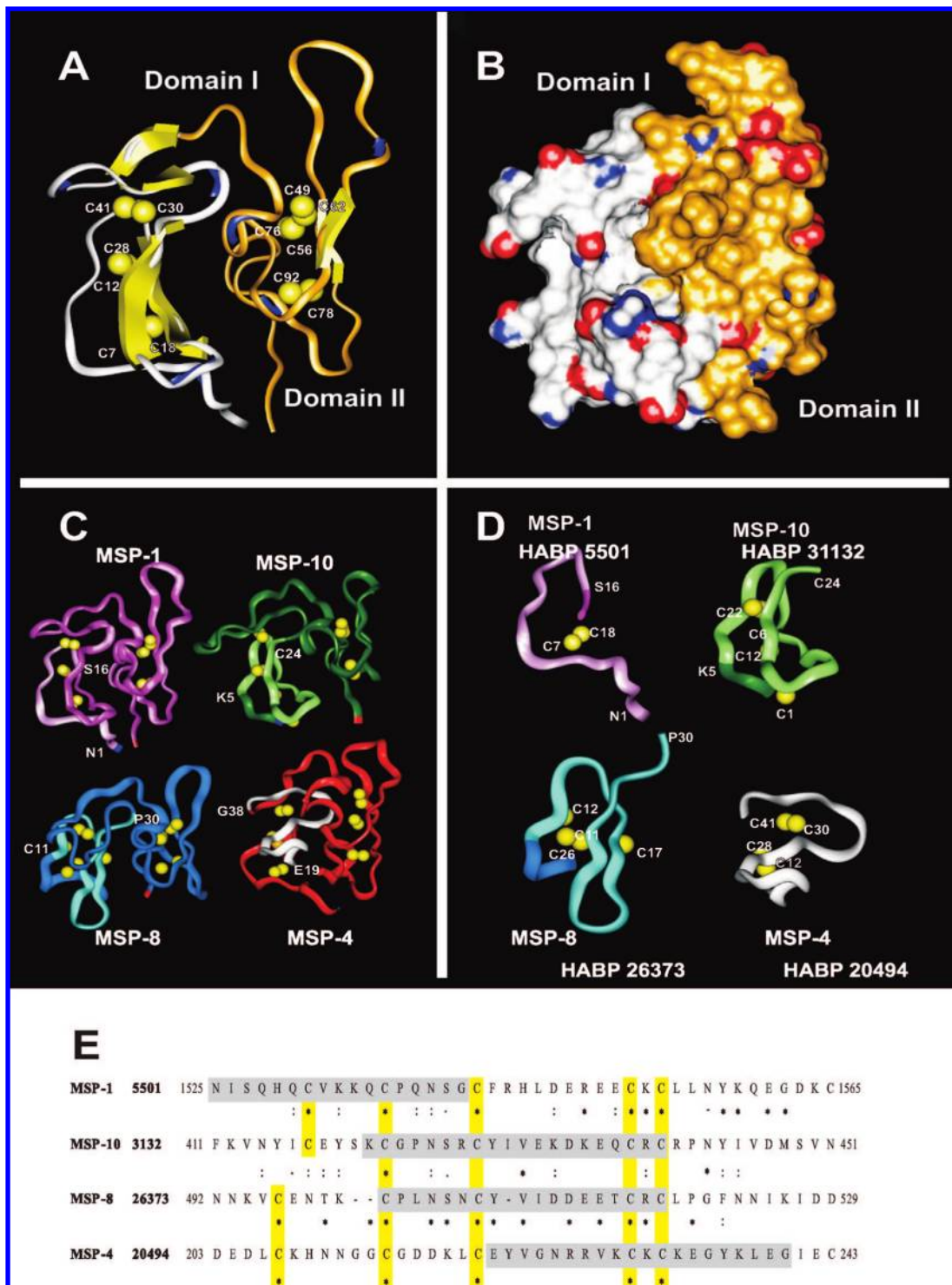


**Figure 12.** 3D structure. (A) MSP-1 19 kDa fragment determined by X-ray crystallography showing domains I (white) and II (gold) in which each EGF-like domain I and II are located displaying parallel and antiparallel  $\beta$ -sheets (yellow) and  $\beta$ -turns. (B) Connolly representation of each domain I (white) and II (gold). Blue indicates positively charged atoms and red negatively charged atoms. (C) 3D structure of the 19 kDa MSP-1 fragment in fuchsia and energy-minimization-based 3D structure predicted for the same 19 kDa homologous sequence in MSP-10 (green), MSP-8 (blue), and MSP-4 (red). The location of MSP-1 HABP 5501 is shown in pink, MSP-10 31132 is shown in lemon green, MSP-8 26373 is shown in pale blue, and MSP-4 20494 is shown in white. (D) MSP-1 19 kDa 5501 HABP determined by NMR and MSP-4 20494 based predicted structures for MSP-10 31132 HABP (lemon green), MSP-8 26373 HABP (pale blue), and MSP-4 20494 (white). Yellow balls correspond to cysteines determining EGF-like domains and establishing S-S bridges. 5501 (MSP-1) and 31132 (MSP-10) located in the highly unordered or nonstructurally organized region of EGF-like domain I showed the highest RBC invasion inhibition, while 26373 (MSP-8) and 20494 (MSP-4) entirely included in the structurally ordered EGF-like domain inhibited RBC invasion (low percentage binding) in spite of them all binding with high affinity to RBCs. (E) On the basis of these GPI-anchored MSP HABP amino acid sequences and Cys alignment, it can be clearly seen that, when 5501 (MSP-1) HABP was used as template, HABPs displaying a lower RBC invasion ability, such as 26373 (MSP-8) and 20494 (MSP-4), were displaced 11 and 18 residues, respectively, toward the C-terminal region of the MSP 19 kDa-like sequences. This suggested a shift in evolutionarily and functionally related proteins toward the molecule's C-terminus and a new parasite strategy for evading the host's genetic variability and immune response, using alternative binding motif redundancy.

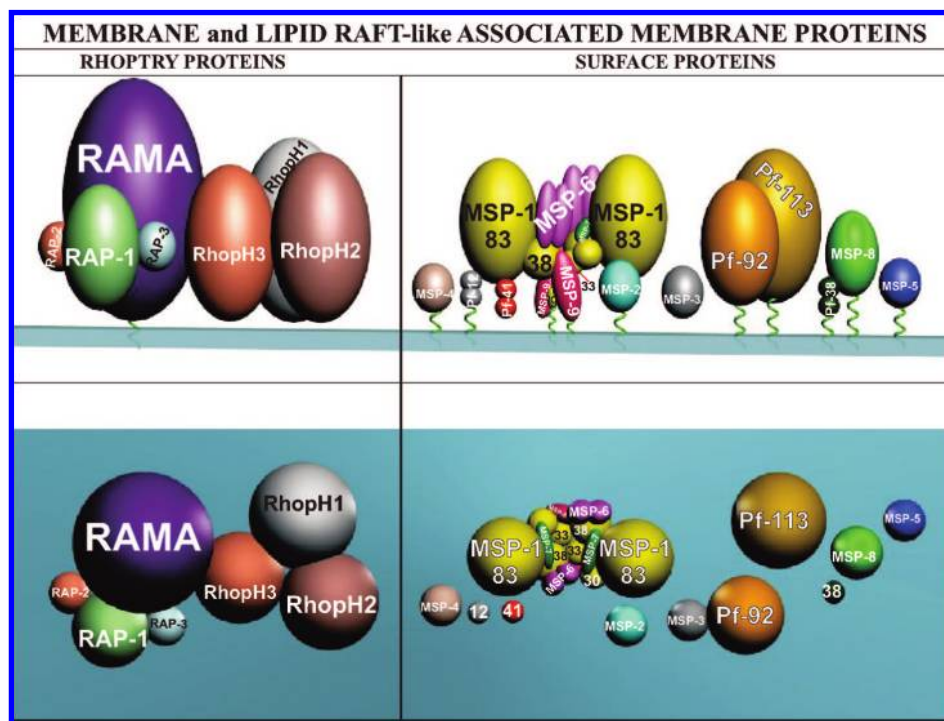


**Figure 13.** Membrane and detergent resistant lipid raft-like membrane-associated proteins (DRM). Molecule sizes are drawn at their approximate molecular weight. The figure's right-hand panel shows DRM rafts formed by MSP-1 83, 30, and 38 kDa fragments (yellow) and noncovalently associated molecules such as MSP-6 (fuchsia) and MSP-7 (green). MSP-1 33 kDa (yellow) and the only 19 kDa (yellow) fragment anchored to the merozoite membrane via GPI tail are also displayed. Other GPI tail (shown as black twists traversing the pale-green membrane) anchored membrane surface proteins such as MSP-2 (clear blue), MSP-4 (clear brown), MSP-5 (dark blue), MSP-8 (green) and Pf113 (dark gold), Pf92 (brown), Pf41 (red), and Pf12 (gray), recently identified in DRM proteome analysis, are also shown. The left-hand panel shows RAMA anchored to the membrane via a GPI tail and proteins noncovalently associated to RAMA and involved in merozoite invasion of RBC (recognized in DRM proteomes). All high (RhopH) and low (RAP-1, -2, -3) molecular weight rhoptry protein members are also shown. The top panel shows the lateral view of the hypothetical organization of these proteins; the low panel is a view from the top.

KKQIEK<sup>1378</sup>), which has been recognized by more than 30% of immune individuals living in holoendemic areas.<sup>99</sup> This HABP has bound promiscuously to HLA-DR $\beta$ 1\* 0101, 0102, 0401, and 0701 alleles,<sup>129</sup> and HABP 1585 pseudopeptides have induced antibodies able to inhibit in vitro merozoite invasion of RBCs recognizing the MSP-1 protein.<sup>130</sup>

Conserved HABP 5501 (<sup>1542</sup>QGMLNLSQHCVCV-KKQCPQNS<sup>1561</sup>) was located at the N-terminal region of the MSP-1<sub>19</sub> fragment, 15 residues upstream of the EGF-1 domain, displaying a random structure, according to its 3D structure as determined by X-ray crystallography of the 19 kDa fragment<sup>131</sup> (Figure 12) and circular dichroism (CD) studies of this peptide performed by us<sup>132</sup> (Figure 10).

Conserved HABPs 1522, 1585, and 5501 were poorly antigenic and weakly or nonimmunogenic.<sup>133–135</sup> However, when HABP sequences were carefully modified to alter peptide flexibility (with critical amino acid charge, mass, and volume being taken into account), such modified HABPs induced high antibody levels against the parasite when used as immunogens (as assessed by different immunological methods) and induced protection against experimental challenge in *Aotus* monkeys.<sup>133–136</sup>

It has been found that MSP-1 HABPs' binding to RBCs was saturable and their  $K_d$  ranged from 140 to 250 nM, with between 6 000 to 13 000 binding sites per cell. The binding of these conserved HABPs was not neuraminidase-treatment-susceptible or sialic-acid-dependent, suggesting that the RBC receptors were protein in essence.<sup>64</sup> Some evidence for this lies in the fact that the MSP-1<sub>42</sub> domain (where HABPs 1585 and 5501 were located) together with ABRA bind to band 3

on RBCs to facilitate merozoite invasion<sup>115</sup> (Figure 13), involving both the MSP-1 33 and 19 kDa fragments.

Some conserved (1513 and 1522) and variable (1582) MSP-1 HABPs have inhibited in vitro merozoite invasion of RBCs by up to 50% but have not inhibited their intraerythrocytic development,<sup>64</sup> suggesting the absence of a toxic effect on the parasite's intraerythrocytic growth.

Nuclear magnetic resonance (NMR) studies determining conserved HABP 1513, 1522, and 1585 3D structure have shown that all of them have an  $\alpha$ -helical structure,<sup>133,134,136</sup> while HABP 5501 has presented a random structure as revealed by CD (Figure 10) and NMR studies of free peptide. It should be stressed that conserved 5501 HABP displayed the same random structure that it displayed in the recombinant fragment in X-ray crystallography studies of the MSP-1<sub>19</sub> fragment<sup>131,132,135</sup> (Figures 12 and 14A, shown in white), suggesting that the 3D structure adopted by small synthetic peptides (~20 mer long) in solution is very similar to that which they display in the native molecule.

### 3.2. Merozoite Surface Protein-2 (MSP-2)

MSP-2 (PFB0300c) is a 44–55 kDa protein anchored to the merozoite surface via a GPI tail.<sup>137</sup> MSP-2 has two conserved regions located at the N-terminal (43 residues) and at the C-terminal (73 residues) plus a highly variable central region in terms of amino acid sequence and extension, flanked by nonrepeat variable sequences.<sup>138,139</sup> MSP-2 variation among different parasite strains is mainly due to

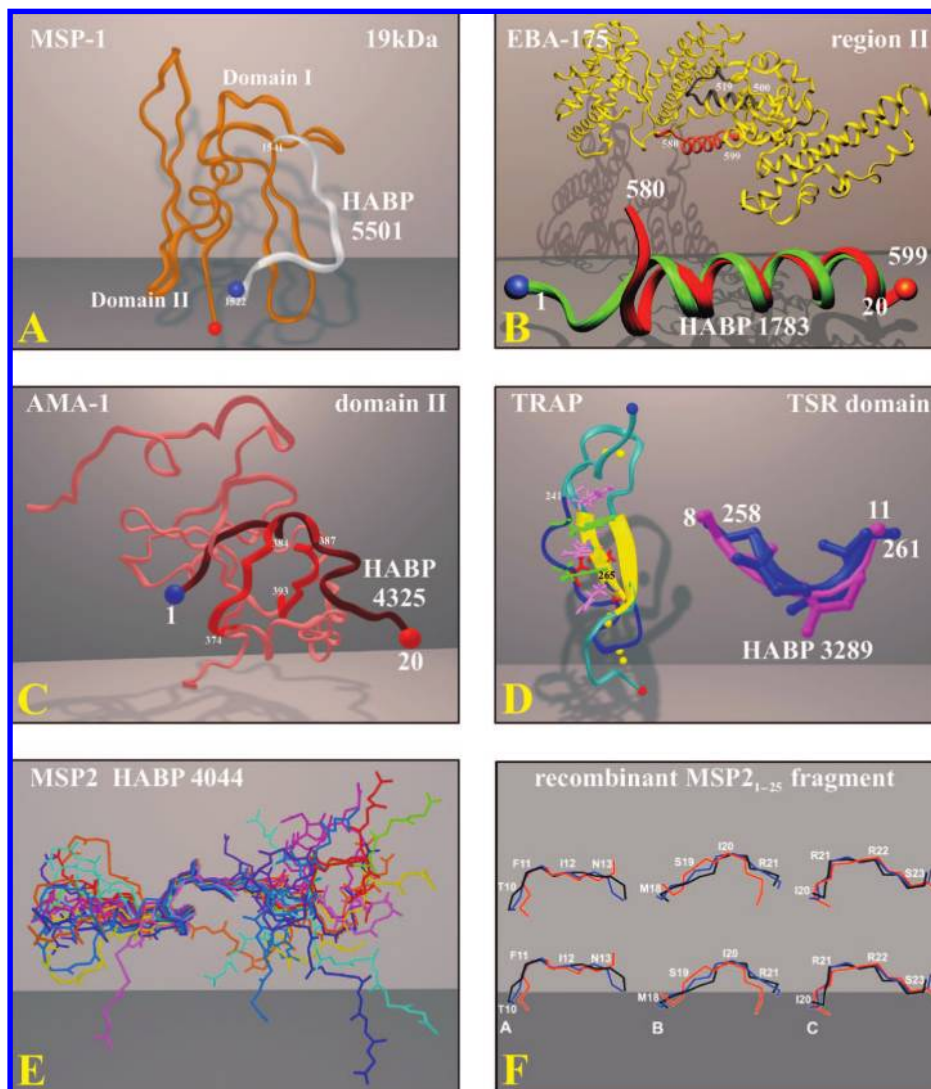


**Figure 14.** (A) 3D structure of the MSP-1 19 kDa fragment (PDB accession number 1OB1) (light brown) showing that this fragment's N-terminal region (where our HABP 5501 was located) is totally random (shown in white), confirmed by CD spectra (Figure 10) and  $^1\text{H}$  NMR analysis. (B) X-ray crystallography of recombinant EBA-175 region II fragment (PDB accession number 1ZRL) (in yellow) showing that the  $\alpha$ -helical fragment located between residues 580–589 (in red) completely corresponds to our HABP 1783 amino acid sequence. These amino acid sequences (in red) from recombinant protein and HABP 1783 (in green) displayed 0.89 Å rmsd when they were overlapped (red and dark-green structures). The secondary structure of HABP 1779 (located in residues 500–519 in the EBA-175 protein and colored in sepia) determined by CD spectra displayed a clearly distorted  $\alpha$ -helical structure confirmed in recombinant EBA-175 region II 3D structure. (C) X-ray crystallographic structure determined for AMA-1 protein domain II (in pink) (PDB accession number 1YXE) where RBC HABP 4325 was located (residues 374–393, in red) showing in this protein a short  $\alpha$ -helical structure between residues 384–387, similar to that displayed by native HABP 4325 (in dark brown) between residues 13–16. When the two structures were overlapped, they displayed a 0.99 Å rmsd. (D) 3D structure of the *P. falciparum* TRAP sporozoite protein as determined by  $^1\text{H}$  NMR (PDB accession number 2BBX) where our hepatocyte HABP 3287/3289 was located, displaying a  $\beta$ -turn structure between residues 241–265 (in dark blue), similar to our TRAP HABP 3287/3289 displaying the same  $\beta$ -turn structure between residues 8–11 (fuchsia) A 1.5 Å rmsd was determined when the two fragments were overlapped, thereby completely agreeing with our CD and  $^1\text{H}$  NMR structural determinations. (E)  $^1\text{H}$  NMR studies show that HABP 4044 displays a classical  $\beta$ -turn type III structure. (F) Stereo view of the 3D structure of the recombinant MSP-2 protein's conserved N-terminal region (residues 1–25). A  $\beta$ -turn type III was also found in such a structure, similar to our structural results corresponding to HABP 4044 determined by  $^1\text{H}$  NMR in dimethylsulfoxide (DMSO).

the presence of this large block of repeat sequences in the MSP-2 central region.<sup>139</sup>

The role of MSP-2 during invasion has still not been clarified; however, it is highly antigenic since it is recognized by immunocluster-eluted antibodies.<sup>61</sup> Antibodies against MSP-2 have inhibited merozoite invasion in a dose-dependent way but are strain-specific.<sup>140–142</sup> Antibodies recognizing the MSP-2 protein have been associated with a low risk of acquiring clinical malaria in Gambia and Papua New Guinea.<sup>143–145</sup>

Contrasting with this protection-inducing role, it has been reported that polyclonal antibodies for some MSP-2 regions

have promoted RBC invasion by more than one merozoite,<sup>146</sup> suggesting that inhibition/invasion-blocking antibodies could be induced by some MSP-2 regions. Such an immune response evasion mechanism is critical in choosing antigens for rationally designed candidates for an antimalarial vaccine. Furthermore, some regions have implicated MSP-2 in a clear skewing of the immune response toward short-lived antibody responses, such as that mediated by IgG3 subclass antibodies.<sup>147</sup>

Three HABPs have been identified for MSP-2 protein by using our synthetic peptides strategy: conserved HABP 4044 ( $^{21}\text{KNESKYSNTFINNAYNMSIR}^{40}$ ) and variable HABP

4045 (<sup>31</sup>INNAYNMSIRRSMAESKPPT<sup>50</sup>), located in the N-terminal region, and HABP 4053 (<sup>111</sup>NPNHKNAETNP-KGKGEVQKP<sup>130</sup>) located in the central variable region<sup>54</sup> (Figures 3 and 9). HABPs 4045 and 4053 binding to trypsin-treated RBCs became extremely reduced, suggesting that glycoporphins could be receptors for these HABPs.<sup>148</sup> It has also been suggested that band 3 does not play a primordial role in MSP-2 binding, since no effect was found when RBCs were treated with chymotrypsin.

HABP 4044 (<sup>21</sup>KNESKYSNTFINNAYNMSIR<sup>40</sup>) contains an eight-residue-long sequence (underlined) reported as being a B-cell epitope, which is specifically recognized by monoclonal antibodies inhibiting merozoite invasion.<sup>149</sup> It is worth noting that this peptide has induced specific anti-SNTFINNA antibodies in rabbits inhibiting *P. falciparum* merozoite invasion by more than 60%.<sup>53</sup> The SNTFINNA sequence has also been used in designing the antimalarial, multistage vaccine candidate CDC/NIIMALVAC-1.<sup>150,151</sup> The HABP 4044 sequence has also been previously reported as containing a T-cell epitope recognized by individuals exposed to malaria.<sup>101</sup>

Saturation assay analysis has revealed that there are 5 000–12 000 binding sites per cell for MSP-2 HABPs, having 200–250 nM dissociation constants ( $K_d$ ), suggesting that these peptides have high affinity for receptors present on RBC surface.<sup>54</sup> These three peptides have inhibited in vitro merozoite invasion of RBCs.<sup>54</sup>

Conserved HABP 4044 has displayed a classical type 3  $\beta$ -turn structure in our <sup>1</sup>H NMR studies<sup>152</sup> (Figure 14E); such data have been recently corroborated by another group's NMR studies with a recombinant fragment including this HABP and expressed in *E. coli* (Figure 14F), also showing this fragment's tendency to aggregate and form fibrils.<sup>153</sup>

### 3.3. Merozoite Surface Protein-3 (MSP-3)

The MSP-3 protein (PF10\_0345), also known as secreted polymorphic antigen associated with the merozoite (SPAM),<sup>154</sup> has a 48 kDa molecular weight and is derived from a variable higher molecular weight precursor protein.<sup>155,156</sup> Some evidence has suggested that MSP-3 undergoes proteolytic processing in the PV before being secreted on merozoite surface where it associates with some other merozoite surface molecules such as MAL13P1.60 and PFD0230c.<sup>154,157</sup> Polymorphic sequences are located in the MSP-3 N-terminal region, while the MSP-3 C-terminal region is highly conserved among different parasite strains.<sup>48,158,159</sup>

MSP-3 C-terminal and MSP-6 protein sequences present 85% similarity, sharing a specific ILGWEFGGG-A/V-P sequence pattern (peptide 31203 in MSP-3 and 31182 in MSP-6) and a glutamic acid-rich region.<sup>78,113,160</sup> MSP-3 has an important domain composed of three 7-residue long repeat blocks having the AXXAXXX consensus sequence, identified as an antigenic diversity site among different MSP-3 polypeptides.<sup>159</sup> The AXXAXXX motif is highly conserved, in spite of presenting variability within it and at the heptapeptide extreme. Structural analysis has revealed an  $\alpha$ -helix charged repeat structure having a coil-coil structure within the protein.<sup>161</sup> MSP-3 also contains a glutamic acid-rich region and a putative leucine zipper sequence toward the C-terminal region.<sup>154,159</sup> It has also been reported that parasites having a truncated form of MSP-3 do not localize this protein or MSP-9 on merozoite surface, thus reducing merozoite ability to invade RBCs.<sup>162</sup>

MSP-3 could be an important target for inducing antibody-mediated protective immunity, since anti-MSP-3 antibodies have blocked parasite schizogony when antibody-dependent cell inhibition (ADCI) assays have been performed.<sup>156,163</sup> It has been reported that *Saimiri sciureus* monkeys immunized with MSP-3 have been able to totally or partially control parasitaemia following experimental infection with *P. falciparum*,<sup>164</sup> while MSP-3 and glutamate-rich protein (GLURP)-specific IgG3 antibodies have been associated with inducing clinical malaria protection.<sup>165</sup> Mouse anti GLURP-MSP-3 IgG antibodies have inhibited monocyte-dependent parasite growth.<sup>166</sup>

An MSP-3 long synthetic peptide (LSP), including residues 186–276, has been used recently in a phase I clinical trial and found to be well-tolerated and immunogenic when subcutaneously administered to volunteers naturally and previously exposed to *P. falciparum* in Burkina Faso, Africa.<sup>167</sup>

Our studies of the *P. falciparum* FC27 strain MSP-3 protein have identified conserved HABPs 31193 (<sup>21</sup>NNVA-SKEIVKKYNLNLRNAI<sup>40</sup>) and 31209 (<sup>341</sup>VKEAAESIMK-TLAGLIKGNNY<sup>360</sup>) and variable HABP 31202 (<sup>201</sup>YQ-KANQAVLKAKEASSYDYI<sup>220</sup>) (Figures 3 and 9), having 120–270 nM  $K_d$ .<sup>78</sup> HABP binding ability has been seen to be susceptible to treatment with neuraminidase and trypsin and resistant to treatment with chymotrypsin, suggesting a glycoprotein-like receptor. HABPs having a functional role at the moment of invasion could be supported by the fact that all of them inhibited in vitro merozoite invasion of RBCs at 100–200  $\mu$ M concentration.<sup>78</sup> CD spectra analysis has revealed that all these HABPs displayed  $\alpha$ -helix structural characteristics (Figure 10).

### 3.4. Merozoite Surface Protein-4 (MSP-4)

MSP-4 (PFB0310c) contains an EGF-like domain in its C-terminal region. EGF-like domains contain six cysteine residues separated by characteristic spacers, which were initially identified in human EGF. It is currently known that the presence of these EGF-like domains is related to protein-protein recognition, control functions, and ion binding.<sup>17,168</sup>

The *msp4* gene encodes a 272 amino acid protein having a 40 kDa molecular mass that is characterized by a GPI binding motif for membrane anchoring. Its localization on merozoite membrane has been demonstrated by Triton X-114 partitioning and immunofluorescence. The mature protein is relatively hydrophilic, made up by 14.3% glutamic acid, 9.6% aspartic acid, 11.4% lysine, and 8.8% serine.<sup>168</sup> The MSP-4 N-terminal region consists of 15 hydrophobic amino acids, characteristic of a secretory signal sequence, while the MSP-4 C-terminal region corresponds to a typical GPI-anchor attachment signal sequence, having 19 hydrophobic residues preceded by three consecutive serine residues.<sup>168,169</sup>

The presence of a singular EGF-like domain in the C-terminal region is particularly interesting as it presents the typical cysteine residue spacing observed in MSP-1, possibly related to protein-protein interactions during merozoite invasion.<sup>168</sup> It is also worth pointing out that MSP-4 has 53% homology with a hepatic stage sporozoite surface protein (sporozoite and liver stage antigen-SALSA), which is possibly involved in sporozoite invasion of the liver.<sup>170</sup>

Only one HABP (20494, <sup>221</sup>EYVGNNRRVKCKCKEG-YKLEG<sup>240</sup>) has been located at the C-terminal end (Figures 3 and 9) within the EGF-like domain.<sup>171</sup> HABP 20494

binding was sensitive to neuraminidase and trypsin treatment, and it recognized a 52 kDa RBC membrane protein.<sup>171</sup> However, the MSP-4 HABP had low invasion inhibition, suggesting that the protein could have been involved in initial RBC-merozoite recognition or some other physiological event. CD spectra analysis has shown that this peptide displays a random structure<sup>171</sup> (Figures 10 and 12).

### 3.5. Merozoite Surface Protein-5 (MSP-5)

MSP-5 (PFB0305c) is located on trophozoite surface and on free merozoites; it contains an EGF-like domain in its C-terminal region and a putative GPI anchoring sequence. The gene encoding this molecule is located in *P. falciparum* chromosome 2, having a 272 amino acid-long open reading frame and encoding a protein of around 40 kDa molecular weight.<sup>172,173</sup> The MSP-5 sequence has two hydrophobic regions, one in the N-terminal and the other in the C-terminal end, is rich in asparagine (16.6%), and has a relatively high proportion of glutamic acid (12.1%) and serine residues (10.3%).<sup>172</sup> However, it is not so highly charged as MSP-4, as it also has large proportions of leucine (8.4%) and isoleucine (7.3%).<sup>172</sup>

Immunization with *P. yoelii yoelii* MSP-4/MSP-5 *P. falciparum* homologues has protected mice in homologous challenge.<sup>174</sup> However, elegant studies by Sanders et al. have shown that *msh-5* gene knockdown did not affect the in vitro blood-stage growth rate,<sup>18</sup> casting doubts about this protein's critical role in invasion.

Three HABPs were found in MSP-5; HABPs 20498 (<sup>21</sup>LNNKNENFLVRRRLMNDEKGY<sup>40</sup>) and 20499 (<sup>41</sup>EGGFTSKNKENGNNRNNENY<sup>60</sup>) were located in the N-terminal, and HABP 20502 (<sup>101</sup>NIQKEPEEKENSNNLDSSEY<sup>120</sup>) was located in the central region (unpublished results). No HABPs were found in the C-terminal domain (Figures 3 and 9).

### 3.6. Merozoite Surface Protein-6 (MSP-6)

MSP-6 (PF10\_0346) has a 371 amino acid sequence and 48 kDa molecular weight. MSP-6 contains a predicted signal peptide (<sup>1</sup>Met to <sup>19</sup>Asn) and a glutamic acid-rich region lying between residues 237–293 and is cleaved in <sup>161</sup>Ser to produce a 36 kDa fragment called MSP-6<sub>36</sub>. This fragment presents a hydrophilic and negatively charged sequence (211 residues) containing around 42% charged residues (23% Glu, 8% Asp, 10% Lys) and a calculated 3.96 isoelectric point (pI).<sup>113</sup> The C-terminal region of MSP-6 (MSP-6<sub>36</sub>) has great similarity with the *P. falciparum* MSP-3 C-terminal region, sharing the specific ILGWFEFGG-(A/V)-P sequence (peptides 31182 in MSP-6 and 31203 in MSP-3) and a glutamic acid-rich region.<sup>113</sup> MSP-6<sub>36</sub> forms a complex with MSP-1 and MSP-7 (MSP-7<sub>22</sub>) on the surface of merozoites (Figure 13), which are released from the parasite around the time of the RBC being invaded<sup>113,175</sup>

MSP-6 is a highly conserved dimorphic protein among several 3D7-type *P. falciparum* isolates (3D7, NF7, D10, 7G8, and HB3 strains), while MSP-6 sequences in MC, W2mef, and K1 strains (only detected in parasites from mainland Southeast Asia) are also almost identical to each other but longer than 3D7-type sequences.<sup>175</sup> The MSP-6 sequence in the K1 strain contains three blocks of extra amino acids inserted into different parts of the molecule, being 427 amino acids long, whereas 3D7-type has 371

amino acids. A slightly higher pI in K1-type molecules is related to a disproportionate increase in positively charged residues.<sup>175</sup>

Even though MSP-6's function is not yet known, it is probably involved in the invasion of RBCs and could be an important vaccine candidate. Individuals naturally infected with *P. falciparum* present MSP-6 reactive antibodies.<sup>176</sup> IgG antibodies from rabbits immunized with MSP-6 recombinant protein (3D7 strain) have inhibited merozoite (*Pf* 3D7) invasion of RBC by up to 20%.<sup>175</sup>

MSP-6-derived synthetic peptides with high binding activity to RBCs have been identified in this protein,<sup>160</sup> such as 31175 (<sup>41</sup>MYNNDKILSKNEVDNIESN<sup>60</sup>) and 31178 (<sup>101</sup>YDIQATYQFPSTSGGNNVIP<sup>120</sup>), which are located in the N-terminal cleaved and released fragment at <sup>161</sup>S, and 31191 (<sup>36</sup>IEIDSTINNLVQEMIHLSNNY<sup>380</sup>) located in the C-terminal region of MSP-6<sub>36</sub>, (Figures 3 and 9). These HABPs are probably involved in invasion since peptides 31175 and 31191 have inhibited in vitro invasion by up to 40% and peptide 31178 has inhibited in vitro invasion by up to 27% at 200 μM. CD studies determining structural elements have shown that HABP 31191 displays α-helix structural characteristics while 31175 displayed random structural features<sup>160</sup> (Figure 10).

### 3.7. Merozoite Surface Protein-7 (MSP-7)

MSP-7 (PF13\_0197) consists of 351 amino acids, having 41 kDa molecular weight and a 4.74 pI. A 27 amino acid putative N-terminal sequence precedes a 324 amino acid polypeptide (38 kDa). The protein is mainly hydrophilic (33% charged residues), having a negatively charged cluster from residue 94 to 148.<sup>112</sup> This polypeptide is the precursor of a 22 kDa protein (MSP-7<sub>22</sub>) (Figure 9) present on the merozoite surface, which is noncovalently associated with the MSP-1 complex shed from the merozoite surface following RBC invasion, even though the role of this complex formed by MSP-1 fragments with MSP-7<sub>22</sub> and MSP-6<sub>36</sub> (Figure 13) is still not completely clear. MSP-7<sub>22</sub> is then cleaved between residues <sup>194</sup>Gln and <sup>195</sup>Glu, with 18 amino acids being removed from the N-terminal extreme to produce an 18.7 kDa fragment called MSP-7<sub>19</sub>.<sup>177</sup>

MSP-7 has been seen to be highly conserved among different *P. falciparum* strains; only four substitutions have been identified when comparing the FCB-1 with the 3D7 and T9/96 strains. All substitutions have been presented in the MSP-7<sub>22</sub> C-terminal, including one of the cleavage sites leading to formation of MSP-7<sub>19</sub>.<sup>112</sup> The *msh7* gene is expressed in mature schizonts at the same time as *msh1*; deleting the *msh7* gene is reflected in altered parasite invasion of RBCs, suggesting a possible role for this protein in merozoite invasion.<sup>178</sup>

Five HABPs were found in the MSP-7 protein: 26101 (<sup>41</sup>IKNKKLEKLKNIVSGDFVGN<sup>60</sup>) in the N-terminal region, 26107 (<sup>161</sup>NLGLFGKNVLSKVKAQSETDY<sup>180</sup>) in the central region, and 26114 (<sup>301</sup>EKDKEYHEQFKNYIYGVYSYA<sup>320</sup>), 26115 (<sup>321</sup>KQNSHLSEKKIKPEEEYKKF<sup>340</sup>), and 26116 (<sup>332</sup>EKPEEEYKFFLEYSFNLLNTM<sup>351</sup>) in the C-terminal region.<sup>171</sup> HABP 26101 and 26107 localization corresponded to the N- and C-terminal extremes (respectively) of the removed 22 kDa fragment, while HABPs 26114, 26115, and 26116 were located at the 19 kDa fragment's C-terminal end<sup>171</sup> (Figures 3 and 9).

HABP 26101 binding to RBCs was not susceptible to neuraminidase, trypsin, or chymotrypsin treatment. HABP

26114 and 26116 binding was very sensitive to trypsin and chymotrypsin treatment, suggesting that the receptor could be a glycoprotein, while HABP 26107 binding was highly susceptible to just trypsin treatment, suggesting that the receptor is probably the putative “X” receptor.<sup>171,179</sup> CD spectra have revealed that HABPs 26101, 26107, 26114, and 26115 display random structures and HABP 26116 displays  $\alpha$ -helical features.<sup>171</sup>

### 3.8. Merozoite Surface Protein-8 (MSP-8)

MSP-8 (PFE0120c) is a merozoite membrane protein having a 597 amino acid long sequence in the *P. falciparum* 3D7 strain and a 69.4 kDa predicted molecular weight.<sup>17</sup> The MSP-8 sequence shares similar structural aspects with MSP-1, MSP-4, and MSP-5, including a hydrophobic signal sequence in the N-terminal (residues 1–19), a hypothetical GPI binding sequence located in the C-terminal (residues 577–597) and two EGF-like regions similar to those found in MSP-1 and MSP-10.<sup>17,180</sup> However, MSP-8 presents very little homology with MSP-1, MSP-4, and MSP-5 in regions located outside the EGF-like domains.<sup>17</sup> There are 15 cysteine residues in MSP-8, with 12 of them presumably being involved in forming disulfide bridges for EGF-like domains. Two of the other cysteines are located in the C-terminal region, which is likely to be removed during GPI attachment.<sup>17</sup> It has been reported that antibodies against the MSP-8 C-terminal recognize 98, 50, 25, and 19 kDa proteins in *P. falciparum*, whereas antibodies to the N-terminal recognize the 98 and 50 kDa bands, suggesting that MSP-8 may undergo processing in a similar way to MSP-1.<sup>17,85</sup>

MSP-8 immunofluorescence labeling of *P. falciparum* 3D7 parasites revealed a staining pattern consistent with MSP-8 surface location in ring stages, trophozoites, schizonts, and free merozoites, with the highest levels of expression being seen at 21 h during ring and trophozoite stages.<sup>17</sup>

Differently to other *P. falciparum* proteins, genetic variability studies of the complete MSP-8 gene using different laboratory isolates from different geographical regions have shown a limited degree of polymorphism at the N-terminal region. The variations were only detected in the protein's first 350 amino acids, while the C-terminal portion, including the two EGF-like domains, was completely conserved in 13 *P. falciparum* isolates.<sup>17</sup>

It has been shown that several MSP-8 regions are antigenic during natural malarial infection and that MSP-8 recombinant proteins have a structural conformation recognized by human immune sera.<sup>17</sup> MSP-8 also shows significant similarity with the protection-inducing sequence reported for the *P. yoelii* merozoite surface protein pypAg-2.<sup>181</sup> Comparing the two EGF-like domains in MSP-8 to pypAg-2 has revealed 55.3% identity in the first EGF-like domain and 58.3% identity in the second EGF-like domain, suggesting that the two proteins are homologues.<sup>17</sup>

The MSP-8 gene has recently been disrupted in *P. falciparum*, thereby validating the specificity of the antibodies used in the study by Drew et al.<sup>182</sup> and also demonstrating that MSP-8 does not seem to play an essential role in RBC cycle maintenance. This finding, together with the observation that MSP-8 is exclusively intracellular, casts doubts over this antigen's viability as a vaccine candidate. However, it is still possible that MSP-8 is involved in an early PV function, which is significant for pathogenesis in the human host.<sup>182</sup>

The function of MSP-8 remains unknown, but five amino acid sequences able to specifically bind to RBCs have been identified by using synthetic peptides. HABPs 26360 (<sup>241</sup>QNIF-STNNKGLNKYNIDNEL<sup>260</sup>) and 26361 (<sup>261</sup>KEVDALLKND-NYLILNKYHVS<sup>280</sup>) have been located in the central region, HABPs 26368 (<sup>401</sup>HEDSDIFLETYNLISGLNSN<sup>420</sup>) and 26369 (<sup>421</sup>IEETSIEKLKYAILQGKQIN<sup>440</sup>) have been located in the C-terminal, and HABP 26373 (<sup>501</sup>CPLNSN-CYVIDDEETCRCLP<sup>520</sup>) has been located in the EGF-like domain.<sup>74</sup> All the identified HABPs were conserved among the different parasite strains<sup>74</sup> (Figures 3 and 9).

MSP-8 HABPs have dissociation constants ranging from 450 to 800 nM with 200 000–800 000 binding sites per cell. Receptor proteins of around 28, 46, and 73 kDa have been identified on the RBC surface by cross-linking assays. HABPs binding to RBCs were sensitive to treatment with neuraminidase (except for HABP 26368) and chymotrypsin, while only HABP 26360 binding to RBCs was affected by trypsin treatment. HABPs 26361 and 26368 inhibited in vitro merozoite invasion of RBCs by more than 90%.<sup>74</sup> CD structure studies have shown that HABPs 26360 and 26373 presented  $\beta$ -turn and random structural elements, respectively, while HABPs 23361, 23368, and 23369 displayed typical  $\alpha$ -helical structures<sup>132</sup> (Figure 10).

### 3.9. Merozoite Surface Protein-9 (MSP-9) or Acid Basic Repeat Antigen (ABRA)

ABRA (PFL1385c) is a protein having 743 residues with an apparent 101 kDa molecular weight; it is located on merozoite surface and on iRBCs within the PV.<sup>183</sup> The ABRA protein sequence begins with a probable signal peptide containing 11 hydrophobic amino acids and a likely signal peptidase cleavage site following <sup>22</sup>Cys. This protein has two tandem repeat regions, the 8 hexapeptide T/V-N-D-E/D-E-D sequence repeats in the N-terminal and the KE and KEE sequences close to the C-terminal end.<sup>183</sup>

ABRA has a calculated 87 kDa molecular weight, which is considerably less than the apparent 101 kDa molecular weight estimated from mobility on sodium dodecyl sulfate (SDS)–polyacrylamide gels. There are nine potential N-glycosylation sites from the N-X-S/T sequence (where X represents any amino acid) in the ABRA protein; the high apparent molecular weight is, thus, probably due to glycosylation.<sup>183</sup>

ABRA is an acidic and hydrophilic protein. Its pI is 5.6, calculated from the mature protein's amino acid sequence. There are six cysteine residues in ABRA, all located in the N-terminal region. No segments in the protein indicate ABRA anchoring to the membrane (except for the putative signal peptide), consistent with the observation that ABRA is an exoantigen secreted within the PV space.<sup>183,184</sup> ABRA seems to be a highly conserved antigen, according to studies carried out with different *P. falciparum* laboratory isolates. No evidence has been presented of wide polymorphism in ABRA.<sup>50,60</sup> It has been reported that ABRA is a protease with chymotrypsin-like activity resident in its N-terminal region and has slight homology with papain, rat chymotrypsin, and a *Trichomonas vaginalis*-derived extracellular cysteine protease.<sup>185–187</sup>

Reports have indicated that ABRA could be involved in merozoite invasion of RBCs and that it specifically binds to band 3, maybe associated with MSP-1.<sup>62,115</sup> We have found that regions located between residues 121–180 and 201–240, located in the ABRA protein's N-terminal, bound to human

RBCs.<sup>71</sup> These were highly conserved HABPs 2148 (<sup>121</sup>LQSH-KKLIKALKKNIESYQN<sup>140</sup>), 2149 (<sup>141</sup>KKHLIYKNKSYN-PLLLSCVK<sup>160</sup>), 2150 (<sup>161</sup>KMNMLKENVDYIQKNQN-LFK<sup>180</sup>), 2152 (<sup>201</sup>YKSQGHKKETSQNQENNDN<sup>220</sup>), and 2153 (<sup>221</sup>QKYQEVNDEDDVNDDEEDTND<sup>240</sup>) (Figures 4 and 9), whose critical residues in invasion are underlined above. HABPs 2148 and 2149 inhibited in vitro merozoite invasion of RBCs, and its binding was trypsin- and chymotrypsin-sensitive.<sup>71</sup> HABP 2149 presented high homology with a fragment from a human cytosolic A<sub>2</sub> phospholipase (PLA<sub>2</sub>) and PLA<sub>2</sub> peptide activator; HABP 2149 also presented hemolytic and antibacterial activity,<sup>71</sup> suggesting that ABRA could be involved in merozoite release.

Kushwaha et al.<sup>188</sup> have reported that the Ncys ABRA recombinant fragment (residues 24–195) binds to intact human RBCs and solubilized protein band 3, thereby confirming and expanding our data. It has recently been reported that MSP-9/Δ1 (Δ1 corresponds to residues 77–183) and MSP-9/Δ2 (Δ2 corresponds to residues 364–528) (Figure 4, fuchsia) recombinant fragments bind to the band 3 recombinant extracellular domain named 5ABC (residues 720–761) and inhibit in vitro merozoite invasion of RBCs.<sup>116</sup> Bearing in mind that the MSP-1-derived MSP-1<sub>42</sub> fragment also binds to the band 3 5ABC fragment, the authors proposed that the ABRA protein could be acting as coligand in invasion.<sup>115,116</sup>

Other authors have shown that two ABRA-derived synthetic peptides, named AB1 (residues 19–30) and AB5 (residues 518–531), have induced a strong IgG antibody response in rabbits inhibiting in vitro merozoite invasion of RBCs by more than 90%. Such peptides were recognized by the sera of patients recovering from *P. falciparum* infection and stimulated peripheral blood mononuclear cells in convalescent patients living in endemic areas.<sup>189</sup>

Even though studies carried out with recombinant fragments have shown that the ABRA N-terminal is poorly immunogenic,<sup>190</sup> modifying HABP 2150 peptide sequence (located in the N-terminal) produced a peptide analogue able to induce partial protection-inducing immunity in *Aotus* monkeys.<sup>191</sup> This indicates the importance of the ABRA protein in the search for epitopes inducing a protective immune response in developing a multiantigen, antimalarial vaccine.

HABP 2150 three-dimensional structure (determined by NMR) presented two α-helical fragments between residues <sup>8</sup>N to <sup>11</sup>Y and <sup>13</sup>Q to <sup>17</sup>N, while HABP 2148 displayed α-helical structure (by CD). HABP 2149 showed peculiar spectral behavior, while 2152 and 2153 displayed a typical random spectrum (Figure 10).

### 3.10. Merozoite Surface Protein-10 (MSP-10)

MSP-10 (PFF0995c) has a 524 amino acid length, a theoretical 61.2 kDa molecular weight, and is anchored to the merozoite membrane via GPI. Similar to other members of the MSP family, this protein presents two EGF-like domains and undergoes post-translational processing.<sup>180</sup> The protein's sequence is characterized by an asparagine-rich region very close to the N-terminal region, similar to that of the MSP-8 protein (MSP-8-like) and a block of 8 amino acid long degenerated repeat sequences containing the (N/D)EN(I/V/N)EN sequence, comprising residues 126–173.<sup>192</sup>

Comparison with MSP-1 has revealed 31.4% identity in the first EGF-like domain and 40.0% identity in the second one. Cysteine distribution (being typical of EGF-like do-

main) was consistent with that found in other *P. falciparum* proteins presenting such domains. Studies have indicated that MSP-10 can also be processed to produce a C-terminal polypeptide containing both EGF-like domains.

Immunofluorescence assays have revealed a staining pattern for MSP-10 around the circumference of trophozoites and merozoites with both intact schizonts and free merozoites produced from schizont rupture. Triton X-114 partition properties, sequence features, and characteristic immunofluorescence appearance has led to the conclusion that MSP-10 is a merozoite surface-anchored membrane protein. Interestingly, MSP-10 has also been found to be associated (in merozoites) with an apical organelle consistent with the rhoptries or, alternatively, located over the apical polar prominence.<sup>180</sup>

When protein sequences derived from different *P. falciparum* laboratory isolates were studied, it was found that they displayed limited amino acid diversity. When the 3D7 sequence was compared to other *P. falciparum* isolates, only three variations were detected in the region comprising residues 199–515 (L<sup>325</sup>S, R<sup>406</sup>K, and H<sup>489</sup>Q). The last substitution was located within the second MSP-10 EGF-like domain. The isolates can be divided into three allele types based on their substitution pattern within this region. Type 1 (IMR143, IMR147, MAD71, NF7) has the same sequence as 3D7, type 2 (AA01, IMR144, ItG2, K1, V1) has the S<sup>325</sup>, K<sup>406</sup>, Q<sup>489</sup> sequence, and type 3 (FF7) has the S<sup>325</sup>, K<sup>406</sup>, H<sup>489</sup> sequence. All 12 cysteine residues in the sequenced region are conserved, leading to formation of both EGF-like structures.<sup>180</sup>

Interestingly, human immune serum has shown greater recognition of an MSP-10 C-terminal recombinant fragment than other regions from the same protein; such results contrast with those obtained for MSP-4, MSP-8, and MSP-1<sub>19</sub>, where it has been reported that EGF-like domains are poorly antigenic in humans.<sup>193–195</sup>

The function of MSP-10 is still not known; however, synthetic peptides covering the entire protein sequence have been used for defining three RBC binding regions.<sup>196</sup> HABPs 31121 (<sup>201</sup>KKEEDLIEAFFPFILKLDNY<sup>220</sup>) and 31122 (<sup>221</sup>ESLSLDNKYDDYYNLPNDHN<sup>240</sup>) are located in the central region, and HABP 31132 (<sup>421</sup>KCGPNSRCYIVEKD-KEQCRC<sup>440</sup>) is located in the EGF-like domain (Figures 4 and 9). HABPs 31121, 31122, and 31132 have inhibited in vitro merozoite invasion by 70%, 45%, and 65%, respectively.<sup>196</sup> Our results have shown that MSP-10 HABPs specifically and saturably interact (*K<sub>d</sub>* from 130 to 600 nM) with 3 RBC surface proteins having 36, 50, and 77 kDa molecular weights and 4 000 to 26 000 binding sites per cell.<sup>196</sup>

CD spectra analysis confirmed that HABP 31132 had a random structure, similar to that displayed when superimposing this structure on its corresponding N-terminal structure from peptide 5501 in the MSP-1<sub>19</sub> domain. HABP 31122 also displayed a random structure by CD, while HABP 31121 showed a clearly α-helix structure (Figure 10).

MSP-10 HABP 31132 presented homology with MSP-8 HABP 26373, MSP-4 HABP 20494, and MSP-1 HABP 5501, suggesting the existence of a similar conserved RBC binding motif in these proteins and that this domain has a similar or equivalent biological function in the four different proteins (Figures 10 and 12E).<sup>196</sup> Molecular modeling studies between MSP-1 19 kDa fragment 3D structure (determined by X-ray crystallography) and MSP-1, MSP-4, MSP-8, and

MSP-10 conserved HABPs 5501, 20494, 26373, and 31112 have been done to compare their 3D structures and correlate their localization and configuration in MSP-1 19 kDa structure with their RBC invasion inhibition ability. The 6  $\beta$ -sheets, the 7- $\beta$  turns, and the disulfide bridges stabilizing the structure between residues Cys6–Cys22, Cys7–Cys18, Cys11–Cys26, and Cys30–Cys41 located in the EGF-like domain I were identified in the MSP-1 19 kDa fragment (Figure 12).

Molecular modeling and energy-minimization studies revealed a hierarchy of RBC invasion inhibition for these HABPs that correlated very well with their structural localization and configuration. The two HABPs displaying the highest invasion-inhibition activity (MSP-1 5501 and MSP-10 31132) had disulfide bridges between Cys-7 and Cys-18 (5501) and between Cys-6 and Cys-22 (31132), while those having low inhibitory activity had their disulfide bridges between the cysteine residues located further back in the structurally configured or ordered EGF-like domain I in such a way that MSP-8 26373 had the S–S bridge between Cys-11 and Cys-26 and MSP-4 20494 had it between Cys-12 and Cys-28.

The data clearly showed that, despite the fact that all these peptides bound with high affinity to RBCs, only those located in the N-terminal unordered region located between Cys-7 and Cys-18 and between Cys-6 and Cys-22 were highly relevant in RBC invasion, stressing the importance of localization in these HABPs' functional activity and the structural configuration determined by these intracysteine domains (Figures 12C and 12D). Such functional and structural data suggest that these GPI-anchored EGF-like bearing MSP proteins could use their corresponding binding motifs redundancy as alternative routes for invasion or immune response distracters.

### 3.11. Glycophorin Binding Protein-130 (GBP-130)

GBP-130 (PF10\_0159) is a merozoite surface protein consisting of a charged, 225-residue-long N-terminal region and 11 50-residue-long repeat sequences.<sup>197,198</sup> The protein is recognized by merozoite immunocloner-eluted antibodies and binds to the RBC surface. GBP-130 binding to RBCs seems to be mediated by the repeat sequences, since this region binds to glycophorin A (GpA), independently of sialic acid, and antibodies recognizing this region have inhibited merozoite in vitro invasion of RBCs.<sup>199</sup>

Immunizing splenectomized *Saimiri* monkeys with parasite proteins (GBP-130 being among those having the greatest concentration) has induced protection-inducing immunity against *P. falciparum*.<sup>200</sup> Immunising *Aotus* monkeys with DNA encoding a recombinant protein containing 3 of the 50 amino acid long repeat regions has induced high antibody titers. However, protection-inducing immunity has not been induced on monkeys intravenously challenged with *P. falciparum*-infected RBCs, and sera from immunized *Aotus* monkeys have not inhibited parasite development.<sup>201</sup>

Our studies have shown that peptide 2220 (<sup>701</sup>FYKILT-NTDPNDEVERDNAD<sup>721</sup>) binds to RBC surface with high affinity (Figure 4) and does so independently of sialic acid. The binding could be via GpA and/or GpC protein moieties, according to the binding presented when RBCs were treated with trypsin.<sup>68</sup> This peptide has inhibited in vitro merozoite invasion of RBCs by up to 90% but did not inhibit parasite development. The peptide sequence forms part of the 50

amino acid long repeat region, which is recognized by antibodies inhibiting merozoite in vitro invasion of RBCs.<sup>199</sup>

This protein has been found to be involved in protein trafficking between the merozoite's endoplasmic reticulum and the PV, through one of the mechanisms involving the use of consensus amino acid sequences named *Plasmodium* export elements (PEXEL) used for molecular trafficking between the merozoite, the RBC cytoplasm, and the external environment.<sup>202,203</sup>

CD analysis has revealed that peptide 2220 has random structural elements (Figure 10).

### 3.12. Serine Repeat Antigen-5 (SERA-5)

The serine repeat antigen-encoding gene is located in *P. falciparum* chromosome 2, with this being the fifth gene from a cluster of 9 homologous genes shaping the SERA family.<sup>204</sup> This family consists of 8 open reading frames grouped in tandem within chromosome 2 (designated SERA-1 to SERA-8) and a ninth homologous gene located in chromosome 9. All the homologues were differentially transcribed in trophozoite and schizont stages containing cysteine protease (SERA-6, -7, and -8) or serine protease motifs (SERA-1 to -5 and -9) having a typical cysteine protease structure, suggesting that this protein could belong to this enzyme family. However, catalytic activity has not been well-established.<sup>205</sup> SERA-5 has chymotrypsin-like proteolytic activity-processing substrates downstream of aromatic residues, with activity being blocked by the serine protease inhibitor 3,4-diisocoumarin. SERA-5 and -6 have characteristic papain-like folding; catalytic clefts and the catalytic triad are appropriately located in each one.<sup>206</sup>

Studies carried out with detergent-resistant membranes (DRMs) using Triton X-100 have shown that SERA proteins are associated with some of the proteins anchored to the membrane by an as yet to be established mechanism.<sup>114</sup> Gene-disruption experiments have shown that, whereas genes encoding SERA-2, -3, -7, and -8 could be disrupted without an obvious deleterious effect on parasite growth, genes encoding SERA-4, -5, and -6 cannot.<sup>204</sup>

SERA protein (also known as p126 or serine-rich protein, SERP) located in trophozoite and schizont PV is a 989 residue long, highly conserved 111 kDa protein.<sup>207</sup> SERA is produced in large quantities at the end of the asexual cycle.<sup>207</sup> Following its synthesis, the protein undergoes proteolytic processing, producing shorter 50, 47, and 18 kDa fragments (Figures 4 and 9).<sup>208</sup>

The 47 kDa fragment is processed in turn into two 25 kDa fragments remaining bound to the 18 kDa fragment by disulfide bonds; these are associated with the merozoite membrane.<sup>209</sup> The 47 kDa N-terminal fragment has been subjected to extensive immunological and biochemical characterization.<sup>210–212</sup> It contains a B-cell epitope that is the target for specific antibodies inhibiting the parasite's invasion of goats and murines.<sup>207,213–220</sup> Murine inhibitory monoclonal antibody mAb 43E5 recognizes the P47 fragment; such epitopes contained in P47 have produced significant protection against experimental challenge with *P. falciparum* in *Aotus* and *Saimiri* monkeys.<sup>210,211</sup> A positive correlation has recently been found between naturally induced antibodies against the *P. falciparum* SERA 47 kDa domain and progressive protection-inducing immunity in adults and children in endemic areas.<sup>221,222</sup>

Mouse monoclonal antibodies directed against SERA N- and C-terminal regions and against the complete protein have

inhibited in vitro merozoite invasion of RBCs.<sup>214,215,218</sup> It has been reported that SERA N-terminal specific antibodies bind to merozoites at the moment of schizont rupture and, therefore, inhibit merozoite invasion of RBCs.<sup>219</sup> Some epitopes inducing inhibitory antibodies are located in the 17–165 residue region.<sup>216</sup> It has also been reported that monoclonal antibodies and affinity-purified human antibodies directed against the SERA protein can act in cooperation with blood monocytes to inhibit a large percentage of *P. falciparum* development in vitro.<sup>223</sup>

The 50 kDa fragment is completely secreted in culture medium and is not present on merozoites. This fragment contains a papain-like cysteine-protease domain, present in the central region of all 9 members of the SERA family, except for SERA-5, where the active cysteine site has been replaced by serine. Even though this domain's role in the SERA protein family remains unknown, it is probable that this soluble fragment participates in releasing merozoites during the rupture of the PV or iRBC membrane.<sup>224</sup> These processing events occur within the parasitised RBCs in the stage prior to schizont rupture.<sup>208</sup> Protection against malaria has been associated with SERA-induced immunity.<sup>210–212,221,222</sup> SERA is recognized by immunocluster-eluted antibodies.<sup>60,61</sup>

The SERA protein binds to human and mouse RBC membranes, inverted vesicles, and intact mouse RBCs.<sup>225,226</sup> Our studies with synthetic peptides have led to determining seven SERA protein HABPs that specifically bind to RBCs, having 150–1 100 nM  $K_d$ . Six HABPs have presented conserved sequences: 6725 (<sup>141</sup>YLKETNNAISFESNSGSLEKK<sup>160</sup>), 6733 (<sup>321</sup>YALGSDIPEKCDTLASNCFLS<sup>340</sup>), 6737 (<sup>401</sup>YDNILVKMFKTENNDKSELI<sup>421</sup>), 6746 (<sup>581</sup>DQGNCDTSWIFASKYHLETI<sup>600</sup>), 6754 (<sup>741</sup>YKKVQNLGDDTADHAVNIVG<sup>760</sup>), and 6762 (<sup>901</sup>NEVSERVHVYHILKHIKDGK<sup>920</sup>) (Figures 4 and 9). Three peptides (6725, 6727, and 6733) were located in the 47 kDa fragment. The area corresponding to the 50 kDa fragment contained peptides 6737, 6746, and 6754, while peptide 6762 was located in the 18 kDa fragment. We have reported that peptides 6725 and 6737 interact with some 17 and 35 kDa proteins on the RBC surface.<sup>227</sup> HBP binding was not affected by enzymatic treatment of RBCs; similar results have been reported when binding was done with the complete protein.<sup>225,226</sup> Interestingly, HBP 6727 (<sup>181</sup>VRGDTEPISDSSSSSSSS<sup>200</sup>) contains the RGD motif in its sequence; this has been reported as being an adhesion motif to fibronectin.<sup>228,229</sup>

HBP 6725 shared its sequence with a peptide that induced antibodies recognizing native SERA protein in mice (FESNSGSLEKKKYVKLPSNG), indicating that this sequence (or part of it) was exposed to the immune system. Monkeys immunized with a SERA fragment (residues 24–285), including HABPs 6725 and 6727, or with the 18 kDa fragment including HBP 6762 have induced protection against experimental infection with *P. falciparum* in *Aotus* monkeys.<sup>210–212</sup>

Replacing some critical amino acids in the peptides' sequences has modified their 3D structure and induced immunogenicity and protection against *P. falciparum* challenge in *Aotus* monkeys, suggesting that such modifications made to high binding peptide sequences allows a better fit with immune system molecules. CD studies determining structural characteristics have shown that HABPs 6733, 6737, 6746, and 6762 present  $\alpha$ -helix structural features<sup>132</sup> (Figure 11); this was later confirmed by <sup>1</sup>H NMR studies.<sup>133,230</sup>

### 3.13. Lipid Raft-Associated *Plasmodium falciparum* Cys6 Peptide Family

The Cys6 family represents a very recently identified group of proteins that is present on asexual-stage (merozoites) and sexual-stage (gametocytes) parasite surfaces.<sup>231</sup> All Cys6 family proteins present a conserved cysteine residue pattern in their primary sequence, forming a unit that is repeated in two structurally similar domains, in spite of having different lengths and characteristics.<sup>232</sup> The group of asexual-stage proteins belonging to the Cys6 family (Pf12, Pf38, Pf41, Pf92, and Pf113) has been recently validated as being merozoite membrane proteins associated with other surface proteins in raft-like lipidic structures via confocal immunofluorescence microscopy studies and solubilization detergent-resistant membranes (DRM), such as Triton-X.<sup>114,232</sup>

The PFF0615c gene encoding the 39.4 kDa Pf12 protein has been isolated and expressed in COS7 cells.<sup>233</sup> Pf12 has been located on merozoite surface anchored by a GPI domain at the C-terminal end; it has been shown to be recognized by antibodies from naturally infected patients.<sup>233</sup> HBP 33625 (<sup>101</sup>VIGSSMFMRRSLTPNKINEV<sup>120</sup>) located in the N-terminal region in domain 1 and 33633 (<sup>261</sup>MDHYNNTFYSLPLSLISDNW<sup>280</sup>) in the C-terminal region in domain 2 were found in Pf12 protein (Garcia et al., submitted) (Figures 4 and 9).

The 40.6 kDa Pf38 protein is encoded by the previously described PFE0395c gene. Prior studies have shown that this protein expressed on gametocyte and merozoite surface is anchored by a GPI tail.<sup>114,231,232</sup> Pf38 has shown reactivity with antibodies from humans exposed to malaria and has been located in the apical organelle extreme in early schizonts.<sup>114</sup>

Two HABPs have been found for protein Pf38: 33645 (<sup>141</sup>VLRIHISNGVLRKIPGCDNF<sup>160</sup>) and 33648 (<sup>201</sup>YSIKPDGCFNSVYVKRYPN<sup>220</sup>), both located in domain 2, presenting 35–45% hydrophobic residues while 25% of these peptides' residues were charged (Garcia et al., submitted) (Figure 9).

The Pf41 protein encoded by the PFD0240c gene does not have a GPI domain, and its location on the membrane is subject to noncovalent but strong interactions with other GPI-anchored merozoite membrane proteins. Antibodies present in immune human sera have recognized the central Pf41 fragment expressed in *E. coli*.<sup>114</sup> Four Pf41 HABPs were found: 33708 (<sup>161</sup>ALNRFKMKDLKFFNDQAD<sup>180</sup>), 33709 (<sup>181</sup>NTTKLNLPKSLNIPNDILNY<sup>200</sup>), 33713 (<sup>261</sup>AGKVNNKVKIQGKPGELVG<sup>280</sup>), and 33715 (<sup>301</sup>LHKNKVTDLKTLIPGYASYT<sup>320</sup>). The first two HABPs mentioned above were found in the protein's central region outside both domains, while the other two peptides were found in the C-terminal region in domain 2 (Garcia et al., submitted).

The Pf92 protein (PF13\_0338) was initially detected on blood-stage parasites' DRMs.<sup>114</sup> It has a molecular weight of around 90 kDa, has a GPI anchoring domain at its C-terminal extreme,<sup>18</sup> and is located on the merozoite surface.<sup>114</sup> The mature form of the protein has 14 cysteine residues that may form 7 disulfide bridges.<sup>18</sup>

Six HABPs have been identified in Pf92, five of them in the protein's central region: 33667 (<sup>221</sup>RLSDYGGKILVKGTAQNLN<sup>240</sup>), 33672 (<sup>321</sup>FVLAPDEMVFYH-GNEKKN<sup>340</sup>), 33675 (<sup>381</sup>KTCKVPSSHLKYSSDGLYKL<sup>400</sup>), 33677 (<sup>421</sup>LSDLNNKYHTTIKTRVINK<sup>440</sup>), and 33680 (<sup>481</sup>YIRNHIDLDFPFDTDTVKLY<sup>500</sup>). 33689

(661GTAMESLLYLNNNNVKKLID<sup>680</sup>) has been located toward the C-terminal extreme (unpublished results).

The Pf113 protein (PF14\_0201), having a predicted 112.5 kDa molecular weight, presents a putative GPI anchoring domain at its C-terminal extreme.<sup>18</sup> It also has a cysteine-rich region in its N-terminal and a repeat region in its C-terminal.<sup>18</sup> The same as Pf92, Pf113 was initially detected on DRMs.<sup>114</sup>

Pf113 protein has 7 HABPs, two of them located in the cysteine-rich region in its N-terminal: 33723 (<sup>81</sup>YFFEYEL-RKKTQSFNRKNSI<sup>100</sup>) and 33728 (<sup>181</sup>DNNKECLIDPLD-VQKNLLNEY<sup>200</sup>). The other five HABPs were located in the protein's central region: 33740 (<sup>421</sup>ASLKETMNKIDTIEK-KIEEFY<sup>440</sup>), 33745 (<sup>521</sup>NYRRRKRITELRKILVEKLR<sup>540</sup>), 33746 (<sup>541</sup>ILYLEKNLNFNTQASCIKSY<sup>560</sup>), 33748 (<sup>581</sup>RLKENKDYDVVSSIIQHLDN<sup>600</sup>), and 33749 (<sup>601</sup>VDAN-KKKKWL THERILKKLQY<sup>620</sup>) (unpublished results).

Enzymatic treatment revealed possible binding between Pf12 and Pf38 HABPs and GpA, GpB, and GpC since the binding of HABPs 33625 and 33633 was sensitive to all enzymatic treatment. HABP 33645 lost its binding ability on treating RBC with neuraminidase and chymotrypsin, while Pf41 HABP 33708 and 33709 binding was affected by neuraminidase and trypsin treatment. Moreover, other receptors could be involved in HABP–RBC interactions since HABP 33648 binding was sensitive to chymotrypsin and trypsin treatment of RBCs, suggesting a band 3 protein-like receptor; HABP 33715 binding was only reduced when RBCs were treated with neuraminidase, indicating the putative “Y” as possible receptor. Pf41 HABPs 33713 and 33715 binding became increased by enzymatic treatment, indicating the existence of a cryptic receptor for these peptides.

CD studies have shown that HABP 33625 from Pf12, 33709 from Pf41, and 33648 from Pf38 displayed typical  $\alpha$ -helix structural elements in part of their sequences while HABPs 33645, 33713, and 33715 had greater random coil tendency and low helical content. HABP 33708 displayed a distorted  $\alpha$ -helical configuration, and HABP 33633 contained a mixture of structural elements (none of them predominant).

## 4. Microneme Proteins

### 4.1. Erythrocyte Binding-like (EBL) Family

Parasite ligands recognizing host RBC receptors represent a crucial step in invasion and are presumed necessary for junction formation. Parasites such as *Plasmodium knowlesi* and *P. vivax* depend on recognizing a specific receptor (i.e., Duffy blood-group antigen). *P. knowlesi* merozoites bind to human RBCs, whether they have the Duffy blood-group antigen or not. However, the parasite cannot form the junction and invade if the Duffy blood-group antigen receptor, at least, is not present.<sup>234</sup>

Adams et al.<sup>21</sup> have proposed that Duffy binding proteins (DBPs) and sialic acid binding proteins form part of a family of genes having structurally, evolutionary, and functionally related products based on gene structure and amino acid sequence homology, bearing in mind the level of conservation in amino acid sequence (especially that of cysteines) located in regions 5' and/or 3' cysteine-rich regions between *P. vivax* proteins and 3 *P. knowlesi* DBPs.<sup>21</sup> Duffy binding-like (DBL) domains have been defined in *P. falciparum* proteins and in other species based on the high homology

between the sequences of amino acids from regions located in these proteins' N-terminal fragments.<sup>21</sup>

Parasites such as *P. falciparum* can use alternative receptors in the absence of a primary receptor (i.e., GpA) or when this receptor is blocked; *P. falciparum* clones or isolates have developed the ability to use alternate invasion routes. These routes use different receptors such as GpA, GpB, GpC, band 3, and unknown receptors (X, Y, Z). It is thought that using such alternative invasion routes is associated with the expression of different or single *ebf* products or both.<sup>20</sup>

Trafficking to the micronemes of the most abundant *ebf* family proteins (EBA-175, EBA-140, and EBA-181) is dependent on the carboxyl-terminal-cysteine-rich domain but not the transmembrane nor the cytoplasmic tail, with the latter being essential for invasion but not for trafficking.<sup>235,236</sup>

#### 4.1.1. Erythrocyte Binding Antigen-175 (EBA-175)

The *P. falciparum* FCR3 isolate EBA-175 protein (the first described) (GenBank No. Accession AAA29600) is a 1 463 amino acid long microneme-soluble protein obtained from culture supernatant following schizont rupture.<sup>237</sup> The gene encoding the EBA-175 protein belongs to the family of *ebf* genes encoding proteins involved in specific recognition of host-cell receptors, including *P. vivax* and *P. knowlesi* DBL proteins.<sup>20</sup> EBA-175 has limited polymorphism among the different strains. An extra amino acid sequence (segment F) is displayed in the FCR3 strain, which is not found in the CAMP strain (segment C).<sup>43,238–240</sup> This allele region has been found to be conserved in all cultured and wild strains studied to date. It is thought that the protein acts as a bridge between the merozoite and the RBC at the moment of invasion.<sup>241</sup> EBA-175 binds to sialic acid on the mucin domain of GpA, preferentially to Neu5Ac( $\alpha$ 2-)-Gal-(Neu5Ac( $\alpha$ 2,6)Gal) on O-linked tetrasaccharides,<sup>242–244</sup> and is probably involved in forming a junction between the RBC and the apical portion of the merozoite just before invasion.<sup>245</sup> This step forms a key part of RBC invasion.

It has been postulated that EBA-175 binding to RBCs occurs in two steps. The complete protein first binds to the RBC, depending on the presence of sialic acid and the GpA skeleton on RBC.<sup>244,246</sup> EBA-175 is cleaved afterward by endogenous proteases in a second step, producing a 65 kDa fragment located between CAMP strain amino acids 354 and 1061 including the C-terminal portion of region II (RII). RII is a highly conserved EBA-175 616 amino acid fragment consisting of 2 Cys-rich regions (F1 and F2) homologous to the DBL domain. It has been shown that F2 alone can bind to RBCs but that F1 by itself cannot.<sup>244</sup>

It has been reported that the EBA-175 protein is functionally active in invasion of RBCs, independent of whether the process is sialic acid dependent.<sup>247</sup> It has been found that the invasion routes used by the merozoite could be independent of EBA-175, since *P. falciparum* strains in which the EBA-175 gene has been disrupted have shown normal human and animal RBC invasion rates, whether enzymatically treated or not.<sup>37</sup>

The complete culture supernatant isolated EBA-175 protein, recombinant fragments (including RII), and peptide 4 (comprising amino acids 1062–1103) are recognized by merozoite immunocloner-eluted antibodies.<sup>43,60,248</sup> All these recombinant fragments or synthetic peptides induce antibodies that are able to inhibit merozoite invasion of RBCs.<sup>43,44,246</sup> Interestingly, RII-induced antibodies may also interfere with merozoite invasion routes that do not involve sialic acid.<sup>45</sup>

Antibodies recognizing the EBA-175 region comprising amino acids 1085–1096 are able to inhibit merozoite invasion of RBCs; however, this sequence is weakly antigenic during *P. falciparum* infection in humans.<sup>249</sup>

Six conserved HABPs have been found using peptides covering the whole EBA-175 protein sequence in RBC binding assays<sup>67</sup> (Figures 5 and 9); their critical binding residues (underlined) have been identified. One of them, HABP 1758 (<sup>80</sup>KSYGTPDNIDKNMSLIHKHN<sup>99</sup>), has inhibited merozoite invasion but not their development.<sup>67</sup>

HABPs 1779 (<sup>500</sup>NIDRIYDKNLLMIKEHILAI<sup>519</sup>), 1783 (<sup>580</sup>HRNKKNDKLYRDEWWKVIK<sup>599</sup>), 1814 (<sup>1200</sup>ODRN-SNTLHLKDYRNEEMERH<sup>1219</sup>), 1815 (<sup>1220</sup>YTNQNINISQER-DLQKHGFH<sup>1239</sup>), and 1818 (<sup>1280</sup>NNNFNNIPSRYNLYD-KKLDL<sup>1299</sup>) have 60–180 nM  $K_d$ , showing the ligands' high affinity for their respective receptor molecules. Hill coefficients ( $n_H$ ) greater than 1 showed positive cooperativity, suggesting the ability to facilitate a second ligand's binding. 7 000–15 000 receptor sites per RBC were calculated for these HABPs when saturation was analyzed.<sup>67</sup>

Our studies have reported three binding regions. The first was in the N-terminal portion including peptide 1758 (located in region I); the second was in region II, more specifically in the so-called 5'Cys fragment F2 region (containing peptides 1779 and 1783); and the third was close to the 3'Cys-rich region (including HABPs 1814, 1815, and 1818).

HABPs 1758 and 1818 receptor sites on RBCs seemed to be cryptic according to results obtained from enzymatically treated RBC binding assays. HABPs 1814, 1815, and 1818 were located in regions recognized by merozoite immunocluster-eluted antibodies (indicating that these sequences are exposed during invasion) and by antibodies inhibiting merozoite invasion of RBCs.

HABPs 1779 and 1783 were located in the F2 RBC binding region, and anti-F2 antibodies have inhibited merozoite invasion of RBCs.<sup>244</sup> HABPs 1779 and 1783 have partially inhibited region II binding to RBCs; however, a mixture of HABPs 1779 and 1783 better inhibited merozoite invasion of RBCs than any single peptide.

The 3D structure of the EBA-175 protein's region II has been determined by X-ray crystallography. RII dimer organization has revealed two prominent channels containing four out of six glycans observed at binding sites. Each monomer consisted of two DBL domains (F1 and F2) where F2 formed a more prominent channel and allowed better contact with the glycans. Since the cocrystallized glycans were bound to the dimer's interface making contact with both monomers, then the dimer could have possibly been assembled around the GpA extracellular domain.

Crystallographic analysis of RII has shown that HABPs 1779 and 1783 form part of the channels formed by the dimer, with HABP 1783 forming part of the F2 cavity dimerization interface (Figure 14B). Both interact with the glycans with which this fragment was cocrystallized. This confirms our findings that HABPs 1779 and 1783 are EBA-175 ligands used to interact with these sialoglycoproteins.<sup>242</sup>

It has been proposed that peptide 1783 could be binding directly to GpA and, therefore, encapsulating glycophorin.<sup>242</sup> Replacing critical amino acids also allowed more immunogenic peptides to be produced, which were able to protect monkeys against experimental challenge with *P. falciparum*,<sup>250</sup> probably blocking these HABPs' interaction with the RBC receptors and, thus, blocking invasion or avoiding dimerization by EBA-175 RII binding.

NMR and CD studies have shown that HABPs 1758, 1779, 1783, and 1815 have an  $\alpha$ -helical structure, while 1818 presents a random structure (Figure 10). The perfect overlap of HABP 1783 structure (obtained by NMR) with EBA-175 recombinant RII residues 580–599 (obtained by X-ray crystallography<sup>242</sup>) strongly supports the idea that short synthetic peptides (~20 mer long) might resemble their original conformation in native proteins. This also supports using short peptides for clearly defined functional structures in biological molecules, such as binding to host cells or immunological activities such as antibody or cellular immune reaction induction.

Insoluble HABP 1779 (at the protein concentration required for NMR analysis) presented a distorted  $\alpha$ -helical structure in CD studies (Figure 10), very similar to that adopted by the residues (500–519) where this HABP is located in the RII molecule, once more confirming our original assumption that short peptide structures (~20 mer long) represent excellent tools for intimately analyzing receptor–ligand interactions in merozoite–RBC invasion (Figure 14B).

Peptide 1799 (sharing its sequence with peptide CP-1)<sup>43</sup> and peptides 1807 and 1808 (also sharing their sequence with peptide 4) have presented high, nonspecific binding ability. Conserved HABPs 1758, 1779, 1783, 1815, and 1818 were neither antigenic nor immunogenic, but molecular modifications made for better adjustment with MHC-II molecules have made these peptides become immunogenic, having partially protection-inducing immunogenicity against experimental infection caused by *P. falciparum* parasites in *Aotus* monkeys.<sup>81,250–252</sup>

#### 4.1.2. Erythrocyte Binding Antigen-181 (EBA-181) or JESEBL

EBA-181 (PFA0125c) is a 1 567 amino acid protein having a primary structure characteristic of *eb1* family members. This protein consists of a hydrophobic N-terminal signal sequence, two cysteine-rich regions in the N-terminal extracellular domain (F1/F2 DBL), a 3' Cys-rich domain, a transmembrane domain, and a short cytoplasmatic C-terminal tail. This protein is found in micronemes and is coexpressed at the same time as EBA-175. EBA-181 expression differs among *P. falciparum* strains. Its primary structure (including intron/exon structure) and the fact that EBA-181 binds to RBCs suggests that it plays a role in merozoite invasion and is likely to function in an analogous manner to EBA-175 and EBA-140 as an alternative parasite ligand.<sup>20</sup> Targeted disruption of the *eba-181* gene has had no effect on the parasite's invasion phenotype, suggesting that it might act as an alternate ligand.<sup>236</sup>

We have reported that EBA-181 presents five amino acid sequences binding to RBCs defined by HABP 30030 (<sup>81</sup>KKVKIISRPVENTLHRYPVS<sup>100</sup>), which binds to a receptor on the RBC, which is trypsin-resistant but susceptible to chymotrypsin (different to GpB).<sup>253</sup> HABP 30031 (<sup>101</sup>SFL-NIKKYGRKGEYLNRNSF<sup>120</sup>) was located before the DBL/F1 domain and HABPs 30045 (<sup>381</sup>DIDFKPFFEFYGKY-EEKCM<sup>400</sup>), 30051 (<sup>501</sup>LLWKKHGTILDNQNACKY-IN<sup>520</sup>), and 30060 (<sup>681</sup>KDRKLFSLAKDKNVTTFLKEY<sup>700</sup>) were located in the DBL/F2 domain (where the RBC binding region is located) (Figures 5 and 9). None of these HABPs bound to GpA or GpB, and there were at least four different receptors for these HABPs according to their susceptibility

to treatment with trypsin, chymotrypsin, or neuraminidase. These HABPs have inhibited in vitro merozoite invasion of RBCs.<sup>253</sup>

EBA-181 has presented very limited polymorphism in the RBC binding domain, having only five amino acid residue changes (K<sup>359</sup>R, D<sup>363</sup>V, I<sup>414</sup>N, Q<sup>443</sup>K, and K<sup>637</sup>N) in the different strains. Such variations have modified EBA-181 RBC specific binding according to results obtained using enzyme-treated RBCs.<sup>41</sup> However, such variations have not occurred in any of the HABPs dealt with here.

CD studies for all these peptides have revealed  $\alpha$ -helical structures for conserved HABPs 30030, 30031, 30045, 30051, and 30060 in the presence of trifluoroethanol (30%, TFE) (Figure 10). This has been confirmed by using CONTINLL, CDSSTR, and SELCON3 software to analyze their secondary structures.

#### 4.1.3. Erythrocyte Binding Antigen-140 (EBA-140) or BAEBL

EBA-140 (MAL13PI.60), also known as BAEBL or PfEBP-2, has only shown 24% identity with EBA-175; however, it shares structural and sequential homology with EBA-175 and EBA-181 (JESEBL).<sup>20,41,254,255</sup> Such homology also includes the extracellular domain having a signal peptide,<sup>256</sup> a transmembrane domain,<sup>257</sup> a putative cytoplasmic domain,<sup>38</sup> two cysteine-rich domains with eight conserved cysteines in the F1 domain, and localization in the micronemes.<sup>20,21</sup> All these characteristics have led to it being proposed that these antigens are participating in invasion, whether by producing alternative invasion routes or mediating invasion mechanisms.

Maximum EBA-140 expression has appeared during late schizont development stages, according to IFA detection. Subcellular IFA localization studies have shown that EBA-140 is colocalized with EBA-175 at the merozoites' apical end.<sup>256</sup>

EBA-140 protein binds to GpC (residues 14–22) on RBC surface and is involved in an invasion route that does not depend on GpA, GpB, and/or sialic acid, representing a new route for the parasite to enter the RBC.<sup>38</sup>

Comparing deduced EBA-175 RII and EBA-140 RII amino sequences has shown that 26 out of 27 cysteines were positionally conserved for EBA-140. Comparing EBA-175 RII/F1 and EBA-140 RII/F1 and DBP RII (containing a single cysteine domain) has shown complete positional conservation for all 12 cysteines. EBA-175 RII/F1 contained an additional cysteine.<sup>255</sup> The presence of two or more parasite ligands binding to different RBC surface molecules provides the potential for redundancy and adaptability within the critical process of RBC invasion.

However, EBA-140 is not absolutely required for normal *P. falciparum* merozoite growth and invasion, provided that sufficient function is available from similar parasite ligands and RBC receptors. EBL-140 is not expressed in some *P. falciparum* parasites, suggesting that it also is not essential.<sup>256</sup> Antibodies raised against EBA-140 RII by DNA vaccination have blocked its binding to RBCs.<sup>258</sup>

HABPs 26135 (<sup>361</sup>SYTSFMKSKTQMEVLTNLY<sup>380</sup>), 26144 (<sup>541</sup>DLADIKGSIIKDYYGKKM<sup>560</sup>), 26147 (<sup>601</sup>LKNKETCKDYDKFQKIPQFL<sup>620</sup>), 26160 (<sup>861</sup>GH-SESSLNRTTNAQDIKIGRY<sup>880</sup>), 26170 (<sup>1061</sup>CNNEYSMEYCTYSDERNSSP<sup>1080</sup>), and 26177 (<sup>1191</sup>VQETNISDYS-EYNYNEKNMY<sup>1210</sup>) have defined six protein RBC binding sequences<sup>259</sup> (Figures 6 and 9). These HABPs' binding to

RBCs was mainly mediated by charged residues. Polymorphism studies carried out to date have shown that HAPB sequences are conserved.<sup>255</sup>

Dissociation constants in the range 350–750 nM have been presented in saturation analysis, revealing high binding affinity with  $n_H$  equal to or greater than 1, indicating positive cooperativity in binding. There were 1 800–7 000 binding sites per RBC, indicating that there were not many receptor molecules; however, binding was highly specific.

Cross-linking results and those from enzyme-treated RBC binding assays have suggested that GpC could be the HAPB receptor on RBCs. Invasion inhibition assays using in vitro cultures have shown that all HABPs inhibited invasion by 11–69% at 200  $\mu$ M concentration.<sup>259</sup>

CD studies determining structural elements have shown that HABPs 26135, 26144, 26147, and 26177 presented  $\alpha$ -helix structural characteristics, while 26170 had  $\beta$ -strand structural elements and 26160 had components of distorted  $\alpha$ -helical and random structures<sup>132</sup> (Figure 10).

#### 4.1.4. Erythrocyte Binding-like-1 (EBL-1)

EBL-1 (PF13\_0115) is a putative RBC binding protein encoded by the *eb1-1* gene<sup>260,261</sup> having characteristics similar to the rest of the EBP family members and 306 kDa of predicted molecular weight. It should be noted that EBL-1 protein expression has not yet been reported and may be a pseudogene; however, EBL-1 protein mRNA transcription in late-stage schizonts, its relationship to rapid phenotypical proliferation, and its high homology with other *eb1* products have suggested that it is probably involved in invasion.<sup>20,260,261</sup> EBL-1 has been identified as being a second member of the *eb1* family in *P. falciparum*, based on the family's general characteristics, which are a single copy of the gene encoding two cysteine-rich domains, a DBL domain, and a C-terminal Cys-rich domain.<sup>20,261</sup> EBL-1 has only four conserved cysteines in the DBL domain compared to other proteins that have eight.<sup>20</sup> EBL-1 protein interaction with RBCs has not been characterized to date, but it has been suggested that the DBL domain mediates RBC binding in the EBL protein family.<sup>22,244,246</sup>

We found five RBC binding regions, independent of sialic acid, defined by HAPB 29895 (<sup>41</sup>HKKKSGELNNKSGIL-RSTY<sup>60</sup>) in the N-terminal region, 29903 (<sup>201</sup>LYECGK-KIKEMKWICTDNQF<sup>220</sup>) in the DBL/F1 region, 29923 (<sup>601</sup>CNAILGSYADIGDIVRGLDV<sup>620</sup>) and 29924 (<sup>621</sup>WRD-INTNKLSEKFQKIFMGY<sup>640</sup>) in the DBL/F2 region, and 30018 (<sup>2481</sup>LEDIINLSKSKKKSINDTSFY<sup>2500</sup>) in the EBL-1 C-terminus (Figures 5 and 9).<sup>262</sup> HABPs 29923 and 29924 were located in the F2 domain, which has been described as being an erythrocyte-binding-activity mediator in EBL family members.<sup>22,244,246</sup>

HABP binding to enzyme-treated RBCs and cross-linking assays has revealed three different binding sites for these HABPs on RBCs located in a 36 kDa protein. These HABPs have been able to inhibit merozoite invasion of RBCs.<sup>262</sup>

All EBL family members studied to date have contained RBC binding regions in region II, F1 and F2 domains. Some of these HAPB sequences have presented homology.<sup>67,259,262</sup> CD studies determining structural elements have shown that HABPs 29003, 29907, 29923, 29924, and 30009 displayed regular  $\alpha$ -helix structural characteristics while 30018 presented a distorted  $\alpha$ -helical structure and 28995 had random structural features (Figure 10).

All these microneme proteins have been found to be cleaved by a family of intramembrane proteins (named rhomboid-like proteins upon secretion), thereby removing their cytoplasmic tails.<sup>263</sup> Interestingly, we have found that HABPs 1818 (EBA-175), 26170 (EBA-140), and 30018 (EBL-1) located  $80 \pm 20$  residues upstream from the cleavage site have a distorted type  $\alpha$ -helix or strand structure; they are located at the beginning of the C-terminal Cys region.<sup>132</sup>

## 4.2. Apical Membrane Antigen-1 (AMA-1)

AMA-1 deserves special consideration since it has been found to be associated with reorientation, bringing the merozoite's apical pole into contact with RBC membrane to start invasion after merozoite rolling over RBC membrane.<sup>264</sup> AMA-1 (PF11\_0344) is a highly variable surface antigen located in the merozoite's apical complex,<sup>23</sup> which is expressed during both sporozoite and merozoite stages of the parasite's life cycle.<sup>265</sup> *Pf*AMA-1 has a typical N-terminal signal peptide with two of the first three residues being charged, followed by 10 consecutive hydrophobic residues. There is also a 23-residue hydrophobic sequence beginning at residue 547 and a smaller C-terminal cytoplasmic 55-residue region.<sup>23</sup>

The *Pf*AMA-1 83 kDa precursor is a microneme-targeted protein that is released from the micronemes to the merozoite surface during schizont rupture to become a type I membrane protein. It is then proteolytically processed within the <sup>92</sup>NLFSSVIEIVE<sup>101</sup> sequence to produce a 66 kDa product, which is processed once more into 48 and 44 kDa soluble fragments also found in culture supernatant. It then becomes relocated on merozoite surface around the time of merozoite release.<sup>24,266,267</sup>

The AMA-1 ectodomain is formed by three domains (I, II, and III), according to disulfide bonds.<sup>194</sup> The first, in the N-terminal region (residues 97–307), has great genetic variability, as does domain III located in the C-terminal region (residues 436–546). Domain II, extending from residues 309 to 435, is a most conserved domain, having very few amino acid sequence differences. Domain III is the only one remaining bound to the merozoite membrane.<sup>268–271</sup>

Both inbred and outbred mice immunized with folded *P. chabaudi adami* AMA-1 ectodomain have been protected against parasite infection during experimental challenge, and such protection has been directly related to antibody levels inhibiting merozoite in vitro invasion.<sup>272,273</sup> The passive transfer of specific antibodies induced in mice by refolded AMA-1 ectodomain has also induced protection.<sup>272</sup> *P. yoelii* AMA-1 specific monoclonal antibodies are very effective against parasite infection by passive immunization.<sup>274</sup> *P. falciparum* FVO AMA-1 recombinant protein has induced antibodies recognizing homologous and heterologous *P. falciparum* merozoites; these purified antibodies have convincingly inhibited RBC invasion of homologous and (to a lesser extent) heterologous *P. falciparum* merozoites.<sup>275</sup> It has been reported that anti-*P. knowlesi* AMA-1<sub>66</sub> monoclonal antibodies have inhibited merozoite invasion of RBCs released from schizonts in iRBC.<sup>276</sup> Interestingly, a Fab fragment from an anti-AMA-1 monoclonal antibody has inhibited merozoite in vitro invasion better than the whole antibody.<sup>277</sup>

It has been reported that infection-induced antibodies in humans (blocking the inhibition of merozoite invasion by other antibodies and interrupting proteolytic AMA-1) is one

of the escape mechanisms used by *P. falciparum*.<sup>278</sup> However, AMA-1 polymorphism is highly responsible for immune response evasion<sup>279</sup> since a single mutation in AMA-1 has been seen to drastically affect AMA-1 antibody activity directed against domain I<sup>280,281</sup> or AMA-1 domain III,<sup>270,282</sup> showing the great importance of minimal genetic variations in parasite evasion of the immune response.

AMA-1 exhibits tremendous polymorphism, having 52 amino acid differences, with most of them being dimorphic but a considerable number having more extensive polymorphism. The whole protein is, thus, highly polymorphic.<sup>268,279,280</sup>

It has been proposed that AMA-1 plays a central role in RBC invasion by merozoites<sup>283</sup> since evidence has been presented that AMA-1 is directly involved in the merozoite's apical reorientation.<sup>264</sup> It has been reported that the *P. yoelii* AMA-1 domains I and II, expressed on COS-7 cells, bind to mouse and rat RBCs<sup>284</sup> and that *Pf*AMA-1 domain III binds to the human RBC Kx membrane protein.<sup>285</sup>

Six RBC binding regions have been reported in our studies containing sequences from HABPs 4313 (<sup>134</sup>DAEVAGTQYR-LPSGKCPVFG<sup>153</sup>), 4315 (<sup>172</sup>QYLKDGGFAPPTPEPLM-SPM<sup>193</sup>), 4316 (<sup>194</sup>TLDEMRFYKDNKYVKNLDE<sup>213</sup>), and 4321 (<sup>294</sup>VVDNWEKVCPRKNLQNAKFG<sup>313</sup>) located in domain I.<sup>76</sup> This domain has presented more antigenic diversity than all other AMA-1 domains,<sup>194</sup> mainly in HABPs 4315 and 4316 (highly variable), 4322 (<sup>314</sup>LWVDGNCE-DIPHVNEFSAID<sup>333</sup>) and 4325 (<sup>374</sup>MIKSAFLPTGAFKADRYK-SH<sup>393</sup>) located in domain II, 4328 (<sup>434</sup>PIEVEHNFPCSLYK-NEIMKE<sup>453</sup>) in domain III variable region, and 4337 (<sup>603</sup>WGEEKRASHTTPVLMKPY<sup>622</sup>) in the AMA-1 putative cytoplasmic domain (Figures 5 and 9). Critical residues have been identified for conserved HABPs 4313, 4321, 4325, and 4337 (shown in bold and underlined above).<sup>76</sup>

All peptides have presented dissociation constants of around 130 nM, with peptide 4322 presenting the least affinity (700 nM). There were 5 000–11 000 binding sites per cell. These peptides' RBC binding activity was not affected when the RBC surface was treated with neuraminidase.<sup>76</sup>

HABPs 4313 and 4321 (both in domain I) were covalently bound by a disulfide bond, implying that these two sequences remain bound together in the protein's 3D structure.<sup>76,194</sup> Variable HBP 4328 sequence was exposed on the protein surface, according to domain III 3D structure.<sup>270</sup> HABPs 4313, 4321, and 4322 were located in AMA-1 regions presenting high homology with *P. yoelii* and *P. berghei* MAEBL protein M1 and M2 RBC binding domains. Domain I (containing conserved 4313 and 4321 and variable 4315 and 4316 HABPs) is the target for antibodies able to inhibit merozoite invasion of RBCs and has been implicated in strain-specific protection in mice.<sup>273</sup> Interestingly, HABPs 4313, 4325, and 4337 have inhibited merozoite in vitro invasion of RBCs.<sup>76</sup>

It is clear that some of these HBP sequences are involved in merozoite invasion of RBCs. In fact, variable HBP 4322 (<sup>314</sup>LWVDGNCE-DIPHVNETSAIDL<sup>333</sup>) (containing an underlined B-epitope recognized by parasite-induced antibodies)<sup>151,286</sup> has been used in designing CDC/NIMAL-VAC-1, a multistage, multiepitopic antimalarial vaccine candidate.<sup>150,151</sup> This variable epitope is highly immunogenic, inducing high antibody titers that have efficiently inhibited in vitro merozoite invasion of RBCs.<sup>151</sup>

HABPs require the presence of potent T-helper epitopes in their sequences for inducing a protection-inducing immune response.<sup>150,151</sup> HABPs 4313 and 4328 carry T-helper epitopes in their sequences; however, highly conserved HABPs 4325 and 4337 were neither immunogenic nor antigenic, but molecular modifications made to their sequences have made these HABPs become antigenic, immunogenic, and protection-inducing.<sup>287,288</sup>

AMA-1 and a related protein (MAEBL) present homology in RBC binding sequences,<sup>76,289</sup> suggesting the presence of conserved RBC binding motifs in these proteins. One of these motifs could be RxxYxNKxxK, in which x could be one of the 20 amino acids, according to homology results so far obtained using LALIGN software.<sup>290</sup>

Given the critical importance of conformational epitopes for inducing protection, knowledge of the antigen's 3D structure is essential if one wishes to completely understand protection-inducing mechanisms. The 3D structures of PfAMA-1 I and II domains' recombinant fragments (residues 104–438)<sup>268</sup> and domain III (residue 436–545) recombinant fragment have been published recently, as has the complete *P. vivax* AMA-1 3D structure.<sup>270,271</sup> Such structural analysis has shown that domains I and II (as expressed in *E. coli*) are composed of two tandem plasminogen apple nematode (PAN) domain folds, present in leech antiplatelet protein, plasminogen, and hepatocyte growth factor. They have high polymorphic residues (positions 187, 197, 200, 234, and 243) surrounding a hydrophobic trough or channel consisting of 9 hydrophobic amino acid chains that are solvent-exposed and for which a critical binding function has been postulated.<sup>268,291</sup> The 3D structure of AMA-1 domain I complexed with 1F9 strain-specific<sup>291</sup> invasion inhibitory antibodies has shown that this MoAb interacts with variable residues P<sup>188</sup>, M,<sup>190</sup> M<sup>173</sup>, F<sup>201</sup>, Y<sup>2002</sup>, and M<sup>224</sup>. MoAb 4G2 strongly interacts with residues K<sup>351</sup>, Q<sup>352</sup>, F<sup>385</sup>, D<sup>388</sup>, and R<sup>389</sup>, with the last 3 residues being present in our HABP 4325 (<sup>374</sup>MIKSAFLPTGAFKADRYKSH<sup>393</sup>); it recognizes a conserved epitope in domain 2 and requires the combination of domains I and II.<sup>292</sup> Conserved HABPs 4313, 4322, and 4337 have a random structure (by NMR and CD spectra analysis), but HABP 4325 has a type 3  $\beta$  turn, coinciding with the same structure it displays in the recombinant RII fragment (Figure 14C).<sup>132,268,287,288,293</sup>

### 4.3. MAEBL

MAEBL (PF11\_0486) is an RBC binding protein located on the surface of mature merozoites. MAEBL is a type 1 membrane protein implicated in merozoite invasion of RBCs and sporozoite invasion of mosquitoes' salivary glands. This protein is structurally similar to *eb1* erythrocyte binding proteins, such as EBA-175, except that MAEBL has cysteine-rich duplicate regions (M1 and M2), similar to domains I and II in AMA-1.<sup>294,295</sup> It has been identified in different malarial parasite species in rodents and in *P. falciparum*.<sup>294,295</sup>

The 2 025 amino acid long *P. falciparum* MAEBL protein consists of a putative signal peptide in the N-terminal, characterized by the presence of a hydrophobic amino acid sequence followed by a cleavage site between residues 20 and 21. The cysteine-rich domains (M1 and M2) are then found, followed by a repeat region in the molecule's central portion, a 22 amino acid long transmembrane domain in the C-terminal, and an intracytoplasmic region.<sup>294,296</sup> The conserved M2 domain is considered to be the main ligand used during merozoite invasion of RBCs. In fact, it has been

reported that *P. yoelii* MAEBL M1 and M2 domains expressed in COS-7 cells bind to mouse RBCs but not to human RBCs;<sup>295</sup> by the same token, the recombinant M2 domain in *P. falciparum* binds specifically to human RBCs.<sup>297</sup>

MAEBL has been located both in micronemes and rhoptries;<sup>294,298</sup> different antibodies have been developed for different portions of this protein, including the three cysteine-rich regions and the carboxyl terminus. It has been suggested that MAEBL is post-translationally processed at a site in between the first and second amino cysteine domains; however, such initial processing is not inhibited by Brefeldin A (BFA).<sup>296</sup>

Peptides from this protein have been used to find two RBC binding regions in the M1 domain defined by HABPs 30181 (<sup>121</sup>KYKLPPIEIPLNKSGLSMYQG<sup>140</sup>) and 30195 (<sup>401</sup>TG-SCYFLKPKPTCVLKKENH<sup>420</sup>) and three RBC binding regions in the M2 domain defined by HABPs 30209 (<sup>681</sup>LNFLNEIRTGYLNKYFKKDV<sup>700</sup>), 30212 (<sup>741</sup>KSKIF-SNRFTMKEYDPKTRL<sup>760</sup>), 30213 (<sup>761</sup>FMYYGLYGLG-GR LGANIKRD<sup>780</sup>), 30219 (<sup>881</sup>YVSSFIRPDYETKCP-PRY-PL<sup>900</sup>), and 30220 (<sup>901</sup>KSKVFGTFDQKTGKCKSL-MDY<sup>920</sup>). Two binding regions have also been found to be defined by HABP 30198 (<sup>461</sup>QTNKRVLYENKSKRN-VRT<sup>480</sup>) between regions M1 and M2 and HABP 30253 (<sup>1561</sup>RAEILKQIEKKRIEEVMKLY<sup>1580</sup>) in the protein's repeat region<sup>289</sup> (Figures 6 and 9).

HABP binding to RBCs has presented 180–400 nM dissociation constants. Receptor–ligand interaction has presented positive cooperativity, as has been established in determining physicochemical constants.<sup>289</sup> This is expected for binding sequences that are involved in merozoite invasion. These RBC binding regions seem to have different specific receptors according to HABP binding to enzymatically treated RBCs, in spite of these HABPs binding to a 33 kDa protein on the RBC surface.

HABPs 30198, 30209, 30213, 30219, and 30253 have displayed  $\alpha$ -helix structural characteristics, while 30181, 30195, 30212, and 30220 have mainly displayed strand or random structures (Figure 10). Most of these HABPs have inhibited merozoite in vitro invasion of RBCs, except for HABPs 30209 and 30213.<sup>289</sup> MAEBL and AMA-1 have presented high homology in RBC binding region sequences.<sup>76,289</sup>

### 4.4. Plasmodium Thrombospondin-Related Apical Merozoite Protein (PTRAMP)

*Plasmodium* thrombospondin-related apical merozoite protein (PTRAMP) is another protein, with a 48 kDa molecular weight, that contains and encodes a thrombospondin-related region (TSR), an important domain found in proteins from many different species that have a role in cell–cell interactions.<sup>299,300</sup> PTRAMP is a highly conserved protein, present in all the *Plasmodium* species. This protein is expressed during the 30–36 h of the asexual cycle (schizont stage), even though it is expressed more abundantly at 42–46 h. PTRAMP is redistributed on the parasite surface, undergoing proteolysis some minutes before schizont rupture.<sup>299,300</sup> It is possible that PTRAMP could play a driving role in merozoites, when this parasite uses locomotion systems for the invasion of host cells.<sup>300</sup> Two HABPs were found in this protein: 33405 (<sup>21</sup>YISSNDLTSTNLKVRN-NWEH<sup>40</sup>) and 33413 (<sup>180</sup>LEGPIQFSLGKSSGAFRIN<sup>199</sup>) (Figures 6 and 9). HABP 33405 located in the PTRAMP

amino-terminal region contained a PEXEL-like sequence (in bold), while HABP 33413 was located in the protein's central region. Saturation assays revealed 170 and 200 nM dissociation constants for HABPs 33405 and 33413, respectively, suggesting low receptor–peptide complex dissociation and high receptor affinity. Hill constants were equal to 2, suggesting positive cooperativity for both HABPs. There were around 17 000 binding sites per cell for each HABP.<sup>301</sup>

Enzymatic treatment did not have any effect on HABP 33405 binding to RBCs. On the other hand, HABP 33413 showed a marked decrease in its specific binding when RBCs were treated with the three enzymes: neuraminidase reduced specific binding by almost 30%, chymotrypsin reduced it by almost 80%, and treatment with trypsin reduced it by 100%, completely eliminating binding activity.

The cross-linking assays identified HABP 33405 as being able to specifically bind, although weakly, to a RBC membrane protein having an apparent 72 kDa molecular weight. Additionally, both HABPs presented similar inhibition activity (57% and 56%, respectively) when both peptides were at 100  $\mu$ M concentration.<sup>301</sup>

## 5. Rhoptry Proteins

The rhoptries play an essential role in *P. falciparum* merozoite invasion of RBCs. These electron-dense organelles located in the apical complex are connected to the surface of a merozoite's apical end by a duct-like structure, and their contents are discharged onto the RBC membrane during invasion.<sup>9,10</sup> Several studies have shown the importance of antibody-mediated responses to rhoptry proteins in antimalarial protection.<sup>302–305</sup> Several proteins having varying molecular weight have been identified in *P. falciparum* rhoptries, some of which have been shown to have a defined role in invasion of RBCs; these include RAP-1, RAP-2, RAP-3, RAMA, *Pf*RBP-H1, *Pf*RBP-2Ha, *Pf*RBP-2Hb, and the RhopH1-CLAG family. Some of these proteins become lost during schizont rupture and merozoite release; others are transferred to the RBC membrane during invasion.<sup>27</sup>

### 5.1. Reticulocyte Binding-like Protein Family (RBL)

Reticulocyte binding-like (RBL) family proteins have great complexity, 230–350 kDa molecular weights and are expressed on both merozoite surface and in the rhoptries. These proteins have been identified as being homologues of rhoptry reticulocyte binding proteins in *P. yoelii* and *P. vivax*.<sup>306,307</sup> All RBL family members share a certain degree of homology in amino acid composition and conserved gene structure having two exons. Exon 1 encodes a signal sequence followed by a short intron and then a long exon 2 encoding the rest of the protein. In spite of these similarities, RBLs have clearly developed for performing different roles during invasion in different *Plasmodium* species.<sup>25</sup> As their name suggests, *P. vivax* reticulocyte binding proteins-1 and -2 (*Pv*RBP-1 and -2) only recognize reticulocytes and not mature RBCs (normocytes). It has been presumed that these molecules are used for identifying reticulocytes and also perhaps for provoking events following invasion once reticulocyte/normocyte distinction has been made.<sup>306,308,309</sup> By contrast, it has been estimated that the murine *P. yoelii* parasite has 13 or more genes related to the RBL family, and it seems that different merozoites in a single schizont can express different RBL family members.<sup>310–312</sup> It is still

not known whether all members of the Py235 family have different binding specificities.

A combination of exploring *P. falciparum* genomic DNA libraries and databases has led to identifying five members of the RBL family, known as normocyte binding proteins (*Pf*NBPs) or reticulocyte binding protein homologues (*Pf*RBP-Hs). *Pf*NBP-1 binds to a trypsin-resistant receptor on RBC surface, and antibodies against it can inhibit parasite invasion of trypsinized RBCs.<sup>304</sup> *Pf*NBP-2a or *Pf*RBP-2Ha and *Pf*NBP-2b or *Pf*RBP-2Hb are unusually related, sharing more than 8 Kb sequence identity before the genes diverge following a series of repeats, an arrangement that could result from an ancient duplication event or gene conversion.<sup>313,314</sup> In spite of such identity, they do not seem to perform overlapping roles in invasion.<sup>304,314,315</sup> *Pf*NBP-3 seems to be a pseudogene, having one or two frame shifts in its open reading frame in all *P. falciparum* strains examined to date, and even though the gene is transcribed, there is no evidence of a translation product.<sup>316</sup> *Pf*NBP-4 or *Pf*RBP-H4 is smaller than other members of the *P. falciparum* RBL family, and there is still no evidence that it plays a role during RBC invasion. It has been proposed that the RBL family is located in the rhoptry neck; however, some evidence has shown that *Pf*RBP-H4 is located in the micronemes.<sup>26</sup>

#### 5.1.1. *Plasmodium falciparum* Normocyte Binding Protein-1 (*Pf*NBP-1) or *Plasmodium falciparum* Reticulocyte Binding Protein-Homologue-1 (*Pf*RBP-H1)

*P. falciparum* normocyte binding protein 1 or *Pf*NBP-1 (PFD0110w), having a 35.8 kDa predicted molecular mass, is homologous to the *P. vivax* RBP-1 protein expressed in the merozoite's apical area and possibly forms a complex with at least one of the *P. falciparum* *Pv*RBP-2 homologues.<sup>304</sup> This protein binds to a sialic acid-dependent receptor located on the RBC surface due to its sensitivity to treatment with neuraminidase (even though it is trypsin-resistant). Being a different receptor in invasion to those known to date (GpA, GpB, GpC, receptor X), it has been named receptor Y. *Pf*NBP-1-induced antibodies can inhibit merozoite invasion of trypsin-treated RBCs. However, two *P. falciparum* strains expressing *Pf*NBP-1 fragments are not able to invade trypsinized RBCs.<sup>304</sup>

Two binding sequences have been identified in this protein in RBC binding assays using 7G8 strain *Pf*NBP-1 protein synthetic peptides. HABP 26332 (<sup>101</sup>VFINDLDTYQYEEYFYEWNQ<sup>120</sup>) and 26336 (<sup>181</sup>NTKETYLKELNKKKMLQNKK<sup>200</sup>) have been found to be involved in merozoite invasion of RBCs (Figures 8 and 9). These HABP sequences have been located in the extracellular domain and belong to *Pf*NBP-1 conserved regions.<sup>75</sup> Saturation assays have shown that HABP binding to RBCs is saturable, having 480–650 nM dissociation constants. These peptides have presented Hill coefficients greater than 1 (1.6 for 26332 and 1.4 for 26336), indicating that their interaction with RBCs presents positive cooperativity. It has been established that HABPs bind to a protein on the RBC having a molecular weight of around 31 kDa, with such binding being affected by trypsin, chymotrypsin, and/or neuraminidase treatment.<sup>75</sup> Competition assays with glycine peptide analogues have shown that peptide 26332 possesses six critical amino acids in its binding sequence (<sup>101</sup>VFINDLDTYQYEEYFYEWNQ<sup>120</sup>) while peptide 26336 has three (<sup>181</sup>NTKETYLKELNKKKMLQNKK<sup>200</sup>).

In vitro assays have revealed that HABPs can inhibit merozoite invasion of RBCs by about 85% at 200  $\mu$ M concentration. CD analysis has shown that HAPB 26332 and 26336 displayed an  $\alpha$ -helical structure<sup>75</sup> (Figure 11).

### 5.1.2. Reticulocyte Binding Protein-2 Homologues a and b (PfRBP-2Ha and -2Hb)

*P. vivax* reticulocyte binding proteins (PvRBP-1 and PvRBP-2) bind to reticulocytes, being partially responsible for *P. vivax* merozoite ability to preferentially invade reticulocytes.<sup>306,309</sup> Two related genes in *P. falciparum* and the resulting encoded proteins could be the result of an evolutionary duplication event and the resulting encoded proteins. Both genes encode large hydrophilic proteins of about 350 kDa, having an N-terminal signal sequence and a simple transmembrane domain close to the C-terminal extreme.<sup>313,314</sup> Both amino acid sequences are identical, except in the C-terminal extreme. PfRBP-2Ha (PF13\_0198) and PfRBP-2Hb (Genbank No. AA038039) show a remarkably variable degree of expression where some parasites express no detectable levels of these proteins, and it has been suggested that this provides a phenotypical variation mechanism to allow alternate receptors to be used for merozoite invasion of human RBCs.<sup>313–315</sup>

These proteins are located in the merozoite's invasive apical zone and could be involved in selecting cells to be invaded by *P. falciparum* merozoites. Anti-PfRBP-2Ha and -2Hb antibodies have inhibited 3D7 strain merozoite invasion of RBCs, suggesting that these proteins are involved in invasion.<sup>314</sup> Targeted gene disruption has shown that PfRBP-2Hb is required for a novel invasion pathway using the sialic acid-independent receptor Z.<sup>315</sup>

Common binding sequences have been found in both proteins, represented by HAPB 26711 (<sup>201</sup>TKLLKNIEST-GNMCKTESYV<sup>300</sup>) in the N-terminal region, 26752 (<sup>1101</sup>IE-KVDNYYSLSDKALTKLK<sup>1120</sup>) in the central region, and 26785 (<sup>1761</sup>INDYNINENFEKHQNILNEI<sup>1780</sup>), 26794 (<sup>1941</sup>IT-PENPLEDNLLNLQLYFE<sup>1960</sup>), 26796 (<sup>1981</sup>GSNSDESIDN-LKVVYNDIIEI<sup>2000</sup>), 26801 (<sup>2081</sup>EIFDNVVEYKTLDDT-KNAYI<sup>2100</sup>), 26803 (<sup>2121</sup>IYFNDLDELEKSLTL-SSNEM<sup>2140</sup>), 26805 (<sup>2161</sup>NDIDKEMKTLIPMLDELL-NE<sup>2180</sup>), 26807 (<sup>2201</sup>GNDIKNIREQENDTNICFEY<sup>2220</sup>), 26816 (<sup>2381</sup>LESIQTFNNLYGDLMSNIQD<sup>2400</sup>), and 26818 (<sup>2421</sup>NITNLLGRINTFIKELDKYQ<sup>2440</sup>) in the C-terminal region.

There is also a RBC binding region in PfRBP-2Ha represented by HAPB 26835 (<sup>2761</sup>LEREKQEQLQ-KEEELKRQE<sup>2780</sup>); there are three RBC binding regions in PfRBP-2Hb represented by HAPBs 26529 (<sup>3021</sup>SDIH-MDSVDIHDSIDTDENA<sup>3040</sup>), 26534 (<sup>3221</sup>ITEKLVDIYP-STYRTLDEPM<sup>3140</sup>), and 26540 (<sup>3235</sup>YADKEEIIIVFDE-NEEKYF<sup>3254</sup>) in the C-terminal regions of each protein (Figures 7 and 9).

Saturation curve analysis has revealed that peptide–cell interaction dissociation constants range from 70 to 300 nM; HAPB 26796 has presented the highest affinity, having a 70 nM constant. All HAPBs have exhibited positive cooperativity (>1 Hill coefficient). There were 5 000–140 000 binding sites per cell for these HAPBs which bound to 21, 48, and 79 kDa proteins on RBC surface.<sup>317</sup> Most of these HAPBs inhibited merozoite invasion of RBCs, some of them inducing more than 90% inhibition (HAPBs 26540, 26711, 26796, and 26805). HAPBs 26534, 26752, 26801, and 26835 only inhibited invasion by 0–30%.<sup>317</sup> The CD spectra

showed that HAPBs 26752, 26794, 26796, 26803, 26805, and 26818 displayed  $\alpha$ -helix-like features and only 26534 and 26540 displayed random or turn structural elements.<sup>132</sup>

## 5.2. Rhoptry-Associated Protein-1 (RAP-1)

The rhoptries located in the merozoite's apical extreme discharge their contents into the PV during merozoite release and RBC invasion. Proteins associated with these organelles may, therefore, be involved in merozoite invasion of RBCs. One such *P. falciparum* merozoite molecule is a complex formed by three noncovalently bound proteins (RAP-1, RAP-2, and RAP-3), where RAP-1 and RAP-2 and RAP-1 and RAP-3 might form complexes, but there is no evidence to date of RAP-2 and RAP-3 complex formation.<sup>318–322</sup> The *rap-1* gene (PF14\_0102) encodes a 782 residue (84 kDa) highly conserved polypeptide.<sup>323–328</sup> In common with all rhoptry proteins that have been sequenced, RAP-1 and RAP-2 contain an N-terminal signal peptide, indicating that these proteins are routed to the organelle via the endoplasmic reticulum/Golgi secretion pathway.<sup>325</sup>

RAP-1 is present during parasite asexual blood-stage development, just before merozoite release; it is cleaved at amino acid residue 191 to produce a 67 kDa molecule called p67,<sup>322–329</sup> which is relatively abundant in free merozoites but becomes lost in ring-stage parasites. This suggests that p67 function is restricted to schizont and merozoite stages.<sup>325,330</sup> RAP-1 protein could be involved in an alternative invasion mechanism, since merozoites expressing truncated RAP-1 forms continue invading RBCs in vitro.<sup>28</sup>

It has been reported that RAP-1 induces a strong protection-inducing antibody response against *P. falciparum* challenge in *Saimiri* monkeys.<sup>321</sup> Monoclonal antibodies produced against conserved RAP-1 linear epitopes have also inhibited *P. falciparum* in vitro development, suggesting that anti-RAP-1 antibodies can reduce parasite replication.<sup>322,331,332</sup>

RAP-1 has presented two RBC binding regions defined by HAPB 26188 (<sup>201</sup>TLTPLEELYPTNVNLFNYKY<sup>220</sup>) in the p67 amino terminal region, and HAPBs 26201 (<sup>461</sup>CLLN-PKTLLEEFLLKKKEIKDL<sup>480</sup>), 26202 (<sup>481</sup>MGGDDLIIKYKEN-FDNFMSIS<sup>500</sup>), 26203 (<sup>501</sup>ITCHIESLIYDDIEASQDIA<sup>520</sup>), and 26204 (<sup>521</sup>AVLKIAKSKLHVITSGLSYK<sup>540</sup>) flanked by disulfide bridges, located at the C-terminus (Figures 8 and 9).<sup>79</sup> This is interesting, because cysteine-rich regions are important in *P. vivax*, *P. knowlesi*, and *P. falciparum* antigens that bind to RBCs.<sup>21</sup> Studies with truncated RAP-1 forms have shown that the biological function of the protein's C-terminal region is very important, including interaction with RBCs, since truncated RAP-1 merozoite forms cannot invade RBCs because of the loss of binding sequence.<sup>28</sup>

Most critical peptide–cell interaction amino acids are located in the central part of most HAPB sequences; however, peptides 26202 and 26203 have also presented critical residues in amino and carboxy terminal regions (critical amino acids are shown in bold and underlined in the HAPB sequences given before and below): 26201 (<sup>461</sup>CLLN**PKTLLEEFLLKKKEIKDL**<sup>480</sup>), 26202 (<sup>481</sup>**MGGDDLIIKYKEN**FDNFMSIS<sup>500</sup>), 26203 (<sup>501</sup>**ITCHIESLIYD-DIEASQDIA**<sup>520</sup>), and 26204 (<sup>521</sup>AVLKI**AKSKLHVITSGLSYK**<sup>540</sup>). Critical residues could not be identified in peptide 26188.

These HAPBs have shown high affinity and positive cooperativity, indicating strong HAPB interaction with RBCs, as is to be expected in RBC binding sequences involved in invasion. HAPB dissociation constants ( $K_d$ ) were between

700 and 900 nM, Hill coefficients were  $> 1$ , and there were 72 000–163 000 binding sites per cell. They specifically bound to a 72 kDa protein on the RBC membrane.<sup>79</sup>

HABPs 26188, 26201, and 26203 inhibited merozoite in vitro invasion of RBCs by 65–97%; HABPs 26202 and 26204 only inhibited it by around 20%.<sup>79</sup> Interestingly, HBP 26188 contained a <sup>201</sup>TLTPLEELYPTNVN-LFNYKY<sup>220</sup> epitope (underlined) recognized by antibodies inhibiting *P. falciparum* merozoite in vitro invasion of RBCs.<sup>325,331</sup> These results suggested that RAP-1 could be involved in one of the different interactions between merozoites and RBCs, supporting the idea that it could be binding to the RBC surface during merozoite invasion.

Figure 8 shows each tested peptide's sequence and its position in RAP-1. A schematic representation of RAP-1 is given to the right of the figure, showing the serine-rich region having tandem repeats related to the KSSSPSXT/V motif (black rectangle) and the Cys-rich region (white rectangle). Residues 43–345, corresponding to the truncated form of RAP-1, are shown further to the right. HBP CD spectra were obtained for evaluating secondary structure elements; all HABPs displayed  $\alpha$ -helix-like features, according to 208–222 nm minimum values and 190 nm maximum ellipticity<sup>79</sup> (Figure 11).

### 5.3. Rhopty-Associated Protein-2 (RAP-2)

RAP-2 protein (PFE0080c), associated with RAP-1, is part of the QF3 low molecular weight complex located in merozoite rhoptries.<sup>318,322,333</sup> The mature form of RAP-2 contains 377 amino acids and has a theoretical 44.487 kDa molecular weight. The primary structure consists of a basic protein having an 8.9 pI and a signal peptide that is cleaved in residue 21. RAP-2 SDS-PAGE migration gives an apparent 40–42 kDa size, and RAP-2 appears to have intramolecular disulfide bridges.<sup>318,333</sup>

Monoclonal antibodies directed against RAP-1 and RAP-2 provide substantial inhibition of merozoites in in vitro invasion of RBCs.<sup>322,331</sup> *Saimiri* monkeys immunized with purified RAP-1 and RAP-2 have been partially protected against *P. falciparum* infection.<sup>321</sup>

Experimental evidence supports the idea that RAP-2 is a ligand used by merozoites for invading RBCs. In fact, this protein presents four RBC binding sequences defined by HABPs 26220 (<sup>61</sup>NHFSSADELIKYLEKTNINT<sup>80</sup>) and 26225 (<sup>161</sup>IKKNPFLRVLNKASTTTHAT<sup>180</sup>) in the protein's amino terminal and central parts and HABPs 26229 (<sup>241</sup>RSVN-NVSKNKTGLRKRSS<sup>260</sup>) and 26235 (<sup>361</sup>FLAEDFVELFD-VTMDCYSRQ<sup>380</sup>) in the carboxy terminal region<sup>334</sup> (Figures 8 and 9). Critical residues could not be identified in peptide 26235. All HABPs bound to a 62 kDa protein located on the RBC surface. HABPs 26225 and 26229 also bound to a 42 kDa RBC protein, and HBP 26235 recognized a 77 kDa band that was not recognized by any other HBP.<sup>334</sup>

Dissociation constants obtained by analyzing Hill coefficients and saturation curves ranged from 500 to 950 nM, indicating a strong interaction with their binding sites on RBCs. Hill coefficients (like those for HABPs 26225, 26229, and 26235) showed that interaction with RBC receptors was simple, while positive cooperativity was suggested for peptide 26220, which had a 1.7 Hill coefficient. There were 50 000–120 000 binding sites per cell.<sup>334</sup>

These RAP-2 RBC binding regions suggested redundancy in merozoite ligands that could be very important for achieving an immune response directed against such regions

or fulfilling alternative functions. The four HABPs inhibited in vitro merozoite invasion by 54–94% at 200  $\mu$ M, suggesting that these RAP-2 regions are involved in *P. falciparum* in vitro invasion.<sup>334</sup> CD analysis was used for obtaining general information regarding HBP structural elements; all HABPs displayed  $\alpha$ -helix-like features<sup>132</sup> (Figure 11).

### 5.4. Rhopty-Associated Protein-3 (RAP-3)

RAP-3 (PB301475.00.0) is the third member of the low molecular weight protein complex located in the rhoptries. It has 400 amino acids in its sequence, and its molecular weight varies from 37 to 40 kDa.<sup>335</sup> It has a signal peptide from amino acid 1–23 and a transmembrane domain between residues 5–22.<sup>28,335,336</sup> It has been shown that proteins from the low molecular weight rhopty complex induce an in vivo immune response in the *Saimiri* monkey model, producing antibodies against RAP-1 and RAP-2.<sup>331</sup> Nevertheless, it has not been determined whether RAP-3 is able to induce a protective immune response to date.<sup>28,335</sup> Studies concerning RAP-3 polymorphism and its possible biological activity in invasion of RBCs are lacking; however, it may act as an auxiliary protein in the RAP complex in maintaining the cycle during the blood stage.<sup>28</sup>

RAP-1 controls RAP-2 or RAP-3 transport toward the rhoptries during invasion,<sup>28</sup> when the gene encoding RAP-1 is interrupted, the traffic of either of the other two proteins is affected and such proteins remain trapped in the endoplasmic reticulum. Invasion does not become inhibited when the gene encoding RAP-3 is interrupted but does become reduced to some degree.<sup>335</sup> These observations suggest that the loss of RAP-3 is compensated for by the presence of RAP-2 and vice versa.

Work carried out in our laboratory has shown that the protein presented 2 HABPs: 33860 (<sup>61</sup>FNHFSNVDEAIEY-LKGLNIN<sup>80</sup>) and 33873 (<sup>321</sup>KNRTYALPKVKGFR-FLKQLF<sup>340</sup>). HBP's binding to RBCs had nanomolar range  $K_d$  values. HBP binding was sensitive to treatment with trypsin for both peptides (Figures 8 and 9). CD spectra revealed the presence of  $\alpha$ -helix structural elements for both HABPs (Figure 11) (unpublished results). Transcripts of MSP-2, MSP-5, RAP-1, RAP-2, and SERA have also been determined in sporozoites and infected hepatocytes, suggesting that the rhopty-associated proteins are excellent targets for multiantigen, multistage, subunit-based, antimalarial vaccine development.<sup>337</sup>

### 5.5. Rhopty-Associated Membrane Antigen (RAMA)

This protein is produced during the late ring, early trophozoite, and immature schizont phases in the malaria parasite's asexual-stage cycle and has been reported as being one of the first proteins to be synthesized, since it appears 15–20 h following invasion.<sup>338</sup> RAMA induces high immunological resistance against infection by the *P. falciparum* parasite, since antibodies directed against this protein inhibit merozoite invasion of RBCs.<sup>305,339</sup>

RAMA is a protein that is synthesized as a 170 kDa precursor and then cleaved to produce a mature 60 kDa form. It is associated with the rhopty membranes.<sup>338</sup> This is a mainly hydrophilic 861-residue-long protein, having a hydrophobic 15-residue signal sequence (SS) in its N-terminal region. The final fragment remains bound to the merozoite

membrane, anchored by a GPI tail. RAMA has three highly acidic repeat regions: the first is formed by 25 residues (<sup>96</sup>SFIETDEYEDNEDDKYNKDEDDYSE<sup>121</sup>), the second has 5 consecutive residues (E/V)MKD(E/V), and the third has a EE(S/F)KN sequence in the following repeat regions.<sup>338</sup>

The binding assays involving RBCs and RAMA protein-derived peptides led to identifying HABPs 33426 (<sup>79</sup>NILSSVHRKGRILYDSF<sup>97</sup>) and 33460 (<sup>777</sup>HKKREKSISPHSYQKVSTKVQ<sup>797</sup>)<sup>340</sup> (Figures 7 and 9). The first HABP 33426 contained a classical PEXEL motif in its sequence <sup>88</sup>RKGRILYDS<sup>96</sup> (bold)<sup>202</sup> located 75 residues downstream from the SS, suggesting that RAMA is a soluble protein transported from the PV to iRBC cytosol, where it has been found.

Topolska et al.<sup>341</sup> have revealed that RAMA is antigenic during a natural infection. Three epitopes were recognized by hyper immune sera in immunoblots, with two of them in the protein's C-terminal region. This region was focused on the epitope having immunogenicity, with this being found between residues <sup>759</sup>D and N<sup>840</sup>, where the second HABP 33460 was identified (located in a fairly conserved region by polymorphism studies of *P. falciparum rama* gene).<sup>342</sup>

Dissociation constant values were ~400 nM, suggesting low receptor–peptide complex dissociation. Hill constant values > 1 indicate positive cooperativity; they were 2.1 and 2.5 for 33426 and 33460 RAMA HABPs, respectively. There were ~180 000 and 34 000 binding sites per cell for 33426 and 33460, respectively.<sup>340</sup>

CD analysis data revealed that HABP 33426 had a distorted  $\alpha$ -helicoid structure, while peptide 33460 presented a random coil structure (data not shown). Enzymatic treatment for RBCs in the case of HABP 33426 decreased peptide binding to RBC by 50%, 75%, and 75% when they were treated with neuraminidase, trypsin, and chymotrypsin, respectively, suggesting that the nature of the receptor was probably a glycoprotein or the putative “Y” receptor.<sup>179</sup> A >80% reduction in HABP 33460 binding to RBCs was observed when these cells were treated with chymotrypsin, suggesting that the receptor was essentially a protein, possibly GpB or the putative RBC “E” and/or “Z” receptors.<sup>179</sup>

The HABPs found in RAMA protein inhibited in vitro merozoite invasion of RBCs by 61% at 200  $\mu$ M concentration; this perhaps required lesser concentration, since no concentration–inhibition relationship was observed, suggesting that this receptor–ligand was saturable at lower concentrations than that used in the assay and that there was strong competition for RBC receptor sites between each HABP and the parasite's complete protein.<sup>340</sup>

RAMA has been reported to be a fundamental DRM protein resistant to the action of detergents such as Triton X-100.<sup>114</sup> It is anchored to the membrane via its GPI tail, unlike the other rhoptry proteins (RAP-1, RAP-2, RAP-3, RhopH3), which are noncovalently bound to RAMA forming a macromolecular complex on lipid rafts mediating merozoite invasion of RBCs<sup>114</sup> (Figure 13).

## 5.6. RhopH3

The RhopH protein complex has been shown to bind to the inside of the RBC membrane.<sup>343</sup> Nevertheless, only RhopH3 has been molecularly characterized. Serological studies using human sera from malaria-infected individuals from different geographical areas have shown that anti-RhopH3 antibodies are primarily reactive with epitopes located at the C-terminal region.<sup>344,345</sup> The RhopH3 C-

terminal portion is structurally conserved among different geographical and laboratory *P. falciparum* isolates.<sup>345</sup> Because of its role in RBC binding and its presence in the RBC membrane following invasion, the RhopH3 protein is considered an ideal candidate for vaccine studies.<sup>343,346,347</sup>

The complete *rhoph3* (PFI0265c) gene sequence has been determined, encoding a protein having a 110 kDa molecular weight.<sup>347</sup> It has been found that (contrasting with most other *P. falciparum* genes) the *rhoph3* gene does not encode any repeat amino acid sequences such as RhopH1 and RhopH2.<sup>345</sup> *rhoph3* from *P. falciparum* and *P. vivax* is mainly encoded by a 7 exon gene, having 63, 111, 961, 63, 57, 771, and 668 bp lengths in *P. falciparum*. The six intron sequences span a total of 1 355 bp in *P. falciparum*, being only seven amino acids shorter than *PvRhopH3* (estimated to be 104.5 kDa MW).<sup>345,348</sup>

The RhopH3 protein has been recently identified and characterized in *P. vivax*, finding that RhopH3 is located in homologous chromosome regions in both parasite species, since upstream and downstream genes shared high identity (31.8–79.9%) and similarity (40.9–89.1%) values and displayed the same ORF orientation.<sup>348</sup>

Although the chromosome region comprising all these genes was slightly longer in *P. vivax* than in *P. falciparum*, each gene tends to be smaller in the former parasite species.<sup>348</sup> Studies in our laboratory have defined the specific RBC binding regions for *P. falciparum* RhopH3 protein (Figures 7 and 9) (unpublished results), which could be functionally relevant at the moment of invasion. The HABPs identified in the RhopH3 protein were as follows: 33482 (<sup>21</sup>KVWGKDV FAGFVTKKLTLLY<sup>40</sup>), 33521 (<sup>61</sup>LD-FVDEPEQFYWFVEHFLSV<sup>80</sup>), 33483 (<sup>81</sup>KFRVPKHLKD-KNIHNFTPTLY<sup>100</sup>), 33522 (<sup>101</sup>NRSWVSEFLKEYEPEFVN-PV<sup>120</sup>), 33484 (<sup>241</sup>TKETANSNNILKTIDEFLRKY<sup>260</sup>), 33529 (<sup>281</sup>FLFESLKNPYLDNFKKFMTN<sup>300</sup>), 33531 (<sup>321</sup>KPK-NYLDVQNLDTCEFKKL<sup>340</sup>), 33487 (<sup>421</sup>TQNVKSLD-LEVDVETMKGIIY<sup>440</sup>), 33566 (<sup>521</sup>NFLYKNNKAIRYHV-LVVKPH<sup>540</sup>), 33490 (<sup>561</sup>ILGLSNLVSSNPSPFFDTIY<sup>580</sup>), 33491 (<sup>621</sup>PKEFELIKSRMIHPNIVDRIY<sup>640</sup>), 33570 (<sup>641</sup>LKG-IDNLMKSTRYDKMRTMY<sup>660</sup>), 33580 (<sup>841</sup>NLKKGLEF-YKSSLKLDQLDK<sup>680</sup>), and 33581 (<sup>861</sup>EKPKKKKSKR-KKKRDSDDRY<sup>880</sup>).

HABP dissociation constant values were 410–900 nM; Hill constant values were > 1 (1.4 to 2.2), indicating positive cooperativity. There were 40 000 to 461 000 binding sites per cell for RhopH3 HABPs.

These peptides inhibited merozoite invasion at 200  $\mu$ M concentration; there was 60–94% invasion inhibition. The highest inhibition was achieved by peptides 33482 and 33521, and the mean inhibition was achieved by peptide 33581. Most peptides' CD profiles indicated a clear shift toward an ordered structure, possibly being  $\alpha$ -helical as characterized by double minima at 207 and 220 nm. Only 33491 and 33570 (both in the C-terminal portion) displayed a random structure (unpublished results) (Figure 11).

The binding of HABPs located in the protein's C-terminal region is sensitive to neuraminidase and trypsin RBC-treatment, showing that peptide–receptor interaction could possibly be glycoproteic (maybe GpA and GpC). The binding of these HABPs was not affected by chymotrypsin RBC-treatment, indicating that cleavage of band 3 and GpB proteins did not affect the HABP–RBC interaction. HABPs 33482, 33491, 33521, 33522, 33570, 33580, and 33581

specifically bound to three bands having apparent 35, 26, and 17 kDa molecular weights (unpublished results).

### 5.7. Cytoadherence-Linked Asexual Gene (RhopH-1/CLAG 3.2)

It has been proposed that the cytoadherence-linked asexual gene (*clag*) family plays an important role in iRBC cytoadherence to endothelial cells, different paralogues being involved in binding to different receptors. The first of the *clag* genes characterized in *P. falciparum* is located in chromosome 9, and its product (RhopH-1/CLAG 9 protein) has been implicated in iRBC binding to endothelial cells.<sup>349–351</sup>

RhopH-1/CLAG 2 (PFB0935w), RhopH-1/CLAG 3.1 (PFC0110w), and RhopH-1/CLAG 3.2 (PFC0120w) (in chromosomes 2 and 3, respectively) have been completely sequenced, and it has been found that they are colinear with RhopH-1/CLAG 9 (PFI1730w), having identical splicing patterns and being expressed during asexual stages (except for CLAG 3.2). However, they are very divergent in sequence.<sup>352,353</sup> The fact that deleting the *clag* gene from chromosome 9 prevents binding to CD36 but does not inhibit binding to endothelial cells suggests that different members of the *clag* gene family could have different specificities or that they are not functionally equivalent.<sup>351,352,354</sup>

Ocampo et al.<sup>355</sup> used the information available in the *P. falciparum* genome for designing primers for polymerase chain reaction (PCR) and RT-PCR assays to determine that the RhopH-1/CLAG 3.2 protein-encoding gene (PFC0110w) is transcribed in the *P. falciparum* FCB2 strain. It was also found that polyclonal antibodies from goats (obtained by inoculating polymeric peptides) recognized a protein in schizont lysate having a molecular weight (142 kDa) close to that of RhopH-1/CLAG 3.2, suggesting that the protein may also be expressed in the FCB2 strain.<sup>355</sup>

The foregoing has suggested that the RhopH-1/CLAG 3.2 protein could be involved in some iRBC adhesion phenomena, since we found that the 12 synthetic peptides derived from the protein bound specifically and with high affinity to C32 cells: 30371 (<sup>21</sup>KVLSINENENLGENKNENAY<sup>40</sup>), 30373 (<sup>61</sup>LKSMIGNDELHKNLTILEKLY<sup>80</sup>), 30374 (<sup>81</sup>IL-ESLEKDKLKYPLLKQGTE<sup>100</sup>), 30387 (<sup>340</sup>VYYSEKRRK-TYLKVDRSST<sup>359</sup>), 30403 (<sup>660</sup>VRKHIPNNLVDELEK-LMKSgy<sup>679</sup>), 30407 (<sup>740</sup>FSNYQNPYIRKDLHD-KVLSQ<sup>759</sup>), 30409 (<sup>780</sup>AYDMYFEQRHVKNLYKYH-NI<sup>799</sup>), 30414 (<sup>880</sup>KEVDELYSIYNFNTDIFTD<sup>899</sup>), 30419 (<sup>980</sup>NVDNLDKAYGLSENIQVATS<sup>999</sup>), 30421 (<sup>1020</sup>NSLL-PPYAKKPITQLKYGKT<sup>1039</sup>), 30428 (<sup>1160</sup>LDAYKSFPGG-FGPAIKEQTQ<sup>1179</sup>), and 30435 (<sup>1300</sup>HETNEDIMSNLRRY-DMENAF<sup>1319</sup>). Some of them recognized a 53 kDa protein on CD32 membrane (expressing CD36 having 53–54.3 kDa molecular weight). HABPs 30373, 30403, 30409, 30414, and 30421 peptides also bound to human RBCs<sup>355</sup> (Figures 8 and 9).

A possible role has also been suggested in invasion for peptides specifically binding to RBCs since some of them inhibited in vitro merozoite invasion of RBCs by up to 94%. Interestingly, CD determined the presence of  $\alpha$ -helix structural elements in **all** peptides inhibiting RBC invasion by more than 64%<sup>355</sup> (Figure 11).

## 6. Infected RBC (iRBC) Membrane-Associated *P. falciparum* Proteins and Transportome-Associated Proteins

Parasite-derived antigens and those associated with iRBC membrane are interesting molecules for analysis since they can be indicators of immune evasion, a particular disease's pathogenesis involvement, and important virulence factors. The main variant antigens acting as polypeptide ligands for endothelial receptors are *P. falciparum* erythrocyte membrane protein 1 (*PfEMP-1*), repetitive interspersed family (RIFINs), and subtelomeric variant open reading frame (STEVOR);<sup>49,356,357</sup> some of them are involved in occluding the small vessels and, therefore, in severe malaria, placental adhesion and blood supply inhibition and, therefore, in abortions, etc.<sup>358–360</sup>

Some other antigens such as knob-associated histidine-rich protein or histidine-rich protein I (KAHRP/HRP-I) and histidine-rich proteins II and III (HRP-II and HRP-III) are located on the RBC membrane, being the main components of electron-dense and knob-like structures that have also been involved in cytoadherence and rosette formation and, therefore, in microvascular adhesion.<sup>357,361–364</sup> The genes encoding most of these proteins (*PfEMP-1*, STEVOR, KAHRP, and HRP-III) are located in subtelomeric regions.<sup>364</sup> Some other proteins for which some specific functions were recently documented in the parasite's life cycle have also been included in this section: the ring-infected erythrocyte surface antigen protein (RESA).<sup>365</sup>

### 6.1. Ring-Infected Erythrocyte Surface Antigen (RESA)-155

The gene encoding RESA protein (PFA0110w) is located in *P. falciparum* chromosome 1, encoding a 155 kDa protein. It is a *P. falciparum* molecule expressed on the surface of ring iRBCs (Figures 1E1 and 1E2) located on dense granules, even though it can also be found in culture supernatant.<sup>366</sup>

RESA's function during merozoite invasion is still not fully understood; however, it has been found that this antigen establishes specific interactions via a 108 amino acid long fragment (residues 667–770, shown in fuchsia in Figures 6 and 9) stabilizing spectrin tetramer formation against dissociation during RBC invasion, acting as a cytoskeleton protector during febrile periods (interacting with some heat-shock proteins, HSPs), mechanical degradation, and reinvasion by new merozoites as well as mediating RBC adhesion to healthy RBCs and endothelial cells.<sup>367,368</sup>

Five functional regions have been reported in RESA. Regions II (residues 436–504) and V (residues 885–1073) contained repeat sequences recognized by most of this protein's antibodies, acting as smokescreens or decoys to bias the immune system. Two peptides from these regions have produced antibodies able to efficiently inhibit in vitro merozoite invasion.<sup>369–371</sup> Region III (residues 521–591) confers thermal stability to the RBC cytoskeleton and membrane.<sup>193,372</sup> Region IV (residues 723–770) binds to spectrins. Region I, in the amino terminal extreme (residues 141–200), has been defined as being a RBC-binding region, since HABPs 6671 (<sup>141</sup>MTDVNRYRYSNNYEAIPHIS<sup>160</sup>) and 6673 (<sup>181</sup>LRSDIKKMQTLWDEIM<sup>200</sup>) were found in this region and presented nanomolar dissociation constants<sup>373</sup> (Figure 6).

RESA nonrepeat sequence antibodies have inhibited merozoite invasion<sup>374</sup> and cytoadherence. Passive immunization of *Aotus* monkeys with human anti-RESA immunoglobulin

has provided a degree of protection against *P. falciparum* challenge.<sup>34</sup> Recombinant RESA fragments used for immunization in *Aotus* monkeys have provided some protection against invasion of RBCs,<sup>375</sup> and the presence of anti-RESA antibodies in individuals from holoendemic *P. falciparum* areas has been correlated with acquired clinical immunity against malaria.<sup>376–380</sup>

HABP 6673 sequence superimposed on that of peptide Lj5 (KMOTLWDEIMDINKRK), containing B- and T-epitopes, has been shown to be able to efficiently inhibit *in vitro* merozoite invasion.<sup>373,374,381,382</sup> Interestingly, HABP 6671 (MTDVNRYRYSNNYEAI~~PHIS~~) peptide analogues have been able to induce partial protection against merozoite infection in *Aotus* monkeys.<sup>80</sup> HABP 6671 is located ~50 residues downstream a PEXEL motif,<sup>203</sup> suggesting that this protein is transported from the merozoite to the RBC cytoplasm and from these to the iRBC membrane, making it an excellent target for immune response against iRBCs. CD spectra analysis and NMR studies have shown that HABP 6671 displays a  $\beta$ -turn type III structure while HABP 6673 presented a very distorted short  $\alpha$ -helical region<sup>132</sup> (Figure 11).

Cappai et al.<sup>383</sup> have described the presence of a highly homologous *resa* gene in *P. falciparum*,<sup>383</sup> which has been called *resa-2*. Even though genes encoding RESA and RESA-2 are located in different chromosomes, it is obvious that they belong to the same family. This finding has raised the question of whether RESA-2 could supply RESA's function in parasites that are deficient in this protein. RESA-2 transcription has been observed in different isolates, whether these were able to express the RESA protein or not.<sup>384</sup>

## 6.2. RESA-like Protein

Following completion of the *P. falciparum* genome sequencing project, many protein-encoding sequences have been made available.<sup>385</sup> The challenge lies in characterizing and identifying those which are functionally relevant. Clarifying their biological function is of supreme importance in developing potential targets as candidates for an anti-malarial vaccine. Identifying optimal or functional antigens represents a fascinating alternative and has broadened the perspectives for work in this field since many of the parasite's antigenic proteins have had their sequences described; however, their role regarding protective immunity still remains unknown. The RESA-like protein (PFL2535w) has, thus, been taken as the target for our study in the search for interesting new antigens having biological relevance or fulfilling a possible role during merozoite invasion.

This protein is homologous to *P. falciparum* RESA.<sup>366,385</sup> Specific primers used in PCR and RT-PCR assays have led to determining that the gene encoding this protein is both present and being transcribed in the *P. falciparum* FCB-2 strain 16 h after RBC invasion.<sup>386</sup> *Pf resa-like* gene transcription was assessed by PCR amplification using total RNA extracted from early ring (3 h), late ring (16 h), and schizont (36 h) stages. A 400 bp fragment was obtained after only 16 h in late-ring-stage iRBCs, showing this gene's fundamental transcription during this stage. Indirect immunofluorescence studies with goat antipeptide antiserum have led to detecting this protein on iRBC cytosol in MC-like dense fluorescent granules when the parasites are in both ring and trophozoite stages after 16–20 h (Figures 1E5 and 1E6) and very strongly on iRBC membranes at 22 h.<sup>386</sup> This suggests that this protein is synthesized during early ring

stages (16 h) and transported to the iRBC membrane surface during the trophozoite stage (22 h) (Figures 1E1 and 1E2).

Western blotting has shown that antisera produced against polymerized synthetic peptides from this protein recognized a 72 kDa band in *P. falciparum* schizont lysate.<sup>386</sup> Normal RBC binding assays using *P. falciparum* RESA-like synthetic peptides have revealed that peptides 30326 (<sup>101</sup>NAE-KILGFDDKNILEALDLFY<sup>120</sup>), 30334 (<sup>281</sup>RVTWKKLRT-KMIKALKKSLTY<sup>300</sup>), and 30342 (<sup>431</sup>SSPQRLKFTAGGG-FCGKLRNY<sup>450</sup>) bound with high activity (Figures 6 and 9) and saturability, presenting dissociation constants in the 400–800 nM range.<sup>386</sup>

The peptides being studied inhibited *P. falciparum* *in vitro* invasion of normal RBCs by up to 91%, depending on concentration, suggesting that some RESA-like protein regions are involved in intra-RBC stage *P. falciparum* invasion.<sup>386</sup> CD revealed that they all presented  $\alpha$ -helical structural elements, although HABP 30324 displayed a highly distorted  $\alpha$ -helical structure.<sup>386</sup> Similar to RESA, HABP 30326 is located 30 residues downstream a classical PEXEL motif found in this protein, suggesting that it could be a member of the protein families involved in transport (transportome) of other molecules, nutrients, etc., between the surrounding environment and the parasite.<sup>203,362</sup>

## 6.3. Histidine-Rich Proteins

The RBC stage of *P. falciparum* synthesizes a family of proteins characterized by having unusually high histidine content. The knob-associated histidine-rich protein (KAHRP) (PFB0100c), also known as histidine-rich protein-I (HRP-I), is a conserved protein having molecular weight ranging from 85 to 105 kDa. The gene encoding this protein is located on chromosome 2 and is expressed during the middle and late stages of the malarial parasite's asexual cycle.<sup>387,388</sup> The KAHRP protein is essential for microvascular sequestration, a strategy where an iRBC adheres to capillary vessels via knob-like structures to avoid the parasite being eliminated by the spleen. The knob is a small plate-shaped electrodense structure forming the base of a protuberance on iRBC membranes. Several parasite proteins have been associated with these structures; however, the main component is the KAHRP protein.<sup>389–392</sup> KAHRP has also been involved in rosetting since KAHRP monoclonal antibodies spontaneously disrupt formed *P. falciparum* RBC rosettes.<sup>363</sup>

KAHRP interacts with various RBC cytoskeletal components including spectrin, actin, spectrin–actin–band 4.1 complexes, and the ankyrin band 3 binding domain.<sup>390,393–395</sup> These interactions modify parasite-infected RBCs' mechanical properties.<sup>357</sup>

KAHRP presents three different domains: a histidine-rich amino terminal domain (region I), a central lysine-rich domain (region II), and a repeat decapeptide one in the C-terminal extreme (region III).<sup>387,396</sup> Two KAHRP regions independently bind to the *PfEMP1* acidic terminal sequence: the 63-residue histidine-rich and 70-residue 5' repeats.<sup>397</sup>

The absence of KAHRP on RBC membrane leads to weak interaction between *PfEMP1* protein and vascular endothelium cells, allowing the severity of obstruction to become attenuated, thereby leading to attenuation of vascular complications accompanying cerebral malaria.<sup>389</sup> Histidine-rich protein-II (HRP-II) is a histidine- and alanine-rich protein characterized by repeats having Ala-His-His (AHH) and Ala-His-His-Ala-Ala-Asp (AHHAAD) sequences, with a molecular weight ranging from 65 to 104 kDa.<sup>398</sup>

HRP-II is synthesized in immature parasites (ring stages) and throughout the trophozoite stage. HRP-II is present in parasite cytoplasm, in culture supernatants as a secreted soluble protein,<sup>399,400</sup> as concentrated packets in host-RBC cytoplasm, on iRBC membrane, and in the plasma of humans suffering from malaria.<sup>400</sup>

HRP-II has been implicated as a heme polymerase, and it has been shown that each hexapeptide repeat sequence (AHHAAA) provides one heme binding site. Even though the exact polymerization mechanism remains unknown, it has been proposed that HRP-II may facilitate hemoglobin transport to the food vacuole and catalyze polymerization.<sup>401,402</sup> HRP-II is used as an antigen for the specific diagnosis of malaria.<sup>403,404</sup>

HRP-III, or small histidine alanine-rich protein (SHARP) (MAL13P1.4B), has a 35–40 kDa molecular weight; it is not as abundant as HRP-I and HRP-II proteins. It has been described that the deduced amino acid sequence of HRP-III contains separate blocks of hexapeptide and pentapeptide repeat sequences and that it is highly polymorphic in different *P. falciparum* isolates.<sup>405</sup> *hrp-II* and *hrp-III* genes are closely related in both encoding and nonencoding regions. Experimental evidence has indicated that they are related by an ancestral duplication and interchromosome transposition.<sup>406,407</sup> However, HRP-III's location and specific function have yet to be established.

*P. falciparum* membrane-associated HRP-I (MAHRP-1) is a 29 kDa protein located in MC; it is exclusively expressed during early RBC stages but is present throughout the cycle.<sup>408</sup> The MAHRP-1 sequence contains a predicted transmembrane domain and a polymorphic cluster of histidine-rich repeats and specifically binds to ferriprotoporphyrin in vitro. MAHRP's precise function remains unclear; however, it is likely to be involved in protein trafficking and may protect against oxidative damage.<sup>408</sup>

Our studies using synthetic peptides have shown that KAHRP-derived peptides 6767 (<sup>1</sup>MKSFKNKNTLRRKKAF-PVFT<sup>20</sup>), 6783 (<sup>321</sup>QNYVHPWSGYSAPYGVPHGA<sup>340</sup>), 6786 (<sup>381</sup>KSKKHKDHDGEEKKSKKHKD<sup>400</sup>) and 6789 (<sup>441</sup>KKREKSIMEKNHAAKLLTKK<sup>460</sup>), and HRP-II-derived peptide 6800 (<sup>1</sup>NNSAFNNLCSKNAKGLNLN<sup>20</sup>) specifically interacted with RBCs (Figures 6 and 9) and presented nanomolar dissociation constants.<sup>72</sup> Conserved KAHRP peptide 6767 is located in the protein's N-terminal extreme, and it is located 35 residues upstream to the PEXEL motif required for exporting soluble proteins in *P. falciparum*.<sup>203</sup>

Peptide 6786 is contained in the KAHRP region to which the cytoskeleton ankirin proteins and the *P. falciparum* EMP-1 protein bind, forming part of a 72 amino acid long region from the KAHRP protein (residues 370–441, shown in fuchsia in Figure 6), which also interacts with spectrin,<sup>395</sup> indicating that the peptide could be involved in knob formation.<sup>393,397</sup> We found that the binding of conserved HABP 6786 was inhibited by anti-GpA, B, and C antibodies by up to 84% and that the number of receptor sites per cell for this peptide became reduced when RBCs were enzymatically treated with trypsin and neuraminidase, indicating that binding to RBCs could be associated with glycoporphins and sialic acid.<sup>72</sup> CD analysis of secondary structure showed that peptides 6767 and 6786 had random structural features (Figure 11).

HABP 6786 was not immunogenic and did not induce antibodies when used as an immunogen in *Aotus* monkeys.

However, peptide analogue 24224 (KSKKHMDLDGEMM-MAKKLKD) presented two helical regions, was immunogenic, and induced protection. Immunogenicity and protection induction was associated with peptide 24224 binding to the HLA-DRβ1\* 0301 molecule.<sup>409</sup>

It is interesting to note that HRP-II protein-derived HABP 6800 binding to RBCs was also inhibited by antiGpA, B, and C antibodies, but only by up to 35%. Similar to HABP 6786, the number of receptor sites per cell for HABP 6800 became reduced by up to 50% when RBCs were enzymatically treated before the binding assay. This suggested that HRP-II HABP 6800 binding to RBCs was associated with proteins and/or glycoproteins having sialic acid residues.<sup>72</sup> CD spectra analysis showed that HABP 6800 had a random structure.<sup>132</sup> The HRP-II protein HABP 6800 also forms part of the vacuolar transport mechanism involving the PEXEL motif (located two residues downstream this HABP) required for secreting proteins from the *P. falciparum* vacuole to the human RBC<sup>410</sup> and making it part of the transportome protein family.

#### 6.4. *P. falciparum* Erythrocyte Membrane Protein-1 (PfEMP-1)

The host RBC membrane undergoes a series of changes during the parasite's intraerythrocyte development, including formation of structures such as protrusions, increased rigidity, altered metabolite transport, and insertion of parasite-derived proteins on iRBC membrane. The dominant antigen is *P. falciparum* erythrocyte membrane protein-1, PfEMP-1<sup>357</sup> (PFA0005w). This protein has been related to *P. falciparum*-iRBC binding to the vascular endothelium (cytoadherence or sequestration) and to non-iRBC (rosetting), contributing toward morbidity and mortality caused by severe malaria.<sup>364,411</sup>

PfEMP-1 is an antigenically variant polypeptide having a high molecular weight (200–350 kDa)<sup>412,413</sup> and is encoded by a large multigene family (named *var* genes), which is highly polymorphic and organized into two exons. Most of the molecule is exposed on the iRBC surface, consisting of a long extracellular region, a transmembrane (TM) domain, and an intracellular acidic terminal segment (ATS), with the last two being encoded in exon 2.<sup>357,412,413</sup>

The extracellular region of PfEMP-1 has the N-terminal segment (NTS), 2–9 domains including different DBLs (DBLα–ε), cysteine-rich interdomain regions (CIDRα–γ), and C2 domains.<sup>357,414</sup> Several studies have shown that most PfEMP-1 adhesion activity is located in the semiconserved head structure composed by NTS, DBLα, and CIDRα but associated with the last two domains mediating binding to several independent host receptors.<sup>49,414–416</sup>

The NTS domain, unique to *P. falciparum* and PfEMP-1, is present in all PfEMP-1 proteins, ranging in length from 75 to 107 amino acids, predicted to be globular, and always preceding the DBLα forming PfEMP-1 conserved head structure with CIDRα.<sup>414</sup> No adhesion property has been described for the NTS domain to date.

DBLα is the most conserved DBL domain, has extensive length divergence, and possesses adhesive properties involved in iRBC rosetting and cytoadherence or sequestration.<sup>359,415,417,418</sup> DBLα specifically binds to heparan sulfate (HS), blood group antigen A (BgA), and CD35 (CR1) on uninfected RBCs (rosetting) and binds to HS on endothelial cells (sequestration) and has, thus, been associated with severe malaria.<sup>357,359,417</sup>

DBL $\beta$  binds to CD31 and ICAM-1, and DBL $\gamma$  binds to chondroitin sulfate A (CSA).<sup>360,419</sup> CIDR domains are also variable in sequence but related by the conserved cysteine-rich motif CX<sub>7-12</sub>CX<sub>3-5</sub>CX<sub>3</sub>CX<sub>1-2</sub>CXWX<sub>7-8</sub>W and mediate binding to CD36, CD31, IgM, and CSA.<sup>360,420</sup> Binding to CSA and HS is associated with placental malaria and binding to CD36 and ICAM-1 with cerebral malaria.<sup>360,421</sup>

The acidic PfEMP-1 ATS domain is highly conserved; it binds to the KAHRP protein's 63 amino acid long, histidine-rich region via electrostatic interactions. It has been proposed that this interaction is the point for the PfEMP-1 protein to anchor to the knobs, thereby contributing toward the adhesion phenomena in which PfEMP-1 participates.<sup>422,423</sup>

We used receptor–ligand binding assays for examining NTS and DBL $\alpha$  region amino acid sequences for potential C32 cell RBC binding motifs. Binding assays revealed that eight peptides corresponding to the PfEMP-1 NTS-DBL $\alpha$  region specifically bound to C32 cells: 6504 (<sup>1</sup>MVELAKMGPKEAAGGDDIED<sup>20</sup>), 6505 (<sup>21</sup>ESAKHMFDRIGKDVYDKVKE<sup>40</sup>), and 6506 (<sup>41</sup>YRAKERGKGLQGRLSEAKFEK<sup>60</sup>) in the NTS region, and 6510 (<sup>121</sup>GACAPYRRLHVCQDNLEQIE<sup>140</sup>), 6512 (<sup>161</sup>EGQSITQDYPKYQATYGDSP<sup>180</sup>), 6515 (<sup>221</sup>LKTIEGKIYEKLNAGAEARYG<sup>240</sup>), 6518 (<sup>281</sup>GERTKGYCRCNDDQVPTYED<sup>300</sup>), and 6520 (<sup>321</sup>YNKKIKDVKRNCRGKDKEDKD<sup>340</sup>) in the DBL $\alpha$  domain.<sup>424</sup>

No HABPs were found having specific human RBC binding among those peptides corresponding to the DBL $\alpha$  domain, which specifically bind to RBCs.<sup>415</sup> It is probable that a larger-sized fragment or a specific configuration was required in this case, so that specific DBL $\alpha$ –RBC interaction could take place. It has been reported that PfEMP-1 putative CSA binding sequence activity is formation-dependent, suggesting nonlinear binding motifs.<sup>358</sup>

It has, however, been suggested that DBL $\alpha$  may encode more than one binding domain, depending on the primary sequence.<sup>414</sup> It is worth stressing that HABPs 6504, 6505, and 6506 (semiconserved sequences) were located in the NTS domain. There have been no reports that this domain participates in any adhesion phenomena; however, the PEXEL motif in *P. falciparum* is located in this region.<sup>203</sup>

HABP 6505 (<sup>21</sup>ESAKHMFDRIGKDVYDKVKE<sup>40</sup>) located in the NTS domain was neither immunogenic nor protective; therefore, based on our previous reports, critical amino acids (shown in bold and underlined) in C32 cell binding were recognized and replaced to modify HABP immunogenicity- and protection-inducing qualities. Analogue peptide 12722 (ESAKH**K**FD**R**IGK**D**VYD**M**VKE) produced high antibody titers and completely protected 3 monkeys out of the 12 vaccinated. Analogue 23410 (KH**K**FD**F**IG**K**IVYD**M**V**K**ER) also produced very high titers, protecting 1 out of 8 vaccinated *Aotus*. <sup>1</sup>H NMR studies showed that all peptides were helical. These peptides' binding to isolated HLA-DR $\beta$ 1 molecules revealed no preferences, suggesting that they could be binding to molecules not so far included in our studies.<sup>424</sup>

<sup>1</sup>H NMR studies included lead peptide 6505, as well as analogues 12720 (nonprotective) and 12722, showing that all peptides presented an  $\alpha$ -helical structure, although differences were observed in helix location and extension.<sup>424</sup> This is interesting, since a conserved feature has been reported for the NTS domains in the central block of amino acids (including HABP 6505) which is expected to have an  $\alpha$ -helical fold.<sup>414</sup>

Previous studies with the DBL $\alpha$  domain have shown that antibody responses from semi-immune individuals are predominantly directed toward variable epitopes. It has been suggested that such immune evasion mechanism used by the parasite could be avoided by using conserved epitopes from the extracellular part of PfEMP-1.<sup>425</sup> Our results have shown that modifications made to certain conserved PfEMP-1 HABP segments were effectively able to make these non-immunogenic, nonprotective peptides become immunogenic and protection-inducing and that these changes were associated with 3D structure modifications.<sup>424</sup>

## 7. Supporting Background for the Subunit-based Synthetic Vaccine Concept

### 7.1. Conserved HABP Structural Characteristics

#### 7.1.1. Functional and Structural Compartmentalization of Merozoite Proteins Involved in RBC Invasion

The 150 peptides shown in the present manuscript corresponded to conserved HABPs from the 35 most relevant proteins involved in merozoite invasion of RBC (their secondary structure as determined by CD is shown in Figures 10 and 11). Some principles have begun to emerge: Merozoite **membrane** HABPs from proteins having a GPI tail anchoring them to the membrane (shown with red spheres at the C-terminus in Figure 9), such as 5501 (MSP-1), 4044 (MSP-2), 20494 (MSP-4), 26373 (MSP-8), 31132 (MSP-10), 33633 (Pf12), 33645 and 33648 (Pf38), 33667, 33675 and 33680 (Pf92), and 33746 (Pf113), all had a very high percentage of  $\beta$ -turn and/or unordered nonhelical structures as assessed by CD (Figures 10 and 11) and confirmed by X-ray crystallography and <sup>1</sup>H NMR for HABPs 5501 and 4044.<sup>135,152,426</sup> These data suggest that these GPI-membrane anchored protein fragments display  $\beta$ -turns or unordered structures in their HABPs, which could provide them with tremendous segmental atomic mobility.

Type I transmembrane protein AMA-1 HABPs (4313, 4322, and 4337) also presented highly unordered structures as shown by our CD analysis and the complete AMA-1 structure protein determined by X-ray crystallography.<sup>132,268–270</sup> AMA-1 is originally deposited in the micronemes and located in the merozoite's apical region, later becoming translocated to its membrane and allowing merozoite reorientation toward RBC membrane. The short distorted  $\alpha$ -helix present in this protein's domain II<sup>269</sup> (Figure 14C in pink) and our 4325 HABP 3D structure determined by <sup>1</sup>H NMR (Figure 14C in dark brown) located in this molecule's region displayed 0.99 Å rmsd when overlapped. The previous suggests that these two structures are very similar in spite of the two different methodologies used for determining their 3D structures.

HABPs found in the N-terminal region preceding the PEXEL motif<sup>203</sup> from proteins transported from the merozoite to the RBC (Figure 10), such as those found in GBP-130<sup>68</sup> (2220), RESA<sup>573</sup> (6671), KAHRP<sup>72</sup> (6786), and HRP-II (6800),<sup>72</sup> have displayed a  $\beta$ -turn, a strand, or an unordered structure as determined by our CD analysis and <sup>1</sup>H NMR structural determinations for HABPs 6671, 6786, and 6800.<sup>132</sup>

Supporting our findings, it has been described very recently that many *P. falciparum* proteome proteins are completely unordered or present large unordered regions,<sup>427</sup> these are often involved in key biological processes, such as membrane fusion, transport, cell translation, signaling, and large multi-

protein complex self-assembly regulation processes.<sup>428</sup> RESA, MSP-2, HRP-II, and GBP-130 have been described as being some of them.

Conserved membrane **surface** protein HABPs (MSP HABPs) or their fragments involved in merozoite rolling over the RBC membrane present preponderantly  $\alpha$ -helical structure as determined by <sup>1</sup>H NMR, such as MSP-1 (1513, 1522, and 1585),<sup>133,134,136</sup> MSP-3 (31193, 31202, and 31209),<sup>78</sup> MSP-6 (31191),<sup>160</sup> and MSP-8 (26360, 26361, 26368, and 26369).<sup>74,132</sup> They are not transported inside the RBCs; do not mediate the transport of substances from the interior of the merozoite to the iRBCs and vice versa, and do not have a GPI tail. The same  $\alpha$ -helical pattern has been displayed by MSP-9 or ABRA (2148, 2149, and 2150)<sup>71,132</sup> and MSP-10 (31121) HABPs.<sup>196</sup>

MSP-1 is proteolytically processed in natural conditions during invasion and containing these HABPs forms macromolecular complexes for interacting with some RBC membrane proteins, as occurs with the MSP-1 33 kDa fragment (where conserved HAPB 1585 was located).<sup>64</sup> MSP-1 33 kDa fragment associates with MSP-9 or ABRA, forming a stable macromolecular complex that binds to band 3 RBC protein via a region containing MSP-9 HABPs 2148, 2149, and 2150 (fuschia in Figures 9 and 13).<sup>116</sup>

MSP-1 cleavage fragments also form macromolecular complexes with MSP-6 and MSP-7.<sup>111</sup> MSP-6 in its tetrameric form binds to MSP-1 38 kDa fragment, while the MSP-7 precursor has been shown to interact with MSP-1 83 kDa (where 1513 and 1522 HABPs were located), 30 kDa, and 38 kDa fragments but not with the 42 kDa fragment (Figure 13). All HABPs present in these cleavage fragments have displayed an  $\alpha$ -helical structure.

It should be stressed that none of these fragments is transported within the cytoplasm of newly invaded RBCs, being released into the milieu. Only the MSP-1 19 kDa fragment anchored to the merozoite via a GPI tail (where HAPB 5501 was located) has been found inside newly invaded RBCs.<sup>88</sup>

Regarding MAEBL (presenting a hybrid structure between AMA-1 protein and EBL proteins),<sup>289</sup> the first two conserved HABPs (30181 and 30195) located in the M1 region as well as HABPs 302112 and 30220 located in the M2 region (having the greatest homology with AMA-1) had  $\beta$ -turn, strand, or unordered configurations, as happened with conserved AMA-1 protein HABPs (Figures 10 and 11).<sup>132</sup> Soluble protein-derived HABPs loosely bound to the merozoite **membrane**, performing some enzymatic activity such as SERA-5 (6725, 6733, 6737, 6746, 6754, and 6762),<sup>227</sup> were all  $\alpha$ -helical as determined by CD (Figure 11) and confirmed by <sup>1</sup>H NMR for 6737, 6746, and 6762.<sup>230,429,430</sup>

Similar structural patterns were observed with **microneme** proteins. The main protein from this group (EBA-175)<sup>67</sup> is immediately processed upon being released (exposing  $\alpha$ -helical 1758 HAPB) and further cleaved, liberating a 65 kDa fragment (where conserved HABPs 1779 and 1783 were found) located in this protein's so-called F1 (Figure 5, red square) and F2 (Figure 5, pink square) regions. HABPs 1758, 1779, and 1783 presented  $\alpha$ -helical structure as assessed by CD and <sup>1</sup>H NMR.<sup>67,250–252</sup> This data (confirmed by X-ray crystallography studies of the recombinant fragment called EBA-175 region II) showed that the sequences corresponding to these HABPs' location were entirely  $\alpha$ -helical,<sup>242</sup> totally agreeing with our <sup>1</sup>H NMR and CD studies (Figure 14B). This strongly supports the usefulness of 15–25-mer-long

peptides for assessing biological functions such as receptor–ligand interactions and immunological responses.

All HABPs located in the F1 (red squares) and F2 (pink squares) regions in Figures 5 and 6 presenting high homology with DBL regions and acting as contact sequences with RBC membrane sialoglycoproteins in proteins EBA-181 (30031, 30045, 30051, and 30058), EBA-140 (26128, 26135, 26144, and 26147), and EBL-1 proteins (29903, 29907, 29923, and 29924) displayed  $\alpha$ -helical structures (Figures 5, 6, 9, and 10).

It has been shown that those EBAs and EBL-1 protein fragments staying anchored to the membrane are processed by rhomboid-like enzymes, called shedases,<sup>431</sup> during the last moments before the complete merozoite's penetration into RBCs, leaving their last 100 residues anchored by their transmembrane fragments, with the rest of the molecule being released to the milieu after having fulfilled its RBC adhesion function (i.e., the above-mentioned HABPs).

We have very recently found that conserved HABPs located in close proximity (maximum 20 amino acids upstream) to the cysteine-rich carboxy terminal region, and suggested as being involved in microneme targeting of *P. falciparum* parasite proteins, such as EBA-175 (1818), EBA-140 (26170), EBL-1 (30018), and MAEBL (30270), have displayed  $\beta$ -turn, random, or highly distorted  $\alpha$ -helical structural elements.<sup>132</sup>

A large number of proteins are processed during invasion, and parts of the molecule are trimmed and released.<sup>85,113,177,267</sup> Those HABPs present in regions remaining anchored to the merozoite membrane via GPI tails, or attached to them by intracytoplasmic domains, or containing or being close to PEXEL motifs, or close to regions involved in the trafficking of some EBL proteins to the micronemes, possess a  $\beta$ -turn or random structure. Strikingly, nearly all native HABPs that were released to the milieu when molecules were trimmed have an  $\alpha$ -helical structure.<sup>132</sup>

It is equally interesting to note that all conserved HABPs synthesized in the rhoptries and involved in invasion presented clearly  $\alpha$ -helical structures: RAP-1 (26188, 26201, 26202, and 26204),<sup>79,132</sup> RAP-2 (26220, 26225, 26229, and 26235),<sup>132,334</sup> RAP-3 (33860 and 33873) (unpublished results), NBP-1 (26332),<sup>75,132</sup> and *Pf*RBP-2Ha (26752, 26794, 26796, 26801, 26803, 26805, 26807, and 26818).<sup>132,317</sup> The same happened with CLAG 3.2 HABPs (30373, 30403, 30409, 30414, and 30421)<sup>132,355</sup> and RhopH3 (30482, 30483, 30484, 30487, 30521, 30522, 30529, 30531, and 30536) (unpublished results).

It can, thus, be suggested that all conserved HABPs derived from molecules involved in initial contact phases between merozoites and RBCs (rolling, such as MSPs), microneme (such as EBAs and EBL-1), and rhoptry (such as RAPs and NBPs) proteins involved in adhesion and penetration, as well as those performing some enzymatic activity such as SERA displayed  $\alpha$ -helical structures and are cleaved and released after processing into the milieu once they have fulfilled their function.

This data clearly shows a functional compartmentalization of proteins involved in merozoite invasion of RBCs for performing specific functions associated with specific 3D structural features, suggesting that different receptor–ligand mechanisms could be involved during merozoite invasion of RBC. The first is present in rolling, where the merozoite rolls over the membrane of several RBCs, establishing specific but not very strong interactions, which will be

mediated by those HABPs that, when the molecule is processed, are released into the milieu. When the merozoite stops rolling over RBCs, a second mechanism involving merozoite reorientation and the beginning of their invagination will be mediated by highly specific and strong interactions between membrane protein fragments that remain anchored to the membrane. These are the only fragments from these molecules that enter the RBC along with the parasite.

As an example of such compartmentalization, MSP-1-derived HABPs 1513, 1522, and 1585, EBA-175-derived HABPs 1779, 1783, and 1815, and SERA-5 protein-derived HABPs (6733, 6737, 6746, and 6762) all had  $\alpha$ -helical structure. All these HABPs involved in merozoite invasion were shed (following processing) during such an invasion.<sup>132</sup>

HABP 5501 (located in the 19 kDa C-terminal fragment of the MSP-1 protein, remaining anchored to the merozoite membrane by a GPI tail), MSP-2 protein HABP 4044 (also having a GPI tail), HABPs 4313, 4325, and 4337 (present in AMA-1 protein transmembrane fragments remaining bound to the merozoite membrane), and many more presented in this review have all presented a  $\beta$ -turn or random structure by CD.<sup>132</sup> The importance of CD analysis of HABPs' CD-assessed secondary structure in this manuscript. The above data suggests that using a simple methodology such as CD to determine any peptide's secondary structure could lead to redesigning it so that it could fit into its appropriate HLA-DR molecule and thereby induce a specific protection-inducing immune response.

The Dictionary of Secondary Structure of Proteins (DSSP)<sup>432</sup> has identified three helix-types ( $3_{10}$  or G;  $\alpha$  or H;  $\Pi$  or I), turns (represented by T), strands (E), bridges (B), bends (S), and other secondary structures (L), leaving enough space to recognize native HABPs that could fit properly into any of the HLA-DR $\beta$  molecules' 16 alleles to design molecules able to induce an appropriate immune response.

However, conserved HABPs are not antigenic or immunogenic, nor protection-inducers regarding natural or experimentally induced infection. Critical residues in binding to receptor cells have, therefore, been identified to resolve this problem.<sup>81,134,136,252</sup> Hundreds of peptides having had different modifications made to them have, thus, been synthesized to find a way of making them immunogenic and protection-inducing regarding experimental challenge in a statistically significant number of *Aotus* monkeys, but these results are beyond the scope of this manuscript.

### 7.1.2. Minimal Subunit-based Synthetic Peptide Vaccine Concept is Correct

It has often been suggested that short peptides (15–25 mer long) do not mimic the 3D structure they display in the native protein, casting some doubts on the minimal epitope approach and on the subunit-based synthetic peptide vaccine concept, suggesting that only long or complete proteins could induce protective immunity, because of their folding characteristics.

However, the 3D structure of our native conserved HABPs obtained by <sup>1</sup>H NMR contradicts this concept when compared to the segments where they are located in the few malarial recombinant proteins analyzed by X-ray crystallography or <sup>1</sup>H NMR described in the past few years.<sup>131,135,242,252,271,287</sup>

X-ray crystallographic determination of the 3D structure of the MSP-1 19 kDa fragment<sup>131</sup> (PDB accession no. 1OB1) (Figure 14A, light brown) has shown that this fragment's N-terminal region (where our HABP 5501 is located) is totally random (shown in white), thereby confirming our CD spectra (Figure 10) and <sup>1</sup>H NMR analysis of this peptide.<sup>135</sup>

More recently, X-ray crystallography has revealed an  $\alpha$ -helical region located between residues 580–589 (Figure 14B in red) completely corresponding to our HABP 1783 amino acid sequence present in recombinant EBA-175 region II 3D structure<sup>67,242,252</sup> (PDB accession no. 1ZRL) (Figure 14B in yellow). These amino acid sequences (Figure 14B in red) from recombinant protein and HABP 1783 (Figure 14B in green) displayed 0.89 rmsd when they were overlapped (Figure 14B, red and dark-green structures).

The secondary structure of HABP 1779 (located in residues 500–519 in the EBA-175 protein and colored in sepia in Figure 14B) displayed a clearly distorted  $\alpha$ -helical structure in recombinant EBA-175 region II 3D structure,<sup>242</sup> very similar to that shown in CD spectra analysis, where it also displayed a distorted  $\alpha$ -helix. Unfortunately, this HABP was insoluble for <sup>1</sup>H NMR studies.

X-ray crystallographic 3D structure determined for AMA-1 protein domain II<sup>271</sup> (Figure 14C in pink) (PDB accession no. 1YXE) where RBC HABP 4325 was located (residues 374–393, red) showed that this protein segment contained a short  $\alpha$ -helical structure between residues 384 and 387, similar to that displayed by native HABP 4325<sup>287</sup> (Figure 14C in dark brown) between residues 13 and 16. When the two structures were overlapped, they displayed a 0.99 Å rmsd. Native 4325 HABP presented 46% distorted  $\alpha$ -helix (Hd) and 37% unordered (unrd) structural configuration in CD deconvolution studies, thereby supporting these findings and completely agreeing with the structure that this native conserved HABP displayed in AMA-1 protein domain II and <sup>1</sup>H NMR studies.<sup>287</sup>

The 3D structure of the *P. falciparum* TRAP sporozoite protein as determined by <sup>1</sup>H NMR<sup>433</sup> (PDB accession no. 2BBX) (Figure 14D) where our hepatocyte HABP 3287/3289 was located displayed a  $\beta$ -turn structure between residues 241 and 265<sup>434</sup> (Figure 14D in dark blue). Our TRAP 3287/3289 HABP presented the same  $\beta$ -turn structure between residues 8 and 11 (Figure 14, fuchsia) displaying 1.5 Å rmsd when the two fragments were overlapped, thereby completely agreeing with our CD and <sup>1</sup>H NMR structural determinations<sup>435</sup> (Figure 14D).

The 3D structure of the MSP-2 protein's conserved N-terminal region has been recently determined by <sup>1</sup>H NMR in a recombinant fragment (residues 1–25) produced on *E. coli* and dissolved in TFE (Figure 14F).<sup>153</sup> A  $\beta$ -turn type III was found in such a structure, identical to our results as determined by <sup>1</sup>H NMR in dimethylsulfoxide (DMSO) but displaced by two residues<sup>152</sup> (Figure 14E).

Conserved HABPs 5501, 1783, 4325, and 4044 have shown that they are able to block invasion of new RBCs. We have also shown that their ability to bind to RBCs was specifically inhibited when host cells were enzymatically treated and that radio-labeled conserved HABPs specifically and strongly bound to specific proteins on host-cell membrane,<sup>54,64,67,76</sup> as determined by the cross-linking methodology.

All this structural data provided by different techniques determining identical secondary and 3D structures for configurations in recombinant proteins and synthetic HABPs,

strongly supports the idea that short HABPs (15–25 mer long) mimic the structural configuration they display in their native proteins and that they could, therefore, be performing similar biological functions.

By the same token, these HABPs have displayed very similar secondary structures (as assessed by CD spectra) in monomer<sup>132</sup> or polymer form, making them excellent tools for studying the immunological responses that they will induce when polymerized, suggesting that the immune response elicited by them could be similar to that induced by monomers in natural conditions (infection or immunization). These structural agreements provide strong support for the minimal subunit-based, chemically synthesized vaccine concept, making identifying conserved HABPs essential for a rational, ongoing vaccine development approach.

## 8. Implications for Vaccine Design and Perspectives

The recently described *P. falciparum* genome has shown that it contains genetic information encoding the synthesis of ~5 300 proteins, with a good number of them being unknown or not having an established function.<sup>385</sup> Proteome and transcriptome studies of each of the parasite's stages has suggested that 50–90 of these proteins are directly involved in merozoite invasion of RBCs. Many of them have been analyzed here, and their amino acid sequences involved in binding to RBCs (HABPs) have been described in this manuscript.<sup>436,437</sup>

It has been shown that these proteins form interactive networks<sup>157</sup> where 75 such interactions have been described between 16 of the proteins analyzed here (MSP-1 to MSP-9, EBAs, RAPs, Rhops). A further 19 proteins have still to be characterized, of which 6 have been detected on the merozoite membrane by mass spectrometry and 4 more have signal peptides, suggesting that they display transmembrane domains. Other interactions link MSP proteins to proteins located in the rhoptries, indicating the potential for transient molecular interactions that occur during invasion of RBCs once the content of these organelles has been released.

It has been shown that the proteins covering most of the merozoite surface are bound to the membrane via a GPI tail; this has proved true for MSP-1, -2, -4, -8 and -10 and for the 4 new molecules having this type of anchoring (called *Pf113*, *Pf92*, *Pf38*, and *Pf12*). All these molecules, together with MSP-4 and -5, are bound together on the merozoite membrane, forming raft-like structures. MSP-10 and RAMA (also binding to the membrane via GPI tails) seem to be located in the organelles of the merozoite's apical pole.<sup>18,114,438</sup>

The other MSPs (such as MSP-3, -6, -7, and -9) seem to be associated with GPI-anchored proteins. MSP-8 is known to be associated with parasite membranes during the ring stage. Proteins having a GPI tail seem to be essential for parasite invasion and growth since attempts to disrupt six GPI-anchored merozoite membrane proteins have shown that only MSP-5 is not required for the parasite's normal growth.<sup>18,438</sup>

Thirteen proteins have been identified in DRM-enriched preparations, also known as lipid rafts. They can be classified into those having a demonstrated GPI tail, those having a predicted GPI tail (i.e., presenting a N-terminal signal sequence and a hydrophobic C-terminal domain), proteins binding to those having a GPI tail, and proteins predicted as binding to those having a GPI tail. Proteins from the RhopH-1, -2, and -3 and RAP-1, -2, and -3 complexes that are also

present in DRM preparations seem to be associated with the RAMA protein, which has been shown to have a GPI tail.<sup>114</sup>

The presence of multiple ligands that can be switched-on or turned-off during invasion (as happens with EBAs) must be added to the above complexity. In the absence of a sialic acid receptor on GpA, EBA-175 can use other routes that are independent of sialic acid for mediating invasion.<sup>247</sup> Their absence can also increase the synthesis of other RBC binding proteins such as EBA-140 and EBA-181, which use some other alternative receptors.<sup>254,257</sup> Other proteins act as invasion pathway regulators in the neck of the rhoptries by expressing and/or silencing the *Pfrrbp-h4* gene whose protein is located together with the *PfRBP-2Ha/b* proteins analyzed here, probably acting directly on invasion. When EBA-175 and *PfRBP-H1*, -2Ha, and -2Hb levels are high, *PfRBP-H4* levels are low and vice versa. Multiple receptor–ligand interactions must, thus, be blocked to prevent the parasite adapting itself to invade via alternative routes.<sup>39,315</sup>

The difficulty in blocking merozoite invasion of RBCs becomes more complex as there are whole families of genes (i.e., *var.*, *rif.* or *stevor*) encoding the synthesis of proteins involved in RBC invasion or adhesion to other cells (i.e., endothelial or placental cells), thereby avoiding passage through the spleen and avoiding the action of the immune system. These molecules display tremendous genetic variability that (depending on the receptors present in these and/or other cells) could ensure the switching-on or turning-off of the synthesis of those molecules needed for fulfilling their function or also avoiding the immune response. Many *PfEMP-1*, *STEVOR*, and *RIFIN* proteins display very small, conserved fragments, signifying a formidable challenge for the immune system in dealing with such tremendous genetic variability.<sup>362</sup>

Other molecules accumulate under the iRBC membrane, forming protuberances or knobs that make iRBCs bind to other noninfected RBCs forming rosettes or to endothelial cells. These molecules (such as the histidine-rich KAHRP and HRP-2 proteins studied here) present some common amino acid or PEXEL motifs (as do many other molecules involved in parasite molecular communication and traffic with their exterior) to establish communication pathways between the parasite and its surrounding environment.<sup>203</sup>

Other proteins (such as the RESA family) are expressed on the membrane of recently infected RBCs,<sup>362,366</sup> fulfilling functions similar to the foregoing. All of these, and many more which have still to be described, present a formidable challenge for developing a completely effective vaccine against this parasite stage.

This review has shown that many of these molecules are processed and a large number of their fragments are released into the milieu. This could, therefore, induce an immune response against fragments that could act as decoys, being important but not critical in biasing an immune response directed against relevant but not critical membrane-anchored fragments, which are the only ones present on the newly infected RBCs.

Developing a completely effective vaccine against the parasite's blood stage must, therefore, involve a similar number of conserved HABPs derived from these proteins that are directly involved in RBC invasion being blocked by the immune system. Such data, regarding the number of HABPs, their presence, processed and released fragments, network interactions, and merozoite-membrane-rafts shows

the complexity of the processes involved in merozoite invasion of RBCs.

The reasons why we decided to tackle the problem from the multiantigen, multistage, subunit-based synthetic vaccine point of view have been partially explained in section 2 entitled "Defining target molecules for triggering a protective-inducing immune response", and subsection 2.2 entitled "Rationale for high-activity binding peptide recognition." However, there is another reason that becomes much more evident throughout this review, which is the attempt to avoid the tremendous genetic polymorphism of the molecules involved in invasion by working with conserved HABPs.

Immunization with just one of the native variants of these recombinant proteins, either inserted into vectors or presented in DNA used for immunization, implies inducing a strain-specific immune response, since it has been found that immunity induced by these molecules is strain-specific, as thoroughly shown in AMA-1 and so many other proteins.<sup>140,273,439,440</sup> This means that enormous work must be involved in cloning and producing all the molecules (be they recombinant molecules, integrated in vectors, or DNA), and a large quantity of immunogen is also needed for them to be inoculated during vaccination. The required quantities and quality control for each of these molecules is necessary and must be defined for each method.

Even worse, from the immunological point of view, vaccination with a molecule having genetic variability suppresses the immune response, which could be induced by others from the same family.<sup>441</sup> Many other immunological mechanisms besides genetic variability could be unleashed by immunization with complete molecules: antigenic sin,<sup>442,443</sup> evasion using tandem-repeat sequences used as smoke-screens,<sup>52</sup> suppression, dendritic immunological silence of conserved sequences, etc. Recognizing conserved HABPs is imperative, and this can only be done by chemically synthesizing small fragments or HABPs leading to the recognition of such function.

## 9. Acknowledgments

This research has been supported by Colciencias contract 060/2006. Copyright permissions on all material adapted in the figures of this manuscript were granted by their corresponding publishers as follows: MSP-2<sup>54</sup> (2000) and MSP-1<sup>64</sup> (1996), copyrights Blackwell publishing; MSP-3;<sup>78</sup> EBL-1<sup>262</sup> and CLAG 3.2<sup>355</sup> (copyrights 2005) with permission from Cold Spring Harbor Laboratory Press; PTRAMP,<sup>301</sup> RAMA<sup>340</sup> (2008), MSP-6<sup>160</sup> (2006), EBA-181,<sup>253</sup> MSP-10<sup>196</sup> (2005), MSP-8,<sup>74</sup> NBP-1<sup>75</sup> (2003), MAEBL,<sup>289</sup> PfRBP2-Ha and -Hb,<sup>317</sup> RAP-1,<sup>79</sup> RAP-2<sup>334</sup> (2004), MSP-9<sup>71</sup> (2001), SERA,<sup>227</sup> AMA-1,<sup>76</sup> RESA,<sup>373</sup> KAHRP and HRP-II<sup>72</sup> (2000), copyrights Elsevier; GBP-130<sup>68</sup> (2000), copyright Memórias do Instituto Oswaldo Cruz; EBA-175<sup>67</sup> (2000), copyright Cambridge University Press; and EBA-140<sup>259</sup> (copyright 2003) with permission from Wiley-Blackwell publishing. Additionally, 3D structures for MSP-1<sup>131</sup> (Pizarro et al., copyright Elsevier 2003), EBA-175<sup>242</sup> (Tolia et al., copyright Elsevier 2005), AMA-1<sup>269</sup> (Feng et al., copyright Elsevier 2005), and TRAP<sup>433</sup> (Tossavainen et al., copyright Cold Spring Harbor Laboratory Press 2006) have been adapted with the corresponding copyright permissions. We would like to thank Adriana Bermudez, Armando Moreno, and Jairo Perez for contributing diagrams, John Valbuena, Ricardo Vera, and Alvaro Puentes for contributing initial

manuscript redaction, and Jason Garry for translating and reviewing this manuscript.

## 10. References

- (1) Phillips, R. S. *Clin. Microbiol. Rev.* **2001**, *14*, 208.
- (2) hoSilvie, O.; Franetich, J. F.; Charrin, S.; Mueller, M. S.; Siau, A.; Bodescot, M.; Rubinstein, E.; Hannoun, L.; Charoenvit, Y.; Kocken, C. H.; Thomas, A. W.; Van Gemert, G. J.; Sauerwein, R. W.; Blackman, M. J.; Anders, R. F.; Pluschke, G.; Mazier, D. *J. Biol. Chem.* **2004**, *279*, 9490.
- (3) Garcia, J. E.; Puentes, A.; Patarroyo, M. E. *Clin. Microbiol. Rev.* **2006**, *19*, 686.
- (4) Kappe, S. H.; Buscaglia, C. A.; Nussenzweig, V. *Annu. Rev. Cell Dev. Biol.* **2004**, *20*, 29.
- (5) Sennis, P.; Coppi, A. *Parasitol. Int.* **2007**, *56*, 171.
- (6) Langreth, S. G.; Jensen, J. B.; Reese, R. T.; Trager, W. *J. Protozool.* **1978**, *25*, 443.
- (7) Bannister, L. H.; Dluzewski, A. R. *Blood Cells* **1990**, *16*, 257.
- (8) Sinden, R. E. *Parasitology* **1982**, *84*, 1.
- (9) Kats, L. M.; Black, C. G.; Proellocks, N. I.; Coppel, R. L. *Trends Parasitol.* **2006**, *22*, 269.
- (10) Preiser, P.; Kaviratne, M.; Khan, S.; Bannister, L.; Jarra, W. *Microbes Infect.* **2000**, *2*, 1461.
- (11) Dubremetz, J. F.; Garcia-Reguet, N.; Conseil, V.; Fourmaux, M. N. *Int. J. Parasitol.* **1998**, *28*, 1007.
- (12) Bannister, L. H.; Mitchell, G. H. *J. Protozool.* **1989**, *36*, 362.
- (13) Torii, M.; Adams, J. H.; Miller, L. H.; Aikawa, M. *Infect. Immunol.* **1989**, *57*, 3230.
- (14) Lanzer, M.; Wickert, H.; Krohne, G.; Vincensini, L.; Braun Breton, C. *Int. J. Parasitol.* **2006**, *36*, 23.
- (15) Przyborski, J. M.; Wickert, H.; Krohne, G.; Lanzer, M. *Mol. Biochem. Parasitol.* **2003**, *132*, 17.
- (16) Gaur, D.; Mayer, D. C.; Miller, L. H. *Int. J. Parasitol.* **2004**, *34*, 1413.
- (17) Black, C. G.; Wu, T.; Wang, L.; Hibbs, A. R.; Coppel, R. L. *Mol. Biochem. Parasitol.* **2001**, *114*, 217.
- (18) Sanders, P. R.; Kats, L. M.; Drew, D. R.; O'Donnell, R. A.; O'Neill, M.; Maier, A. G.; Coppel, R. L.; Crabb, B. S. *Infect. Immunol.* **2006**, *74*, 4330.
- (19) Cowman, A. F.; Crabb, B. S. *Cell* **2006**, *124*, 755.
- (20) Adams, J. H.; Blair, P. L.; Kaneko, O.; Peterson, D. S. *Trends Parasitol.* **2001**, *17*, 297.
- (21) Adams, J. H.; Sim, B. K.; Dolan, S. A.; Fang, X.; Kaslow, D. C.; Miller, L. H. *Proc. Natl. Acad. Sci. U.S.A.* **1992**, *89*, 7085.
- (22) Michon, P.; Stevens, J. R.; Kaneko, O.; Adams, J. H. *Mol. Biol. Evol.* **2002**, *19*, 1128.
- (23) Peterson, M. G.; Marshall, V. M.; Smythe, J. A.; Crewther, P. E.; Lew, A.; Silva, A.; Anders, R. F.; Kemp, D. J. *Mol. Cell. Biol.* **1989**, *9*, 3151.
- (24) Howell, S. A.; Hackett, F.; Jongco, A. M.; Withers-Martinez, C.; Kim, K.; Carruthers, V. B.; Blackman, M. J. *Mol. Microbiol.* **2005**, *57*, 1342.
- (25) Taylor, H. M.; Grainger, M.; Holder, A. A. *Infect. Immunol.* **2002**, *70*, 5779.
- (26) Kaneko, O.; Mu, J.; Tsuboi, T.; Su, X.; Torii, M. *Mol. Biochem. Parasitol.* **2002**, *121*, 275.
- (27) Kaneko, O. *Parasitol. Int.* **2007**, *56*, 255.
- (28) Baldi, D. L.; Andrews, K. T.; Waller, R. F.; Roos, D. S.; Howard, R. F.; Crabb, B. S.; Cowman, A. F. *EMBO J.* **2000**, *19*, 2435.
- (29) Rungruang, T.; Kaneko, O.; Murakami, Y.; Tsuboi, T.; Hamamoto, H.; Akimitsu, N.; Sekimizu, K.; Kinoshita, T.; Torii, M. *Mol. Biochem. Parasitol.* **2005**, *140*, 13.
- (30) Lobo, C. A.; Rodriguez, M.; Hou, G.; Perkins, M.; Oskov, Y.; Lustigman, S. *Mol. Biochem. Parasitol.* **2003**, *128*, 59.
- (31) Topolska, A. E.; Black, C. G.; Coppel, R. L. *Mol. Biochem. Parasitol.* **2004**, *138*, 237.
- (32) de Koning-Ward, T. F.; O'Donnell, R. A.; Drew, D. R.; Thomson, R.; Speed, T. P.; Crabb, B. S. *J. Exp. Med.* **2003**, *198*, 869.
- (33) Ramasamy, R.; Ramasamy, M.; Yasawardena, S. *Trends Parasitol.* **2001**, *17*, 194.
- (34) Berzins, K.; Perlmann, H.; Wahlin, B.; Ekre, H. P.; Hogh, B.; Petersen, E.; Wellde, B.; Schoenbechler, M.; Williams, J.; Chulay, J.; et al. *Infect. Immunol.* **1991**, *59*, 1500.
- (35) Saul, A. *Parasite Immunol.* **1987**, *9*, 1.
- (36) Pasvol, G. *Trends Parasitol.* **2003**, *19*, 430.
- (37) Kaneko, O.; Fidock, D. A.; Schwartz, O. M.; Miller, L. H. *Mol. Biochem. Parasitol.* **2000**, *110*, 135.
- (38) Lobo, C. A.; Rodriguez, M.; Reid, M.; Lustigman, S. *Blood* **2003**, *101*, 4628.

- (39) Stubbs, J.; Simpson, K. M.; Triglia, T.; Plouffe, D.; Tonkin, C. J.; Duraisingh, M. T.; Maier, A. G.; Winzeler, E. A.; Cowman, A. F. *Science* **2005**, *309*, 1384.
- (40) Dolan, S. A.; Proctor, J. L.; Alling, D. W.; Okubo, Y.; Wellem, T. E.; Miller, L. H. *Mol. Biochem. Parasitol.* **1994**, *64*, 55.
- (41) Mayer, D. C.; Mu, J. B.; Kaneko, O.; Duan, J.; Su, X. Z.; Miller, L. H. *Proc. Natl. Acad. Sci. U.S.A.* **2004**, *101*, 2518.
- (42) Anders, R. F.; McColl, D. J.; Coppel, R. L. *Acta Trop.* **1993**, *53*, 239.
- (43) Kain, K. C.; Orlandi, P. A.; Haynes, J. D.; Sim, K. L.; Lanar, D. E. *J. Exp. Med.* **1993**, *178*, 1497.
- (44) Mitchell, G. H.; Hadley, T. J.; McGinniss, M. H.; Klotz, F. W.; Miller, L. H. *Blood* **1986**, *67*, 1519.
- (45) Narum, D. L.; Haynes, J. D.; Fuhrmann, S.; Moch, K.; Liang, H.; Hoffman, S. L.; Sim, B. K. *Infect. Immunol.* **2000**, *68*, 1964.
- (46) Okoyeh, J. N.; Pillai, C. R.; Chitnis, C. E. *Infect. Immunol.* **1999**, *67*, 5784.
- (47) Reed, M. B.; Caruana, S. R.; Batchelor, A. H.; Thompson, J. K.; Crabb, B. S.; Cowman, A. F. *Proc. Natl. Acad. Sci. U.S.A.* **2000**, *97*, 7509.
- (48) Escalante, A. A.; Lal, A. A.; Ayala, F. J. *Genetics* **1998**, *149*, 189.
- (49) Rasti, N.; Wahlgren, M.; Chen, Q. *FEMS Immunol. Med. Microbiol.* **2004**, *41*, 9.
- (50) Kemp, D. J.; Cowman, A. F.; Walliker, D. *Adv. Parasitol.* **1990**, *29*, 75.
- (51) Hisaeda, H.; Yasutomo, K.; Himeno, K. *Int. J. Biochem. Cell Biol.* **2005**, *37*, 700.
- (52) Kemp, D. J.; Coppel, R. L.; Anders, R. F. *Annu. Rev. Microbiol.* **1987**, *41*, 181.
- (53) Lougovskoi, A. A.; Okoyeh, N. J.; Chauhan, V. S. *Vaccine* **1999**, *18*, 920.
- (54) Ocampo, M.; Urquiza, M.; Guzman, F.; Rodriguez, L. E.; Suarez, J.; Curtidor, H.; Rosas, J.; Diaz, M.; Patarroyo, M. E. *J. Pept. Res.* **2000**, *55*, 216.
- (55) Amante, F. H.; Crewther, P. E.; Anders, R. F.; Good, M. F. *J. Immunol.* **1997**, *159*, 5535.
- (56) Guevara Patino, J. A.; Holder, A. A.; McBride, J. S.; Blackman, M. J. *J. Exp. Med.* **1997**, *186*, 1689.
- (57) Patarroyo, M. E.; Alba, M. P.; Vargas, L. E.; Silva, Y.; Rosas, J.; Rodriguez, R. *Biochemistry* **2005**, *44*, 6745.
- (58) Patarroyo, M. E.; Bermudez, A.; Salazar, L. M.; Espejo, F. *Biochimie* **2006**, *88*, 775.
- (59) Patarroyo, M. E.; Salazar, L. M.; Cifuentes, G.; Lozano, J. M.; Delgado, G.; Rivera, Z.; Rosas, J.; Vargas, L. E. *Biochimie* **2006**, *88*, 219.
- (60) Chulay, J. D.; Lyon, J. A.; Haynes, J. D.; Meierovics, A. I.; Atkinson, C. T.; Aikawa, M. *J. Immunol.* **1987**, *139*, 2768.
- (61) Lyon, J. A.; Thomas, A. W.; Hall, T.; Chulay, J. D. *Mol. Biochem. Parasitol.* **1989**, *36*, 77.
- (62) Kariuki, M. M.; Li, X.; Yamodo, I.; Chishti, A. H.; Oh, S. S. *Biochem. Biophys. Res. Commun.* **2005**, *338*, 1690.
- (63) Sim, B. K.; Orlandi, P. A.; Haynes, J. D.; Klotz, F. W.; Carter, J. M.; Camus, D.; Zegans, M. E.; Chulay, J. D. *J. Cell Biol.* **1990**, *111*, 1877.
- (64) Urquiza, M.; Rodriguez, L. E.; Suarez, J. E.; Guzman, F.; Ocampo, M.; Curtidor, H.; Segura, C.; Trujillo, E.; Patarroyo, M. E. *Parasite Immunol.* **1996**, *18*, 515.
- (65) Attie, A. D.; Raines, R. T. *J. Chem. Educ.* **1995**, *72*, 119.
- (66) *Fluorescence Polarization Technical Resource Guide*, 4th ed.; Invitrogen Corporation: Madison, WI, 2006.
- (67) Rodriguez, L. E.; Urquiza, M.; Ocampo, M.; Suarez, J.; Curtidor, H.; Guzman, F.; Vargas, L. E.; Trivinos, M.; Rosas, M.; Patarroyo, M. E. *Parasitology* **2000**, *120* (Pt 3), 225.
- (68) Suarez, J. E.; Urquiza, M.; Curtidor, H.; Rodriguez, L. E.; Ocampo, M.; Torres, E.; Guzman, F.; Patarroyo, M. E. *Mem. Inst. Oswaldo Cruz* **2000**, *95*, 495.
- (69) Kaneko, O.; Soubes, S. C.; Miller, L. H. *Exp. Parasitol.* **1999**, *93*, 116.
- (70) Breuer, W. V.; Ginsburg, H.; Cabantchik, Z. I. *Biochim. Biophys. Acta* **1983**, *755*, 263.
- (71) Curtidor, H.; Urquiza, M.; Suarez, J. E.; Rodriguez, L. E.; Ocampo, M.; Puentes, A.; Garcia, J. E.; Vera, R.; Lopez, R.; Ramirez, L. E.; Pinzon, M.; Patarroyo, M. E. *Vaccine* **2001**, *19*, 4496.
- (72) Lopez, R.; Urquiza, M.; Curtidor, H.; Eduardo Caminos, J.; Mora, H.; Puentes, A.; Patarroyo, M. E. *Acta Trop.* **2000**, *75*, 349.
- (73) Valbuena, J. J.; Bravo, R. V.; Ocampo, M.; Lopez, R.; Rodriguez, L. E.; Curtidor, H.; Puentes, A.; Garcia, J. E.; Tovar, D.; Gomez, J.; Leiton, J.; Patarroyo, M. E. *Biochem. Biophys. Res. Commun.* **2004**, *321*, 835.
- (74) Puentes, A.; Garcia, J.; Ocampo, M.; Rodriguez, L.; Vera, R.; Curtidor, H.; Lopez, R.; Suarez, J.; Valbuena, J.; Vanegas, M.; Guzman, F.; Tovar, D.; Patarroyo, M. E. *Peptides* **2003**, *24*, 1015.
- (75) Valbuena, J. J.; Vera, R.; Garcia, J.; Puentes, A.; Curtidor, H.; Ocampo, M.; Urquiza, M.; Rivera, Z.; Guzman, F.; Torres, E.; Patarroyo, M. E. *Peptides* **2003**, *24*, 1007.
- (76) Urquiza, M.; Suarez, J. E.; Cardenas, C.; Lopez, R.; Puentes, A.; Chavez, F.; Calvo, J. C.; Patarroyo, M. E. *Vaccine* **2000**, *19*, 508.
- (77) Curtidor, H.; Ocampo, M.; Rodriguez, L. E.; Lopez, R.; Garcia, J. E.; Valbuena, J.; Vera, R.; Puentes, A.; Leiton, J.; Cortes, L. J.; Lopez, Y.; Patarroyo, M. A.; Patarroyo, M. E. *Biochem. Biophys. Res. Commun.* **2006**, *339*, 888.
- (78) Rodriguez, L. E.; Curtidor, H.; Ocampo, M.; Garcia, J.; Puentes, A.; Valbuena, J.; Vera, R.; Lopez, R.; Patarroyo, M. E. *Protein Sci.* **2005**, *14*, 1778.
- (79) Curtidor, H.; Ocampo, M.; Tovar, D.; Lopez, R.; Garcia, J.; Valbuena, J.; Vera, R.; Suarez, J.; Rodriguez, L. E.; Puentes, A.; Guzman, F.; Torres, E.; Patarroyo, M. E. *Vaccine* **2004**, *22*, 1054.
- (80) Alba, M. P.; Salazar, L. M.; Vargas, L. E.; Trujillo, M.; Lopez, Y.; Patarroyo, M. E. *Biochem. Biophys. Res. Commun.* **2004**, *315*, 1154.
- (81) Cifuentes, G.; Espejo, F.; Vargas, L. E.; Parra, C.; Vanegas, M.; Patarroyo, M. E. *Biochemistry* **2004**, *43*, 6545.
- (82) Patarroyo, M. E.; Cifuentes, G.; Vargas, L. E.; Rosas, J. *ChemBioChem* **2004**, *5*, 1588.
- (83) Cooper, J. A. *Parasitol. Today* **1993**, *9*, 50.
- (84) Holder, A. A.; Blackman, M. J. *Parasitol. Today* **1994**, *10*, 182.
- (85) Holder, A. A.; Blackman, M. J.; Burghaus, P. A.; Chappel, J. A.; Ling, I. T.; McCallum-Deighton, N.; Shai, S. *Mem. Inst. Oswaldo Cruz* **1992**, *87* (Suppl. 3), 37.
- (86) Holder, A. A.; Riley, E. M. *Parasitol. Today* **1996**, *12*, 173.
- (87) Blackman, M. J.; Ling, I. T.; Nicholls, S. C.; Holder, A. A. *Mol. Biochem. Parasitol.* **1991**, *49*, 29.
- (88) Blackman, M. J.; Heidrich, H. G.; Donachie, S.; McBride, J. S.; Holder, A. A. *J. Exp. Med.* **1990**, *172*, 379.
- (89) Tanabe, K.; Mackay, M.; Goman, M.; Scaife, J. G. *J. Mol. Biol.* **1987**, *195*, 273.
- (90) Etlinger, H. M.; Caspers, P.; Matile, H.; Schoenfeld, H. J.; Stueber, D.; Takacs, B. *Infect. Immunol.* **1991**, *59*, 3498.
- (91) Daly, T. M.; Long, C. A. *Infect. Immunol.* **1993**, *61*, 2462.
- (92) Patarroyo, M. E.; Romero, P.; Torres, M. L.; Clavijo, P.; Moreno, A.; Martinez, A.; Rodriguez, R.; Guzman, F.; Cabezas, E. *Nature* **1987**, *328*, 629.
- (93) Siddiqui, W. A.; Tam, L. Q.; Kramer, K. J.; Hui, G. S.; Case, S. E.; Yamaga, K. M.; Chang, S. P.; Chan, E. B.; Kan, S. C. *Proc. Natl. Acad. Sci. U.S.A.* **1987**, *84*, 3014.
- (94) John, C. C.; O'Donnell, R. A.; Sumba, P. O.; Moormann, A. M.; de Koning-Ward, T. F.; King, C. L.; Kazura, J. W.; Crabb, B. S. *J. Immunol.* **2004**, *173*, 666.
- (95) Darko, C. A.; Angov, E.; Collins, W. E.; Bergmann-Leitner, E. S.; Girouard, A. S.; Hitt, S. L.; McBride, J. S.; Diggs, C. L.; Holder, A. A.; Long, C. A.; Barnwell, J. W.; Lyon, J. A. *Infect. Immunol.* **2005**, *73*, 287.
- (96) Gozalo, A.; Lucas, C.; Cachay, M.; Wellde, B. T.; Hall, T.; Bell, B.; Wood, J.; Watts, D.; Wooster, M.; Lyon, J. A.; Moch, J. K.; Haynes, J. D.; Williams, J. S.; Holland, C.; Watson, E.; Kester, K. E.; Kaslow, D. C.; Ballou, W. R. *Am. J. Trop. Med. Hyg.* **1998**, *59*, 991.
- (97) Kumar, S.; Collins, W.; Egan, A.; Yadava, A.; Garraud, O.; Blackman, M. J.; Guevara Patino, J. A.; Diggs, C.; Kaslow, D. C. *Infect. Immunol.* **2000**, *68*, 2215.
- (98) Chang, S. P.; Case, S. E.; Gosnell, W. L.; Hashimoto, A.; Kramer, K. J.; Tam, L. Q.; Hashiro, C. Q.; Nikaido, C. M.; Gibson, H. L.; Lee-Ng, C. T.; Barr, P. J.; Yokota, B. T.; Hut, G. S. *Infect. Immunol.* **1996**, *64*, 253.
- (99) Udhayakumar, V.; Anyona, D.; Kariuki, S.; Shi, Y. P.; Bloland, P. B.; Branch, O. H.; Weiss, W.; Nahlen, B. L.; Kaslow, D. C.; Lal, A. A. *J. Immunol.* **1995**, *154*, 6022.
- (100) Ohta, N.; Iwaki, K.; Itoh, M.; Fu, J.; Nakashima, S.; Hato, M.; Tolle, R.; Bujard, H.; Saitoh, A.; Tanabe, K. *Int. Arch. Allergy Immunol.* **1997**, *114*, 15.
- (101) Rzepczyk, C. M.; Ramasamy, R.; Mutch, D. A.; Ho, P. C.; Battistutta, D.; Anderson, K. L.; Parkinson, D.; Doran, T. J.; Honeyman, M. *Eur. J. Immunol.* **1989**, *19*, 1797.
- (102) Egan, A. F.; Morris, J.; Barnish, G.; Allen, S.; Greenwood, B. M.; Kaslow, D. C.; Holder, A. A.; Riley, E. M. *J. Infect. Dis.* **1996**, *173*, 765.
- (103) Riley, E. M.; Allen, S. J.; Wheeler, J. G.; Blackman, M. J.; Bennett, S.; Takacs, B.; Schonfeld, H. J.; Holder, A. A.; Greenwood, B. M. *Parasite Immunol.* **1992**, *14*, 321.
- (104) Shi, Y. P.; Sayed, U.; Qari, S. H.; Roberts, J. M.; Udhayakumar, V.; Oloo, A. J.; Hawley, W. A.; Kaslow, D. C.; Nahlen, B. L.; Lal, A. A. *Infect. Immunol.* **1996**, *64*, 2716.
- (105) Egan, A. F.; Burghaus, P.; Druilhe, P.; Holder, A. A.; Riley, E. M. *Parasite Immunol.* **1999**, *21*, 133.
- (106) Morgan, W. D.; Birdsall, B.; Frenkiel, T. A.; Gradwell, M. G.; Burghaus, P. A.; Syed, S. E.; Uthaiyibull, C.; Holder, A. A.; Feeney, J. *J. Mol. Biol.* **1999**, *289*, 113.

- (107) Hensmann, M.; Li, C.; Moss, C.; Lindo, V.; Greer, F.; Watts, C.; Ogun, S. A.; Holder, A. A.; Langhorne, J. *Eur. J. Immunol.* **2004**, *34*, 639.
- (108) Parra, M.; Hui, G.; Johnson, A. H.; Berzofsky, J. A.; Roberts, T.; Quakyi, I. A.; Taylor, D. W. *Infect. Immunol.* **2000**, *68*, 2685.
- (109) Egan, A.; Waterfall, M.; Pinder, M.; Holder, A.; Riley, E. *Infect. Immunol.* **1997**, *65*, 3024.
- (110) Sanders, P. R.; Cantin, G. T.; Greenbaum, D. C.; Gilson, P. R.; Nebl, T.; Moritz, R. L.; Yates, J. R., 3rd; Hodder, A. N.; Crabb, B. S. *Mol. Biochem. Parasitol.* **2007**, *154*, 148.
- (111) Kauth, C. W.; Woehlbier, U.; Kern, M.; Mekonnen, Z.; Lutz, R.; Mucke, N.; Langowski, J.; Bujard, H. *J. Biol. Chem.* **2006**, *281*, 31517.
- (112) Pachebat, J. A.; Ling, I. T.; Grainger, M.; Trucco, C.; Howell, S.; Fernandez-Reyes, D.; Gunaratne, R.; Holder, A. A. *Mol. Biochem. Parasitol.* **2001**, *117*, 83.
- (113) Trucco, C.; Fernandez-Reyes, D.; Howell, S.; Stafford, W. H.; Scott-Finnigan, T. J.; Grainger, M.; Ogun, S. A.; Taylor, W. R.; Holder, A. A. *Mol. Biochem. Parasitol.* **2001**, *112*, 91.
- (114) Sanders, P. R.; Gilson, P. R.; Cantin, G. T.; Greenbaum, D. C.; Nebl, T.; Carucci, D. J.; McConville, M. J.; Schofield, L.; Hodder, A. N.; Yates, J. R., 3rd; Crabb, B. S. *J. Biol. Chem.* **2005**, *280*, 40169.
- (115) Goel, V. K.; Li, X.; Chen, H.; Liu, S. C.; Chishti, A. H.; Oh, S. S. *Proc. Natl. Acad. Sci. U.S.A.* **2003**, *100*, 5164.
- (116) Li, X.; Chen, H.; Oo, T. H.; Daly, T. M.; Bergman, L. W.; Liu, S. C.; Chishti, A. H.; Oh, S. S. *J. Biol. Chem.* **2004**, *279*, 5765.
- (117) Alonzo, P. L.; Smith, T. A.; Armstrong-Schellenberg, J. R.; Kitua, A. Y.; Masanja, H.; Hayes, R.; Font, F.; Menendez, C.; Kilama, W. L.; Tanner, M. *J. Infect. Dis.* **1996**, *174*, 367.
- (118) Noya, O.; Gabaldon Berti, Y.; Alarcon de Noya, B.; Borges, R.; Zerpa, N.; Urbaz, J. D.; Madonna, A.; Garrido, E.; Jimenez, M. A.; Borges, R. E.; et al. *J. Infect. Dis.* **1994**, *170*, 396.
- (119) Patarroyo, G.; Franco, L.; Amador, R.; Murillo, L. A.; Rocha, C. L.; Rojas, M.; Patarroyo, M. E. *Vaccine* **1992**, *10*, 175.
- (120) Sempertegui, F.; Estrella, B.; Moscoso, J.; Piedrahita, L.; Hernandez, D.; Gaybor, J.; Naranjo, P.; Mancero, O.; Arias, S.; Bernal, R.; et al. *Vaccine* **1994**, *12*, 337.
- (121) Valero, M. V.; Amador, L. R.; Galindo, C.; Figueroa, J.; Bello, M. S.; Murillo, L. A.; Mora, A. L.; Patarroyo, G.; Rocha, C. L.; Rojas, M.; et al. *Lancet* **1993**, *341*, 705.
- (122) Valero, M. V.; Amador, R.; Aponte, J. J.; Narvaez, A.; Galindo, C.; Silva, Y.; Rosas, J.; Guzman, F.; Patarroyo, M. E. *Vaccine* **1996**, *14*, 1466.
- (123) Patarroyo, M. E.; Amador, R.; Clavijo, P.; Moreno, A.; Guzman, F.; Romero, P.; Tascon, R.; Franco, A.; Murillo, L. A.; Ponton, G.; et al. *Nature* **1988**, *332*, 158.
- (124) Liroy, E.; Suarez, J.; Guzman, F.; Siegrist, S.; Pluschke, G.; Patarroyo, M. E. *Angew. Chem., Int. Ed. Engl.* **2001**, *40*, 2631.
- (125) Lozano, J. M.; Espejo, F.; Diaz, D.; Salazar, L. M.; Rodriguez, J.; Pinzon, C.; Calvo, J. C.; Guzman, F.; Patarroyo, M. E. *J. Pept. Res.* **1998**, *52*, 457.
- (126) Lozano, J. M.; Espejo, F.; Ocampo, M.; Salazar, L. M.; Tovar, D.; Barrera, N.; Guzman, F.; Patarroyo, M. E. *J. Struct. Biol.* **2004**, *148*, 110.
- (127) Helg, A.; Mueller, M. S.; Joss, A.; Poltl-Frank, F.; Stuart, F.; Robinson, J. A.; Pluschke, G. *J. Immunol. Methods* **2003**, *276*, 19.
- (128) Daubenberger, C. A.; Nickel, B.; Ciatto, C.; Grutter, M. G.; Poltl-Frank, F.; Rossi, L.; Siegler, U.; Robinson, J.; Kshala, O.; Patarroyo, M. E.; Pluschke, G. *Eur. J. Immunol.* **2002**, *32*, 3667.
- (129) Vargas, L. E.; Parra, C. A.; Salazar, L. M.; Guzman, F.; Pinto, M.; Patarroyo, M. E. *Biochem. Biophys. Res. Commun.* **2003**, *307*, 148.
- (130) Lozano, J. M.; Alba, M. P.; Vanegas, M.; Silva, Y.; Torres-Castellanos, J. L.; Patarroyo, M. E. *Biol. Chem.* **2003**, *384*, 71.
- (131) Pizarro, J. C.; Chitarra, V.; Verger, D.; Holm, I.; Petres, S.; Darteville, S.; Nato, F.; Longacre, S.; Bentley, G. A. *J. Mol. Biol.* **2003**, *328*, 1091.
- (132) Reyes, C.; Patarroyo, M. E.; Vargas, L. E.; Rodriguez, L. E.; Patarroyo, M. A. *Biochem. Biophys. Res. Commun.* **2007**, *354*, 363.
- (133) Cubillos, M.; Espejo, F.; Purmova, J.; Martinez, J. C.; Patarroyo, M. E. *Proteins* **2003**, *50*, 400.
- (134) Espejo, F.; Cubillos, M.; Salazar, L. M.; Guzman, F.; Urquiza, M.; Ocampo, M.; Silva, Y.; Rodriguez, R.; Liroy, E.; Patarroyo, M. E. *Angew. Chem., Int. Ed. Engl.* **2001**, *40*, 4654.
- (135) Torres, M. H.; Salazar, L. M.; Vanegas, M.; Guzman, F.; Rodriguez, R.; Silva, Y.; Rosas, J.; Patarroyo, M. E. *Eur. J. Biochem.* **2003**, *270*, 3946.
- (136) Espejo, F.; Bermudez, A.; Torres, E.; Urquiza, M.; Rodriguez, R.; Lopez, Y.; Patarroyo, M. E. *Biochem. Biophys. Res. Commun.* **2004**, *315*, 418.
- (137) Smythe, J. A.; Coppel, R. L.; Brown, G. V.; Ramasamy, R.; Kemp, D. J.; Anders, R. F. *Proc. Natl. Acad. Sci. U.S.A.* **1988**, *85*, 5195.
- (138) Fenton, B.; Clark, J. T.; Khan, C. M.; Robinson, J. V.; Walliker, D.; Ridley, R.; Scaife, J. G.; McBride, J. S. *Mol. Cell. Biol.* **1991**, *11*, 963.
- (139) Smythe, J. A.; Coppel, R. L.; Day, K. P.; Martin, R. K.; Oduola, A. M.; Kemp, D. J.; Anders, R. F. *Proc. Natl. Acad. Sci. U.S.A.* **1991**, *88*, 1751.
- (140) Fluck, C.; Smith, T.; Beck, H. P.; Irion, A.; Betuela, I.; Alpers, M. P.; Anders, R.; Saul, A.; Genton, B.; Felger, I. *Infect. Immunol.* **2004**, *72*, 6300.
- (141) Clark, J. T.; Donachie, S.; Anand, R.; Wilson, C. F.; Heidrich, H. G.; McBride, J. S. *Mol. Biochem. Parasitol.* **1989**, *32*, 15.
- (142) Epping, R. J.; Goldstone, S. D.; Ingram, L. T.; Upcroft, J. A.; Ramasamy, R.; Cooper, J. A.; Bushell, G. R.; Geysen, H. M. *Mol. Biochem. Parasitol.* **1988**, *28*, 1.
- (143) Metzger, W. G.; Okenu, D. M.; Cavanagh, D. R.; Robinson, J. V.; Bojang, K. A.; Weiss, H. A.; McBride, J. S.; Greenwood, B. M.; Conway, D. J. *Parasite Immunol.* **2003**, *25*, 307.
- (144) al-Yaman, F.; Genton, B.; Anders, R.; Taraika, J.; Ginny, M.; Mellor, S.; Alpers, M. P. *Parasite Immunol.* **1995**, *17*, 493.
- (145) Taylor, R. R.; Allen, S. J.; Greenwood, B. M.; Riley, E. M. *Am. J. Trop. Med. Hyg.* **1998**, *58*, 406.
- (146) Ramasamy, R.; Yasawardena, S.; Kanagaratnam, R.; Buratti, E.; Baralle, F. E.; Ramasamy, M. S. *Parasite Immunol.* **1999**, *21*, 397.
- (147) Tonhosolo, R.; Wunderlich, G.; Ferreira, M. U. *J. Eukaryot. Microbiol.* **2001**, *48*, 556.
- (148) Pasvol, G. *Philos. Trans. R. Soc. London, Ser. B: Biol. Sci.* **1984**, *307*, 189.
- (149) Saul, A.; Lord, R.; Jones, G. L.; Spencer, L. *J. Immunol.* **1992**, *148*, 208.
- (150) Shi, Y. P.; Das, P.; Holloway, B.; Udhayakumar, V.; Tongren, J. E.; Candal, F.; Biswas, S.; Ahmad, R.; Hasnain, S. E.; Lal, A. A. *Vaccine* **2000**, *18*, 2902.
- (151) Shi, Y. P.; Hasnain, S. E.; Sacci, J. B.; Holloway, B. P.; Fujioka, H.; Kumar, N.; Wohlhueter, R.; Hoffman, S. L.; Collins, W. E.; Lal, A. A. *Proc. Natl. Acad. Sci. U.S.A.* **1999**, *96*, 1615.
- (152) Cifuentes, G.; Patarroyo, M. E.; Urquiza, M.; Ramirez, L. E.; Reyes, C.; Rodriguez, R. *J. Med. Chem.* **2003**, *46*, 2250.
- (153) Low, A.; Chandrashekar, I. R.; Adda, C. G.; Yao, S.; Sabo, J. K.; Zhang, X.; Soetopo, A.; Anders, R. F.; Norton, R. S. *Biopolymers* **2007**, *87*, 12.
- (154) McColl, D. J.; Silva, A.; Foley, M.; Kun, J. F.; Favaloro, J. M.; Thompson, J. K.; Marshall, V. M.; Coppel, R. L.; Kemp, D. J.; Anders, R. F. *Mol. Biochem. Parasitol.* **1994**, *68*, 53.
- (155) Oeuvray, C.; Bouharoun-Tayoun, H.; Grass-Masse, H.; Lepers, J. P.; Ralamboranto, L.; Tartar, A.; Druilhe, P. *Mem. Inst. Oswaldo Cruz* **1994**, *89 Suppl 2*, 77.
- (156) Oeuvray, C.; Bouharoun-Tayoun, H.; Gras-Masse, H.; Bottius, E.; Kaidoh, T.; Aikawa, M.; Filgueira, M. C.; Tartar, A.; Druilhe, P. *Blood* **1994**, *84*, 1594.
- (157) LaCount, D. J.; Vignali, M.; Chettier, R.; Phansalkar, A.; Bell, R.; Hesselberth, J. R.; Schoenfeld, L. W.; Ota, I.; Sahasrabudhe, S.; Kurschner, C.; Fields, S.; Hughes, R. E. *Nature* **2005**, *438*, 103.
- (158) Huber, W.; Felger, I.; Matile, H.; Lipps, H. J.; Steiger, S.; Beck, H. P. *Mol. Biochem. Parasitol.* **1997**, *87*, 231.
- (159) McColl, D. J.; Anders, R. F. *Mol. Biochem. Parasitol.* **1997**, *90*, 21.
- (160) Lopez, R.; Valbuena, J.; Rodriguez, L. E.; Ocampo, M.; Vera, R.; Curtidor, H.; Puentes, A.; Garcia, J.; Ramirez, L. E.; Patarroyo, M. E. *Peptides* **2006**, *27*, 1685.
- (161) Mulhern, T. D.; Howlett, G. J.; Reid, G. E.; Simpson, R. J.; McColl, D. J.; Anders, R. F.; Norton, R. S. *Biochemistry* **1995**, *34*, 3479.
- (162) Mills, K. E.; Pearce, J. A.; Crabb, B. S.; Cowman, A. F. *Mol. Microbiol.* **2002**, *43*, 1401.
- (163) Singh, S.; Soe, S.; Mejia, J. P.; Roussillon, C.; Theisen, M.; Corradin, G.; Druilhe, P. *J. Infect. Dis.* **2004**, *190*, 1010.
- (164) Carvalho, L. J.; Oliveira, S. G.; Theisen, M.; Alves, F. A.; Andrade, M. C.; Zanini, G. M.; Brigido, M. C.; Oeuvray, C.; Povoia, M. M.; Muniz, J. A.; Druilhe, P.; Daniel-Ribeiro, C. T. *Scand. J. Immunol.* **2004**, *59*, 363.
- (165) Soe, S.; Theisen, M.; Roussillon, C.; Aye, K. S.; Druilhe, P. *Infect. Immunol.* **2004**, *72*, 247.
- (166) Theisen, M.; Soe, S.; Brunstedt, K.; Follmann, F.; Bredmose, L.; Israelsen, H.; Madsen, S. M.; Druilhe, P. *Vaccine* **2004**, *22*, 1188.
- (167) Sirima, S. B.; Nebie, I.; Ouedraogo, A.; Tiono, A. B.; Konate, A. T.; Gansane, A.; Derme, A. I.; Diarra, A.; Ouedraogo, A.; Soulama, I.; Cuzzin-Ouattara, N.; Cousens, S.; Leroy, O. *Vaccine* **2007**, *25*, 2723.
- (168) Marshall, V. M.; Silva, A.; Foley, M.; Cranmer, S.; Wang, L.; McColl, D. J.; Kemp, D. J.; Coppel, R. L. *Infect. Immunol.* **1997**, *65*, 4460.
- (169) Wang, L.; Richie, T. L.; Stowers, A.; Nhan, D. H.; Coppel, R. L. *Infect. Immunol.* **2001**, *69*, 4390.
- (170) Puentes, A.; Garcia, J.; Vera, R.; Lopez, R.; Suarez, J.; Rodriguez, L.; Curtidor, H.; Ocampo, M.; Tovar, D.; Forero, M.; Bermudez, A.; Cortes, J.; Urquiza, M.; Patarroyo, M. E. *Vaccine* **2004**, *22*, 1150.

- (171) Garcia, Y.; Puentes, A.; Curtidor, H.; Cifuentes, G.; Reyes, C.; Barreto, J.; Moreno, A.; Patarroyo, M. E. *J. Med. Chem.* **2007**, *50*, 5665.
- (172) Marshall, V. M.; Tieqiao, W.; Coppel, R. L. *Mol. Biochem. Parasitol.* **1998**, *94*, 13.
- (173) Black, C. G.; Wang, L.; Hibbs, A. R.; Werner, E.; Coppel, R. L. *Infect. Immunol.* **1999**, *67*, 2075.
- (174) Goschnick, M. W.; Black, C. G.; Kedzierski, L.; Holder, A. A.; Coppel, R. L. *Infect. Immunol.* **2004**, *72*, 5840.
- (175) Pearce, J. A.; Triglia, T.; Hodder, A. N.; Jackson, D. C.; Cowman, A. F.; Anders, R. F. *Infect. Immunol.* **2004**, *72*, 2321.
- (176) Singh, S.; Soe, S.; Roussilhon, C.; Corradin, G.; Druilhe, P. *Infect. Immunol.* **2005**, *73*, 1235.
- (177) Pachebat, J. A.; Kadekoppala, M.; Grainger, M.; Dluzewski, A. R.; Gunaratne, R. S.; Scott-Finnigan, T. J.; Ogun, S. A.; Ling, I. T.; Bannister, L. H.; Taylor, H. M.; Mitchell, G. H.; Holder, A. A. *Mol. Biochem. Parasitol.* **2007**, *151*, 59.
- (178) Tewari, R.; Ogun, S. A.; Gunaratne, R. S.; Crisanti, A.; Holder, A. A. *Blood* **2005**, *105*, 394.
- (179) Baum, J.; Maier, A. G.; Good, R. T.; Simpson, K. M.; Cowman, A. F. *PLoS Pathog.* **2005**, *1*, e37.
- (180) Black, C. G.; Wang, L.; Wu, T.; Coppel, R. L. *Mol. Biochem. Parasitol.* **2003**, *127*, 59.
- (181) Burns, J. M., Jr.; Belk, C. C.; Dunn, P. D. *Infect. Immunol.* **2000**, *68*, 6189.
- (182) Drew, D. R.; Sanders, P. R.; Crabb, B. S. *Infect. Immunol.* **2005**, *73*, 3912.
- (183) Weber, J. L.; Lyon, J. A.; Wolff, R. H.; Hall, T.; Lowell, G. H.; Chulay, J. D. *J. Biol. Chem.* **1988**, *263*, 11421.
- (184) Stahl, H. D.; Bianco, A. E.; Crewther, P. E.; Anders, R. F.; Kyne, A. P.; Coppel, R. L.; Mitchell, G. F.; Kemp, D. J.; Brown, G. V. *Mol. Biol. Med.* **1986**, *3*, 351.
- (185) Garber, G. E.; Lemchuk-Favel, L. T.; Meysick, K. C.; Dimock, K. *Appl. Parasitol.* **1993**, *34*, 245.
- (186) Nwagwu, M.; Haynes, J. D.; Orlandi, P. A.; Chulay, J. D. *Exp. Parasitol.* **1992**, *75*, 399.
- (187) Kushwaha, A.; Rao, P. P.; Duttu, V. S.; Malhotra, P.; Chauhan, V. S. *Mol. Biochem. Parasitol.* **2000**, *106*, 213.
- (188) Kushwaha, A.; Perween, A.; Mukund, S.; Majumdar, S.; Bhardwaj, D.; Chowdhury, N. R.; Chauhan, V. S. *Mol. Biochem. Parasitol.* **2002**, *122*, 45.
- (189) Sharma, P.; Kumar, A.; Singh, B.; Bharadwaj, A.; Sailaja, V. N.; Adak, T.; Kushwaha, A.; Malhotra, P.; Chauhan, V. S. *Infect. Immunol.* **1998**, *66*, 2895.
- (190) Kushwaha, A.; Rao, P. P.; Suresh, R. P.; Chauhan, V. S. *Parasite Immunol.* **2001**, *23*, 435.
- (191) Salazar, L. M.; Alba, M. P.; Curtidor, H.; Bermudez, A.; Luis, E. V.; Rivera, Z. J.; Patarroyo, M. E. *Biochem. Biophys. Res. Commun.* **2004**, *322*, 119.
- (192) Higgins, D. G.; McConnell, D. J.; Sharp, P. M. *Nature* **1989**, *340*, 604.
- (193) Foley, M.; Corcoran, L.; Tilley, L.; Anders, R. *Exp. Parasitol.* **1994**, *79*, 340.
- (194) Hodder, A. N.; Crewther, P. E.; Matthew, M. L.; Reid, G. E.; Moritz, R. L.; Simpson, R. J.; Anders, R. F. *J. Biol. Chem.* **1996**, *271*, 29446.
- (195) Holder, A. A. *Proc. Natl. Acad. Sci. U.S.A.* **1999**, *96*, 1167.
- (196) Puentes, A.; Ocampo, M.; Rodriguez, L. E.; Vera, R.; Valbuena, J.; Curtidor, H.; Garcia, J.; Lopez, R.; Tovar, D.; Cortes, J.; Rivera, Z.; Patarroyo, M. E. *Biochimie* **2005**, *87*, 461.
- (197) Perkins, M. E. *J. Exp. Med.* **1984**, *160*, 788.
- (198) Perkins, M. E.; Rocco, L. J. *J. Immunol.* **1988**, *141*, 3190.
- (199) Kochan, J.; Perkins, M.; Ravetch, J. V. *Cell* **1986**, *44*, 689.
- (200) Dubois, P.; Dedet, J. P.; Fandeur, T.; Roussilhon, C.; Jendoubi, M.; Pauillac, S.; Mercereau-Puijalon, O.; Pereira Da Silva, L. *Proc. Natl. Acad. Sci. U.S.A.* **1984**, *81*, 229.
- (201) Aronson, N. E.; Silverman, C.; Wasserman, G. F.; Kochan, J.; Hall, B. T.; Esser, K.; Young, J. E.; Chulay, J. D. *Am. J. Trop. Med. Hyg.* **1991**, *45*, 548.
- (202) Horrocks, P.; Muhia, D. *Trends Parasitol.* **2005**, *21*, 396.
- (203) Marti, M.; Good, R. T.; Rug, M.; Knuepfer, E.; Cowman, A. F. *Science* **2004**, *306*, 1930.
- (204) Miller, S. K.; Good, R. T.; Drew, D. R.; Delorenzi, M.; Sanders, P. R.; Hodder, A. N.; Speed, T. P.; Cowman, A. F.; de Koning-Ward, T. F.; Crabb, B. S. *J. Biol. Chem.* **2002**, *277*, 47524.
- (205) Bourgon, R.; Delorenzi, M.; Sargeant, T.; Hodder, A. N.; Crabb, B. S.; Speed, T. P. *Mol. Biol. Evol.* **2004**, *21*, 2161.
- (206) Hodder, A. N.; Drew, D. R.; Epa, V. C.; Delorenzi, M.; Bourgon, R.; Miller, S. K.; Moritz, R. L.; Frecklington, D. F.; Simpson, R. J.; Speed, T. P.; Pike, R. N.; Crabb, B. S. *J. Biol. Chem.* **2003**, *278*, 48169.
- (207) Bzik, D. J.; Li, W. B.; Horii, T.; Inselburg, J. *Mol. Biochem. Parasitol.* **1988**, *30*, 279.
- (208) Li, J.; Mitamura, T.; Fox, B. A.; Bzik, D. J.; Horii, T. *Parasitol. Int.* **2002**, *51*, 343.
- (209) Sato, D.; Li, J.; Mitamura, T.; Horii, T. *Parasitol. Int.* **2005**, *54*, 261.
- (210) Inselburg, J.; Bathurst, I. C.; Kansopon, J.; Barchfeld, G. L.; Barr, P. J.; Rossan, R. N. *Infect. Immunol.* **1993**, *61*, 2041.
- (211) Inselburg, J.; Bathurst, I. C.; Kansopon, J.; Barr, P. J.; Rossan, R. N. *Infect. Immunol.* **1993**, *61*, 2048.
- (212) Inselburg, J.; Bzik, D. J.; Li, W. B.; Green, K. M.; Kansopon, J.; Hahm, B. K.; Bathurst, I. C.; Barr, P. J.; Rossan, R. N. *Infect. Immunol.* **1991**, *59*, 1247.
- (213) Banyal, H. S.; Inselburg, J. *Am. J. Trop. Med. Hyg.* **1985**, *34*, 1055.
- (214) Barr, P. J.; Inselburg, J.; Green, K. M.; Kansopon, J.; Hahm, B. K.; Gibson, H. L.; Lee-Ng, C. T.; Bzik, D. J.; Li, W. B.; Bathurst, I. C. *Mol. Biochem. Parasitol.* **1991**, *45*, 159.
- (215) Bathurst, I. C.; Gibson, H. L.; Kansopon, J.; Hahm, B. K.; Green, K. M.; Chang, S. P.; Hui, G. S.; Siddiqui, W. A.; Inselburg, J.; Millet, P.; et al. *Vaccine* **1993**, *11*, 449.
- (216) Fox, B. A.; Horii, T.; Bzik, D. J. *Exp. Parasitol.* **2002**, *101*, 69.
- (217) Horii, T.; Bzik, D. J.; Inselburg, J. *Mol. Biochem. Parasitol.* **1988**, *30*, 9.
- (218) Pang, X. L.; Horii, T. *Vaccine* **1998**, *16*, 1299.
- (219) Pang, X. L.; Mitamura, T.; Horii, T. *Infect. Immunol.* **1999**, *67*, 1821.
- (220) Sugiyama, T.; Suzue, K.; Okamoto, M.; Inselburg, J.; Tai, K.; Horii, T. *Vaccine* **1996**, *14*, 1069.
- (221) Fox, B. A.; Xing-Li, P.; Suzue, K.; Horii, T.; Bzik, D. J. *Exp. Parasitol.* **1997**, *85*, 121.
- (222) Okech, B. A.; Nalunkuma, A.; Okello, D.; Pang, X. L.; Suzue, K.; Li, J.; Horii, T.; Ekwang, T. G. *Am. J. Trop. Med. Hyg.* **2001**, *65*, 912.
- (223) Soe, S.; Singh, S.; Camus, D.; Horii, T.; Druilhe, P. *Infect. Immunol.* **2002**, *70*, 7182.
- (224) Wickham, M. E.; Culvenor, J. G.; Cowman, A. F. *J. Biol. Chem.* **2003**, *278*, 37658.
- (225) Perkins, M. E.; Ziefer, A. *Infect. Immunol.* **1994**, *62*, 1207.
- (226) Sam-Yellowe, T. Y. *Exp. Parasitol.* **1993**, *77*, 179.
- (227) Puentes, A.; Garcia, J.; Vera, R.; Lopez, Q. R.; Urquiza, M.; Vanegas, M.; Salazar, L. M.; Patarroyo, M. E. *Parasitol. Int.* **2000**, *49*, 105.
- (228) D'Souza, S. E.; Ginsberg, M. H.; Plow, E. F. *Trends Biochem. Sci.* **1991**, *16*, 246.
- (229) McDonald, J. A.; Quade, B. J.; Broekelmann, T. J.; LaChance, R.; Forsman, K.; Hasegawa, E.; Akiyama, S. *J. Biol. Chem.* **1987**, *262*, 2957.
- (230) Alba, M. P.; Salazar, L. M.; Purmova, J.; Vanegas, M.; Rodriguez, R.; Patarroyo, M. E. *Vaccine* **2004**, *22*, 1281.
- (231) Thompson, J.; Janse, C. J.; Waters, A. P. *Mol. Biochem. Parasitol.* **2001**, *118*, 147.
- (232) Gerloff, D. L.; Creasey, A.; Maslau, S.; Carter, R. *Proc. Natl. Acad. Sci. U.S.A.* **2005**, *102*, 13598.
- (233) Elliott, J. F.; Albrecht, G. R.; Gilladoga, A.; Handunnetti, S. M.; Neequaye, J.; Lallinger, G.; Minjas, J. N.; Howard, R. J. *Proc. Natl. Acad. Sci. U.S.A.* **1990**, *87*, 6363.
- (234) Miller, L. H.; McAuliffe, F. M.; Johnson, J. G. *Prog. Clin. Biol. Res.* **1979**, *30*, 497.
- (235) Treeck, M.; Struck, N. S.; Haase, S.; Langer, C.; Herrmann, S.; Healer, J.; Cowman, A. F.; Gilberger, T. W. *J. Biol. Chem.* **2006**, *281*, 31995.
- (236) Gilberger, T. W.; Thompson, J. K.; Reed, M. B.; Good, R. T.; Cowman, A. F. *J. Cell Biol.* **2003**, *162*, 317.
- (237) Sim, B. K.; Toyoshima, T.; Haynes, J. D.; Aikawa, M. *Mol. Biochem. Parasitol.* **1992**, *51*, 157.
- (238) Carrillo, E. F.; Patarroyo, M. A.; Patarroyo, M. E.; Murillo, L. A. *Mol. Biochem. Parasitol.* **1997**, *85*, 255.
- (239) Kain, K. C.; Lanar, D. E. *J. Clin. Microbiol.* **1991**, *29*, 1171.
- (240) Ware, L. A.; Kain, K. C.; Lee Sim, B. K.; Haynes, J. D.; Baird, J. K.; Lanar, D. E. *Mol. Biochem. Parasitol.* **1993**, *60*, 105.
- (241) Camus, D.; Hadley, T. J. *Science* **1985**, *230*, 553.
- (242) Tolia, N. H.; Enemark, E. J.; Sim, B. K.; Joshua-Tor, L. *Cell* **2005**, *122*, 183.
- (243) Klotz, F. W.; Orlandi, P. A.; Reuter, G.; Cohen, S. J.; Haynes, J. D.; Schauer, R.; Howard, R. J.; Palese, P.; Miller, L. H. *Mol. Biochem. Parasitol.* **1992**, *51*, 49.
- (244) Sim, B. K.; Chitnis, C. E.; Wasniowska, K.; Hadley, T. J.; Miller, L. H. *Science* **1994**, *264*, 1941.
- (245) Hadley, T. J.; Erkmen, Z.; Kaufman, B. M.; Futrovsky, S.; McGuinnis, M. H.; Graves, P.; Sadoff, J. C.; Miller, L. H. *Am. J. Trop. Med. Hyg.* **1986**, *35*, 898.
- (246) Orlandi, P. A.; Klotz, F. W.; Haynes, J. D. *J. Cell Biol.* **1992**, *116*, 901.
- (247) Duraisingh, M. T.; Maier, A. G.; Triglia, T.; Cowman, A. F. *Proc. Natl. Acad. Sci. U.S.A.* **2003**, *100*, 4796.
- (248) Sim, B. K. *Parasitol. Today* **1995**, *11*, 213.

- (249) Jakobsen, P. H.; Heegaard, P. M.; Koch, C.; Wasniowska, K.; Lemnge, M. M.; Jensen, J. B.; Sim, B. K. *Infect. Immunol.* **1998**, *66*, 4203.
- (250) Guzman, F.; Jaramillo, K.; Salazar, L. M.; Torres, A.; Rivera, A.; Patarroyo, M. E. *Life Sci.* **2002**, *71*, 2773.
- (251) Bermudez, A.; Cifuentes, G.; Guzman, F.; Salazar, L. M.; Patarroyo, M. E. *Biol. Chem.* **2003**, *384*, 1443.
- (252) Cifuentes, G.; Guzman, F.; Alba, M. P.; Salazar, L. M.; Patarroyo, M. E. *J. Struct. Biol.* **2003**, *141*, 115.
- (253) Vera-Bravo, R.; Valbuena, J. J.; Ocampo, M.; Garcia, J. E.; Rodriguez, L. E.; Puentes, A.; Lopez, R.; Curtidor, H.; Torres, E.; Trujillo, M.; Tovar, D. R.; Patarroyo, M. A.; Patarroyo, M. E. *Biochimie* **2005**, *87*, 425.
- (254) Gilberger, T. W.; Thompson, J. K.; Triglia, T.; Good, R. T.; Duraisingh, M. T.; Cowman, A. F. *J. Biol. Chem.* **2003**, *278*, 14480.
- (255) Mayer, D. C.; Mu, J. B.; Feng, X.; Su, X. Z.; Miller, L. H. *J. Exp. Med.* **2002**, *196*, 1523.
- (256) Thompson, J. K.; Triglia, T.; Reed, M. B.; Cowman, A. F. *Mol. Microbiol.* **2001**, *41*, 47.
- (257) Maier, A. G.; Duraisingh, M. T.; Reeder, J. C.; Patel, S. S.; Kazura, J. W.; Zimmerman, P. A.; Cowman, A. F. *Nat. Med.* **2003**, *9*, 87.
- (258) Narum, D. L.; Fuhrmann, S. R.; Luu, T.; Sim, B. K. *Mol. Biochem. Parasitol.* **2002**, *119*, 159.
- (259) Rodriguez, L. E.; Ocampo, M.; Vera, R.; Puentes, A.; Lopez, R.; Garcia, J.; Curtidor, H.; Valbuena, J.; Suarez, J.; Rosas, J.; Rivera, Z.; Urquiza, M.; Patarroyo, M. E. *J. Pept. Res.* **2003**, *62*, 175.
- (260) Peterson, D. S.; Miller, L. H.; Wellems, T. E. *Proc. Natl. Acad. Sci. U.S.A.* **1995**, *92*, 7100.
- (261) Peterson, D. S.; Wellems, T. E. *Mol. Biochem. Parasitol.* **2000**, *105*, 105.
- (262) Curtidor, H.; Rodriguez, L. E.; Ocampo, M.; Lopez, R.; Garcia, J. E.; Valbuena, J.; Vera, R.; Puentes, A.; Vanegas, M.; Patarroyo, M. E. *Protein Sci.* **2005**, *14*, 464.
- (263) Baker, R. P.; Wijetilaka, R.; Urban, S. *PLoS Pathog.* **2006**, *2*, e113.
- (264) Mitchell, G. H.; Thomas, A. W.; Margos, G.; Dluzewski, A. R.; Bannister, L. H. *Infect. Immunol.* **2004**, *72*, 154.
- (265) Silvie, O.; Franetich, J. F.; Charrin, S.; Mueller, M. S.; Siau, A.; Bodescot, M.; Rubinstein, E.; Hannoun, L.; Charoenvit, Y.; Kocken, C. H.; Thomas, A. W.; Van Gemert, G. J.; Sauerwein, R. W.; Blackman, M. J.; Anders, R. F.; Pluschke, G.; Mazier, D. *J. Biol. Chem.* **2004**, *279*, 9490.
- (266) Howell, S. A.; Well, I.; Fleck, S. L.; Kettleborough, C.; Collins, C. R.; Blackman, M. J. *J. Biol. Chem.* **2003**, *278*, 23890.
- (267) Howell, S. A.; Withers-Martinez, C.; Kocken, C. H.; Thomas, A. W.; Blackman, M. J. *J. Biol. Chem.* **2001**, *276*, 31311.
- (268) Bai, T.; Becker, M.; Gupta, A.; Strike, P.; Murphy, V. J.; Anders, R. F.; Batchelor, A. H. *Proc. Natl. Acad. Sci. U.S.A.* **2005**, *102*, 12736.
- (269) Feng, Z. P.; Keizer, D. W.; Stevenson, R. A.; Yao, S.; Babon, J. J.; Murphy, V. J.; Anders, R. F.; Norton, R. S. *J. Mol. Biol.* **2005**, *350*, 641.
- (270) Nair, M.; Hinds, M. G.; Coley, A. M.; Hodder, A. N.; Foley, M.; Anders, R. F.; Norton, R. S. *J. Mol. Biol.* **2002**, *322*, 741.
- (271) Pizarro, J. C.; Vulliez-Le Normand, B.; Chesne-Seck, M. L.; Collins, C. R.; Withers-Martinez, C.; Hackett, F.; Blackman, M. J.; Faber, B. W.; Remarque, E. J.; Kocken, C. H.; Thomas, A. W.; Bentley, G. A. *Science* **2005**, *308*, 408.
- (272) Anders, R. F.; Crewther, P. E.; Edwards, S.; Margetts, M.; Matthew, M. L.; Pollock, B.; Pye, D. *Vaccine* **1998**, *16*, 240.
- (273) Crewther, P. E.; Matthew, M. L.; Flegg, R. H.; Anders, R. F. *Infect. Immunol.* **1996**, *64*, 3310.
- (274) Narum, D. L.; Ogun, S. A.; Thomas, A. W.; Holder, A. A. *Infect. Immunol.* **2000**, *68*, 2899.
- (275) Kocken, C. H.; Withers-Martinez, C.; Dubbeld, M. A.; van der Wel, A.; Hackett, F.; Valderrama, A.; Blackman, M. J.; Thomas, A. W. *Infect. Immunol.* **2002**, *70*, 4471.
- (276) Thomas, A. W.; Narum, D.; Waters, A. P.; Trape, J. F.; Rogier, C.; Goncalves, A.; Rosario, V.; Druilhe, P.; Mitchell, G. H.; Dennis, D. *Mem. Inst. Oswaldo Cruz* **1994**, *89 Suppl 2*, 67.
- (277) Thomas, A. W.; Deans, J. A.; Mitchell, G. H.; Alderson, T.; Cohen, S. *Mol. Biochem. Parasitol.* **1984**, *13*, 187.
- (278) Dutta, S.; Haynes, J. D.; Moch, J. K.; Barbosa, A.; Lanar, D. E. *Proc. Natl. Acad. Sci. U.S.A.* **2003**, *100*, 12295.
- (279) Healer, J.; Murphy, V.; Hodder, A. N.; Masciantonio, R.; Gemmill, A. W.; Anders, R. F.; Cowman, A. F.; Batchelor, A. *Mol. Microbiol.* **2004**, *52*, 159.
- (280) Marshall, V. M.; Zhang, L.; Anders, R. F.; Coppel, R. L. *Mol. Biochem. Parasitol.* **1996**, *77*, 109.
- (281) Zhang, L.; Zhan, B.; Wang, J.; Feng, X. *Zhongguo Ji Sheng Chong Xue Yu Ji Sheng Chong Bing Za Zhi* **1995**, *13*, 203.
- (282) Mueller, M. S.; Renard, A.; Boato, F.; Vogel, D.; Naegeli, M.; Zurbriggen, R.; Robinson, J. A.; Pluschke, G. *Infect. Immunol.* **2003**, *71*, 4749.
- (283) Triglia, T.; Healer, J.; Caruana, S. R.; Hodder, A. N.; Anders, R. F.; Crabb, B. S.; Cowman, A. F. *Mol. Microbiol.* **2000**, *38*, 706.
- (284) Fraser, T. S.; Kappe, S. H.; Narum, D. L.; vanBuskirk, K. M.; Adams, J. H. *Mol. Biochem. Parasitol.* **2001**, *117*, 49.
- (285) Kato, K.; Mayer, D. C.; Singh, S.; Reid, M.; Miller, L. H. *Proc. Natl. Acad. Sci. U.S.A.* **2005**, *102*, 5552.
- (286) Udhayakumar, V.; Kariuki, S.; Kolczack, M.; Girma, M.; Roberts, J. M.; Oloo, A. J.; Nahlen, B. L.; Lal, A. A. *Am. J. Trop. Med. Hyg.* **2001**, *65*, 100.
- (287) Cubillos, M.; Salazar, L. M.; Torres, L.; Patarroyo, M. E. *Biochimie* **2002**, *84*, 1181.
- (288) Salazar, L. M.; Alba, M. P.; Torres, M. H.; Pinto, M.; Cortes, X.; Torres, L.; Patarroyo, M. E. *FEBS Lett.* **2002**, *527*, 95.
- (289) Ocampo, M.; Curtidor, H.; Vera, R.; Valbuena, J. J.; Rodriguez, L. E.; Puentes, A.; Lopez, R.; Garcia, J. E.; Tovar, D.; Pacheco, P.; Navarro, M. A.; Patarroyo, M. E. *Biochem. Biophys. Res. Commun.* **2004**, *315*, 319.
- (290) Huang, X.; Miller, W. *Adv. Appl. Math* **1991**, *12*, 373.
- (291) Coley, A. M.; Gupta, A.; Murphy, V. J.; Bai, T.; Kim, H.; Anders, R. F.; Foley, M.; Batchelor, A. H. *PLoS Pathog.* **2007**, *3*, 1308.
- (292) Collins, C. R.; Withers-Martinez, C.; Bentley, G. A.; Batchelor, A. H.; Thomas, A. W.; Blackman, M. J. *J. Biol. Chem.* **2007**, *282*, 7431.
- (293) Purmova, J.; Salazar, L. M.; Espejo, F.; Torres, M. H.; Cubillos, M.; Torres, E.; Lopez, Y.; Rodriguez, R.; Patarroyo, M. E. *Biochim. Biophys. Acta* **2002**, *1571*, 27.
- (294) Blair, P. L.; Kappe, S. H.; Maciel, J. E.; Balu, B.; Adams, J. H. *Mol. Biochem. Parasitol.* **2002**, *122*, 35.
- (295) Kappe, S. H.; Noe, A. R.; Fraser, T. S.; Blair, P. L.; Adams, J. H. *Proc. Natl. Acad. Sci. U.S.A.* **1998**, *95*, 1230.
- (296) Noe, A. R.; Fishkind, D. J.; Adams, J. H. *Mol. Biochem. Parasitol.* **2000**, *108*, 169.
- (297) Ghai, M.; Dutta, S.; Hall, T.; Freilich, D.; Ockenhouse, C. F. *Mol. Biochem. Parasitol.* **2002**, *123*, 35.
- (298) Kariu, T.; Yuda, M.; Yano, K.; Chinzei, Y. *J. Exp. Med.* **2002**, *195*, 1317.
- (299) Green, J. L.; Hinds, L.; Grainger, M.; Knuepfer, E.; Holder, A. A. *Mol. Biochem. Parasitol.* **2006**, *150*, 114.
- (300) Thompson, J.; Cooke, R. E.; Moore, S.; Anderson, L. F.; Janse, C. J.; Waters, A. P. *Mol. Biochem. Parasitol.* **2004**, *134*, 225.
- (301) Calderon, J. C.; Curtidor, H.; Gonzalez, O.; Cifuentes, G.; Reyes, C.; Patarroyo, M. E. *Biochimie* **2008**, *90*, 802.
- (302) Fonjuno, P. N.; Stuber, D.; McBride, J. S. *Infect. Immunol.* **1998**, *66*, 1037.
- (303) Jakobsen, P. H.; Kurtzhals, J. A.; Riley, E. M.; Hviid, L.; Theander, T. G.; Morris-Jones, S.; Jensen, J. B.; Bayoumi, R. A.; Ridley, R. G.; Greenwood, B. M. *Parasite Immunol.* **1997**, *19*, 387.
- (304) Rayner, J. C.; Vargas-Serrato, E.; Huber, C. S.; Galinski, M. R.; Barnwell, J. W. *J. Exp. Med.* **2001**, *194*, 1571.
- (305) Nixon, C. P.; Friedman, J.; Treanor, K.; Knopf, P. M.; Duffy, P. E.; Kurtis, J. D. *J. Infect. Dis.* **2005**, *192*, 861.
- (306) Galinski, M. R.; Medina, C. C.; Ingravallo, P.; Barnwell, J. W. *Cell* **1992**, *69*, 1213.
- (307) Preiser, P. R.; Khan, S.; Costa, F. T.; Jarra, W.; Belnoue, E.; Ogun, S.; Holder, A. A.; Voza, T.; Landau, I.; Snounou, G.; Renia, L. *Science* **2002**, *295*, 342.
- (308) Galinski, M. R.; Barnwell, J. W. *Parasitol. Today* **1996**, *12*, 20.
- (309) Galinski, M. R.; Xu, M.; Barnwell, J. W. *Mol. Biochem. Parasitol.* **2000**, *108*, 257.
- (310) Borre, M. B.; Owen, C. A.; Keen, J. K.; Sinha, K. A.; Holder, A. A. *Mol. Biochem. Parasitol.* **1995**, *70*, 149.
- (311) Khan, S. M.; Jarra, W.; Preiser, P. R. *Mol. Biochem. Parasitol.* **2001**, *117*, 1.
- (312) Preiser, P. R.; Jarra, W.; Capiod, T.; Snounou, G. *Nature* **1999**, *398*, 618.
- (313) Rayner, J. C.; Galinski, M. R.; Ingravallo, P.; Barnwell, J. W. *Proc. Natl. Acad. Sci. U.S.A.* **2000**, *97*, 9648.
- (314) Triglia, T.; Thompson, J.; Caruana, S. R.; Delorenzi, M.; Speed, T.; Cowman, A. F. *Infect. Immunol.* **2001**, *69*, 1084.
- (315) Duraisingh, M. T.; Triglia, T.; Ralph, S. A.; Rayner, J. C.; Barnwell, J. W.; McFadden, G. I.; Cowman, A. F. *EMBO J.* **2003**, *22*, 1047.
- (316) Taylor, H. M.; Triglia, T.; Thompson, J.; Sajid, M.; Fowler, R.; Wickham, M. E.; Cowman, A. F.; Holder, A. A. *Infect. Immunol.* **2001**, *69*, 3635.
- (317) Ocampo, M.; Vera, R.; Rodriguez, L. E.; Curtidor, H.; Suarez, J.; Garcia, J.; Puentes, A.; Lopez, R.; Valbuena, J.; Tovar, D.; Reyes, C.; Vega, S.; Patarroyo, M. E. *Parasitol. Int.* **2004**, *53*, 77.
- (318) Saul, A.; Cooper, J.; Hauquitz, D.; Irving, D.; Cheng, Q.; Stowers, A.; Limpaboon, T. *Mol. Biochem. Parasitol.* **1992**, *50*, 139.
- (319) Clark, J. T.; Anand, R.; Akoglu, T.; McBride, J. S. *Parasitol. Res.* **1987**, *73*, 425.
- (320) Crewther, P. E.; Culvenor, J. G.; Silva, A.; Cooper, J. A.; Anders, R. F. *Exp. Parasitol.* **1990**, *70*, 193.

- (321) Ridley, R. G.; Takacs, B.; Lahm, H. W.; Delves, C. J.; Goman, M.; Certa, U.; Matile, H.; Woollett, G. R.; Scaife, J. G. *Mol. Biochem. Parasitol.* **1990**, *41*, 125.
- (322) Schofield, L.; Bushell, G. R.; Cooper, J. A.; Saul, A. J.; Uproft, J. A.; Kidson, C. *Mol. Biochem. Parasitol.* **1986**, *18*, 183.
- (323) Howard, R. F. *Mol. Biochem. Parasitol.* **1992**, *51*, 327.
- (324) Howard, R. F.; Jensen, J. B.; Franklin, H. L. *Infect. Immunol.* **1993**, *61*, 2960.
- (325) Howard, R. F.; Narum, D. L.; Blackman, M.; Thurman, J. *Mol. Biochem. Parasitol.* **1998**, *92*, 111.
- (326) Howard, R. F.; Peterson, C. *Mol. Biochem. Parasitol.* **1996**, *77*, 95.
- (327) Howard, R. F.; Reese, R. T. *Exp. Parasitol.* **1990**, *71*, 330.
- (328) Howard, R. F.; Schmidt, C. M. *Mol. Biochem. Parasitol.* **1995**, *74*, 43.
- (329) Campbell, G. H.; Miller, L. H.; Hudson, D.; Franco, E. L.; Andrysiak, P. M. *Am. J. Trop. Med. Hyg.* **1984**, *33*, 1051.
- (330) Ridley, R. G.; Lahm, H. W.; Takacs, B.; Scaife, J. G. *Mol. Biochem. Parasitol.* **1991**, *47*, 245.
- (331) Harnyuttanakorn, P.; McBride, J. S.; Donachie, S.; Heidrich, H. G.; Ridley, R. G. *Mol. Biochem. Parasitol.* **1992**, *55*, 177.
- (332) Perrin, L. H.; Ramirez, E.; Lambert, P. H.; Miescher, P. A. *Nature* **1981**, *289*, 301.
- (333) Bushell, G. R.; Ingram, L. T.; Fardoulis, C. A.; Cooper, J. A. *Mol. Biochem. Parasitol.* **1988**, *28*, 105.
- (334) Lopez, R.; Valbuena, J.; Curtidor, H.; Puentes, A.; Rodriguez, L. E.; Garcia, J.; Suarez, J.; Vera, R.; Ocampo, M.; Trujillo, M.; Ramirez, L. E.; Patarroyo, M. E. *Biochimie* **2004**, *86*, 1.
- (335) Baldi, D. L.; Good, R.; Duraisingh, M. T.; Crabb, B. S.; Cowman, A. F. *Infect. Immunol.* **2002**, *70*, 5236.
- (336) Bahl, A.; Brunk, B.; Crabtree, J.; Fraunholz, M. J.; Gajria, B.; Grant, G. R.; Ginsburg, H.; Gupta, D.; Kissinger, J. C.; Labo, P.; Li, L.; Mailman, M. D.; Milgram, A. J.; Pearson, D. S.; Roos, D. S.; Schug, J.; Stoekert, C. J., Jr.; Whetzel, P. *Nucleic Acids Res.* **2003**, *31*, 212.
- (337) Bodescot, M.; Silvie, O.; Siau, A.; Refour, P.; Pino, P.; Franetich, J. F.; Hannoun, L.; Sauerwein, R.; Mazier, D. *Parasitol. Res* **2004**, *92*, 449.
- (338) Topolska, A. E.; Lidgett, A.; Truman, D.; Fujioka, H.; Coppel, R. L. *J. Biol. Chem.* **2004**, *279*, 4648.
- (339) Nixon, C. P.; Friedman, J. F.; Knopf, P. M.; Duffy, P. E.; Kurtis, J. D. *Transfusion* **2005**, *45*, 81S.
- (340) Pinzon, C. G.; Curtidor, H.; Bermudez, A.; Forero, M.; Vanegas, M.; Rodriguez, J.; Patarroyo, M. E. *Vaccine* **2008**, *26*, 853.
- (341) Topolska, A. E.; Richie, T. L.; Nhan, D. H.; Coppel, R. L. *Infect. Immunol.* **2004**, *72*, 3325.
- (342) Kar, P.; Dash, A. P.; Supakar, P. C. *Mol. Biochem. Parasitol.* **2007**, *155*, 156.
- (343) Sam-Yellowe, T. Y.; Perkins, M. E. *Exp. Parasitol.* **1991**, *73*, 161.
- (344) Yang, J. C.; Blanton, R. E.; King, C. L.; Fujioka, H.; Aikawa, M.; Sam-Yellowe, T. Y. *Infect. Immunol.* **1996**, *64*, 3584.
- (345) Brown, H. J.; Coppel, R. L. *Mol. Biochem. Parasitol.* **1991**, *49*, 99.
- (346) Sam-Yellowe, T. Y.; Perkins, M. E. *Mol. Biochem. Parasitol.* **1990**, *39*, 91.
- (347) Sam-Yellowe, T. Y.; Shio, H.; Perkins, M. E. *J. Cell Biol.* **1988**, *106*, 1507.
- (348) Mongui, A.; Perez-Leal, O.; Rojas-Caraballo, J.; Angel, D. I.; Cortes, J.; Patarroyo, M. A. *Biochem. Biophys. Res. Commun.* **2007**, *358*, 861.
- (349) Craig, A. *Parasitol. Today* **2000**, *16*, 366.
- (350) Manski-Nankervis, J. A.; Gardiner, D. L.; Hawthorne, P.; Holt, D. C.; Edwards, M.; Kemp, D. J.; Trenholme, K. R. *Mol. Biochem. Parasitol.* **2000**, *111*, 437.
- (351) Trenholme, K. R.; Gardiner, D. L.; Holt, D. C.; Thomas, E. A.; Cowman, A. F.; Kemp, D. J. *Proc. Natl. Acad. Sci. U.S.A.* **2000**, *97*, 4029.
- (352) Bowman, S.; Lawson, D.; Basham, D.; Brown, D.; Chillingworth, T.; Churcher, C. M.; Craig, A.; Davies, R. M.; Devlin, K.; Feltwell, T.; Gentles, S.; Gwilliam, R.; Hamlin, N.; Harris, D.; Holroyd, S.; Hornsby, T.; Horrocks, P.; Jagels, K.; Jassal, B.; Kyes, S.; McLean, J.; Moule, S.; Mungall, K.; Murphy, L.; Oliver, K.; Quail, M. A.; Rajandream, M. A.; Rutter, S.; Skelton, J.; Squares, R.; Squares, S.; Sulston, J. E.; Whitehead, S.; Woodward, J. R.; Newbold, C.; Barrell, B. G. *Nature* **1999**, *400*, 532.
- (353) Gardner, M. J.; Tettelin, H.; Carucci, D. J.; Cummings, L. M.; Aravind, L.; Koonin, E. V.; Shallom, S.; Mason, T.; Yu, K.; Fujii, C.; Pederson, J.; Shen, K.; Jing, J.; Aston, C.; Lai, Z.; Schwartz, D. C.; Perte, M.; Salzberg, S.; Zhou, L.; Sutton, G. G.; Clayton, R.; White, O.; Smith, H. O.; Fraser, C. M.; Adams, M. D.; Venter, J. C.; Hoffman, S. L. *Science* **1998**, *282*, 1126.
- (354) Gardiner, D. L.; Holt, D. C.; Thomas, E. A.; Kemp, D. J.; Trenholme, K. R. *Mol. Biochem. Parasitol.* **2000**, *110*, 33.
- (355) Ocampo, M.; Rodriguez, L. E.; Curtidor, H.; Puentes, A.; Vera, R.; Valbuena, J. J.; Lopez, R.; Garcia, J. E.; Ramirez, L. E.; Torres, E.; Cortes, J.; Tovar, D.; Lopez, Y.; Patarroyo, M. A.; Patarroyo, M. E. *Protein Sci.* **2005**, *14*, 504.
- (356) Kyes, S.; Horrocks, P.; Newbold, C. *Annu. Rev. Microbiol.* **2001**, *55*, 673.
- (357) Cooke, B. M.; Mohandas, N.; Coppel, R. L. *Adv. Parasitol.* **2001**, *50*, 1.
- (358) Reeder, J. C.; Hodder, A. N.; Beeson, J. G.; Brown, G. V. *Infect. Immunol.* **2000**, *68*, 3923.
- (359) Vogt, A. M.; Barragan, A.; Chen, Q.; Kironde, F.; Spillmann, D.; Wahlgren, M. *Blood* **2003**, *101*, 2405.
- (360) Gamain, B.; Smith, J. D.; Avril, M.; Baruch, D. I.; Scherf, A.; Gysin, J.; Miller, L. H. *Mol. Microbiol.* **2004**, *53*, 445.
- (361) Cooke, B. M.; Mohandas, N.; Coppel, R. L. *Semin. Hematol.* **2004**, *41*, 173.
- (362) Cooke, B. M.; Lingelbach, K.; Bannister, L. H.; Tilley, L. *Trends Parasitol.* **2004**, *20*, 581.
- (363) Carlson, J.; Holmquist, G.; Taylor, D. W.; Perlmann, P.; Wahlgren, M. *Proc. Natl. Acad. Sci. U.S.A.* **1990**, *87*, 2511.
- (364) Craig, A.; Scherf, A. *Mol. Biochem. Parasitol.* **2001**, *115*, 129.
- (365) Cowman, A. F.; Coppel, R. L.; Saint, R. B.; Favaloro, J.; Crewther, P. E.; Stahl, H. D.; Bianco, A. E.; Brown, G. V.; Anders, R. F.; Kemp, D. J. *Mol. Biol. Med.* **1984**, *2*, 207.
- (366) Favaloro, J. M.; Coppel, R. L.; Corcoran, L. M.; Foote, S. J.; Brown, G. V.; Anders, R. F.; Kemp, D. J. *Nucleic Acids Res.* **1986**, *14*, 8265.
- (367) Pei, X.; Guo, X.; Coppel, R.; Bhattacharjee, S.; Haldar, K.; Gratzner, W.; Mohandas, N.; An, X. *Blood* **2007**, *110*, 1036.
- (368) Silva, M. D.; Cooke, B. M.; Guillotte, M.; Buckingham, D. W.; Sauzet, J. P.; Le Scanf, C.; Contamin, H.; David, P.; Mercereau-Puijalon, O.; Bonnefoy, S. *Mol. Microbiol.* **2005**, *56*, 990.
- (369) Kumar, P.; Biswas, S.; Rao, D. N. *Microbiol. Immunol.* **1999**, *43*, 567.
- (370) Perlmann, H.; Perlmann, P.; Berzins, K.; Wahlin, B.; Troye-Blomberg, M.; Hagstedt, M.; Andersson, I.; Hogh, B.; Petersen, E.; Bjorkman, A. *Immunol. Rev.* **1989**, *112*, 115.
- (371) Troye-Blomberg, M.; Sjoberg, K.; Olerup, O.; Riley, E. M.; Kabilan, L.; Perlmann, H.; Marbiah, N. T.; Perlmann, P. *Immunol. Lett.* **1990**, *25*, 129.
- (372) Da Silva, E.; Foley, M.; Dluzewski, A. R.; Murray, L. J.; Anders, R. F.; Tilley, L. *Mol. Biochem. Parasitol.* **1994**, *66*, 59.
- (373) Vera Bravo, R.; Marin, V.; Garcia, J.; Urquiza, M.; Torres, E.; Trujillo, M.; Rosas, J.; Patarroyo, M. E. *Vaccine* **2000**, *18*, 1289.
- (374) Siddique, A. B.; Iqbal, J.; Ahlberg, N.; Wahlin Flyg, B.; Perlmann, P.; Berzins, K. *Parasitol. Res.* **1998**, *84*, 485.
- (375) Collins, W. E.; Anders, R. F.; Papaioanou, M.; Campbell, G. H.; Brown, G. V.; Kemp, D. J.; Coppel, R. L.; Skinner, J. C.; Andrysiak, P. M.; Favaloro, J. M.; et al. *Nature* **1986**, *323*, 259.
- (376) Astagneau, P.; Steketee, R. W.; Wirima, J. J.; Khoromana, C. O.; Millet, P. *Acta Trop.* **1994**, *57*, 317.
- (377) Chizzolini, C.; Dupont, A.; Akue, J. P.; Kaufmann, M. H.; Verdini, A. S.; Pessi, A.; Del Giudice, G. *Am. J. Trop. Med. Hyg.* **1988**, *39*, 150.
- (378) Deloron, P.; Campbell, G. H.; Brandling-Bennett, D.; Roberts, J. M.; Schwartz, I. K.; Odera, J. S.; Lal, A. A.; Osanga, C. O.; de la Cruz, V.; McCutchan, T. M. *Am. J. Trop. Med. Hyg.* **1989**, *41*, 395.
- (379) Petersen, E.; Hogh, B.; Marbiah, N. T.; Perlmann, H.; Willcox, M.; Dolopaie, E.; Hanson, A. P.; Bjorkman, A.; Perlmann, P. *Trans. R. Soc. Trop. Med. Hyg.* **1990**, *84*, 339.
- (380) Riley, E. M.; Allen, S. J.; Troye-Blomberg, M.; Bennett, S.; Perlmann, H.; Andersson, G.; Smedman, L.; Perlmann, P.; Greenwood, B. M. *Trans. R. Soc. Trop. Med. Hyg.* **1991**, *85*, 436.
- (381) Kulane, A.; Siddique, A. B.; Perlmann, H.; Ahlberg, N.; Roussilhon, C.; Tall, A.; Dieye, A.; Perlmann, P.; Troye-Blomberg, M. *Acta Trop.* **1997**, *68*, 37.
- (382) Rzepczyk, C. M.; Ramasamy, R.; Ho, P. C.; Mutch, D. A.; Anderson, K. L.; Duggleby, R. G.; Doran, T. J.; Murray, B. J.; Irving, D. O.; Woodrow, G. C.; et al. *J. Immunol.* **1988**, *141*, 3197.
- (383) Cappai, R.; Kaslow, D. C.; Peterson, M. G.; Cowman, A. F.; Anders, R. F.; Kemp, D. J. *Mol. Biochem. Parasitol.* **1992**, *54*, 213.
- (384) Vazeux, G.; Le Scanf, C.; Fandeur, T. *Infect. Immunol.* **1993**, *61*, 4469.
- (385) Gardner, M. J.; Hall, N.; Fung, E.; White, O.; Berriman, M.; Hyman, R. W.; Carlton, J. M.; Pain, A.; Nelson, K. E.; Bowman, S.; Paulsen, I. T.; James, K.; Eisen, J. A.; Rutherford, K.; Salzberg, S. L.; Craig, A.; Kyes, S.; Chan, M. S.; Nene, V.; Shallom, S. J.; Suh, B.; Peterson, J.; Angiuoli, S.; Perte, M.; Allen, J.; Selengut, J.; Haft, D.; Mather, M. W.; Vaidya, A. B.; Martin, D. M.; Fairlamb, A. H.; Fraunholz, M. J.; Roos, D. S.; Ralph, S. A.; McFadden, G. I.; Cummings, L. M.; Subramanian, G. M.; Mungall, C.; Venter, J. C.; Carucci, D. J.; Hoffman, S. L.; Newbold, C.; Davis, R. W.; Fraser, C. M.; Barrell, B. *Nature* **2002**, *419*, 498.
- (386) Rodriguez, L. E.; Vera, R.; Valbuena, J.; Curtidor, H.; Garcia, J.; Puentes, A.; Ocampo, M.; Lopez, R.; Rosas, J.; Lopez, Y.; Patarroyo, M. A.; Patarroyo, M. E. *Biol. Chem.* **2007**, *388*, 15.

- (387) Triglia, T.; Stahl, H. D.; Crewther, P. E.; Scanlon, D.; Brown, G. V.; Anders, R. F.; Kemp, D. J. *EMBO J.* **1987**, *6*, 1413.
- (388) Vernot-Hernandez, J. P.; Heidrich, H. G. *Mol. Biochem. Parasitol.* **1984**, *12*, 337.
- (389) Crabb, B. S.; Cooke, B. M.; Reeder, J. C.; Waller, R. F.; Caruana, S. R.; Davern, K. M.; Wickham, M. E.; Brown, G. V.; Coppel, R. L.; Cowman, A. F. *Cell* **1997**, *89*, 287.
- (390) Kilejian, A.; Rashid, M. A.; Aikawa, M.; Aji, T.; Yang, Y. F. *Mol. Biochem. Parasitol.* **1991**, *44*, 175.
- (391) Nagao, E.; Kaneko, O.; Dvorak, J. A. *J. Struct. Biol.* **2000**, *130*, 34.
- (392) Rug, M.; Prescott, S. W.; Fernandez, K. M.; Cooke, B. M.; Cowman, A. F. *Blood* **2006**, *108*, 370.
- (393) Magowan, C.; Nunomura, W.; Waller, K. L.; Yeung, J.; Liang, J.; Van Dort, H.; Low, P. S.; Coppel, R. L.; Mohandas, N. *Biochim. Biophys. Acta* **2000**, *1502*, 461.
- (394) Oh, S. S.; Voigt, S.; Fisher, D.; Yi, S. J.; LeRoy, P. J.; Derick, L. H.; Liu, S.; Chishti, A. H. *Mol. Biochem. Parasitol.* **2000**, *108*, 237.
- (395) Pei, X.; An, X.; Guo, X.; Tarnawski, M.; Coppel, R.; Mohandas, N. *J. Biol. Chem.* **2005**, *280*, 31166.
- (396) Ellis, J.; Irving, D. O.; Wellems, T. E.; Howard, R. J.; Cross, G. A. *Mol. Biochem. Parasitol.* **1987**, *26*, 203.
- (397) Waller, K. L.; Cooke, B. M.; Nunomura, W.; Mohandas, N.; Coppel, R. L. *J. Biol. Chem.* **1999**, *274*, 23808.
- (398) Panton, L. J.; McPhie, P.; Maloy, W. L.; Wellems, T. E.; Taylor, D. W.; Howard, R. J. *Mol. Biochem. Parasitol.* **1989**, *35*, 149.
- (399) Rock, E. P.; Marsh, K.; Saul, A. J.; Wellems, T. E.; Taylor, D. W.; Maloy, W. L.; Howard, R. J. *Parasitology* **1987**, *95* (Pt 2), 209.
- (400) Howard, R. J.; Uni, S.; Aikawa, M.; Aley, S. B.; Leech, J. H.; Lew, A. M.; Wellems, T. E.; Rener, J.; Taylor, D. W. *J. Cell Biol.* **1986**, *103*, 1269.
- (401) Lynn, A.; Chandra, S.; Malhotra, P.; Chauhan, V. S. *FEBS Lett.* **1999**, *459*, 267.
- (402) Sullivan, D. J., Jr.; Gluzman, I. Y.; Goldberg, D. E. *Science* **1996**, *271*, 219.
- (403) Leke, R. F.; Djokam, R. R.; Mbu, R.; Leke, R. J.; Fogako, J.; Megnekou, R.; Metenou, S.; Sama, G.; Zhou, Y.; Cadigan, T.; Parra, M.; Taylor, D. W. *J. Clin. Microbiol.* **1999**, *37*, 2992.
- (404) Moody, A. *Clin. Microbiol. Rev.* **2002**, *15*, 66.
- (405) Stahl, H. D.; Kemp, D. J.; Crewther, P. E.; Scanlon, D. B.; Woodrow, G.; Brown, G. V.; Bianco, A. E.; Anders, R. F.; Coppel, R. L. *Nucleic Acids Res.* **1985**, *13*, 7837.
- (406) Wellems, T. E.; Howard, R. J. *Proc. Natl. Acad. Sci. U.S.A.* **1986**, *83*, 6065.
- (407) Wellems, T. E.; Walliker, D.; Smith, C. L.; do Rosario, V. E.; Maloy, W. L.; Howard, R. J.; Carter, R.; McCutchan, T. F. *Cell* **1987**, *49*, 633.
- (408) Spycher, C.; Klonis, N.; Spielmann, T.; Kump, E.; Steiger, S.; Tilley, L.; Beck, H. P. *J. Biol. Chem.* **2003**, *278*, 35373.
- (409) Bermudez, A.; Alba, P.; Espejo, F.; Vargas, L. E.; Parra, C.; Rodriguez, R.; Reyes, C.; Patarroyo, M. E. *Int. J. Biochem. Cell Biol.* **2005**, *37*, 336.
- (410) Hiller, N. L.; Bhattacharjee, S.; van Ooij, C.; Liolios, K.; Harrison, T.; Lopez-Estrano, C.; Haldar, K. *Science* **2004**, *306*, 1934.
- (411) Rowe, A.; Obeiro, J.; Newbold, C. I.; Marsh, K. *Infect. Immunol.* **1995**, *63*, 2323.
- (412) Baruch, D. I.; Pasloske, B. L.; Singh, H. B.; Bi, X.; Ma, X. C.; Feldman, M.; Taraschi, T. F.; Howard, R. J. *Cell* **1995**, *82*, 77.
- (413) Su, X. Z.; Heatwole, V. M.; Wertheimer, S. P.; Guinet, F.; Herrfeldt, J. A.; Peterson, D. S.; Ravetch, J. A.; Wellems, T. E. *Cell* **1995**, *82*, 89.
- (414) Smith, J. D.; Subramanian, G.; Gamain, B.; Baruch, D. I.; Miller, L. H. *Mol. Biochem. Parasitol.* **2000**, *110*, 293.
- (415) Chen, Q.; Barragan, A.; Fernandez, V.; Sundstrom, A.; Schlichtherle, M.; Sahlen, A.; Carlson, J.; Datta, S.; Wahlgren, M. *J. Exp. Med.* **1998**, *187*, 15.
- (416) Chen, Q.; Hedding, A.; Barragan, A.; Fernandez, V.; Pearce, S. F.; Wahlgren, M. *J. Exp. Med.* **2000**, *192*, 1.
- (417) Barragan, A.; Kremsner, P. G.; Wahlgren, M.; Carlson, J. *Infect. Immunol.* **2000**, *68*, 2971.
- (418) Carlson, J.; Wahlgren, M. *J. Exp. Med.* **1992**, *176*, 1311.
- (419) Springer, A. L.; Smith, L. M.; Mackay, D. Q.; Nelson, S. O.; Smith, J. D. *Mol. Biochem. Parasitol.* **2004**, *137*, 55.
- (420) Baruch, D. I.; Ma, X. C.; Singh, H. B.; Bi, X.; Pasloske, B. L.; Howard, R. J. *Blood* **1997**, *90*, 3766.
- (421) Smith, J. D.; Craig, A. G.; Kriek, N.; Hudson-Taylor, D.; Kyes, S.; Fagan, T.; Pinches, R.; Baruch, D. I.; Newbold, C. I.; Miller, L. H. *Proc. Natl. Acad. Sci. U.S.A.* **2000**, *97*, 1766.
- (422) Voigt, S.; Hanspal, M.; LeRoy, P. J.; Zhao, P. S.; Oh, S. S.; Chishti, A. H.; Liu, S. C. *Mol. Biochem. Parasitol.* **2000**, *110*, 423.
- (423) Waller, K. L.; Nunomura, W.; Cooke, B. M.; Mohandas, N.; Coppel, R. L. *Mol. Biochem. Parasitol.* **2002**, *119*, 125.
- (424) Curtidor, H.; Torres, M. H.; Alba, M. P.; Patarroyo, M. E. *Biol. Chem.* **2007**, *388*, 25.
- (425) Staalso, T.; Khalil, E. A.; Elhassan, I. M.; Zijlstra, E. E.; Elhassan, A. M.; Giha, H. A.; Theander, T. G.; Jakobsen, P. H. *Immunol. Lett.* **1998**, *60*, 121.
- (426) Chitarra, V.; Holm, I.; Bentley, G. A.; Petres, S.; Longacre, S. *Mol. Cell* **1999**, *3*, 457.
- (427) Feng, Z. P.; Zhang, X.; Han, P.; Arora, N.; Anders, R. F.; Norton, R. S. *Mol. Biochem. Parasitol.* **2006**, *150*, 256.
- (428) Dyson, H. J.; Wright, P. E. *Nat. Rev. Mol. Cell Biol.* **2005**, *6*, 197.
- (429) Alba, M. P.; Salazar, L. M.; Puentes, A.; Pinto, M.; Torres, E.; Patarroyo, M. E. *Peptides* **2003**, *24*, 999.
- (430) Cubillos, M.; Alba, M. P.; Bermudez, A.; Trujillo, M.; Patarroyo, M. E. *Biochimie* **2003**, *85*, 651.
- (431) Dowse, T. J.; Soldati, D. *Trends Parasitol.* **2005**, *21*, 254.
- (432) Kabsch, W.; Sander, C. *Biopolymers* **1983**, *22*, 2577.
- (433) Tossavainen, H.; Pihlajamaa, T.; Huttunen, T. K.; Raulo, E.; Rauvala, H.; Permi, P.; Kilpelainen, I. *Protein Sci.* **2006**, *15*, 1760.
- (434) Lopez, R.; Curtidor, H.; Urquiza, M.; Garcia, J.; Puentes, A.; Suarez, J.; Ocampo, M.; Vera, R.; Rodriguez, L. E.; Castillo, F.; Cifuentes, G.; Patarroyo, M. E. *J. Pept. Res.* **2001**, *58*, 285.
- (435) Patarroyo, M. E.; Cifuentes, G.; Rodriguez, R. *Int. J. Biochem. Cell Biol.* **2007**,
- (436) Bozdech, Z.; Llinas, M.; Pulliam, B. L.; Wong, E. D.; Zhu, J.; DeRisi, J. L. *PLoS Biol.* **2003**, *1*, E5.
- (437) Pandey, A.; Mann, M. *Nature* **2000**, *405*, 837.
- (438) Gilson, P. R.; Nebl, T.; Vukcevic, D.; Moritz, R. L.; Sargeant, T.; Speed, T. P.; Schofield, L.; Crabb, B. S. *Mol. Cell Proteomics* **2006**, *5*, 1286.
- (439) Fruh, K.; Doumbo, O.; Muller, H. M.; Koita, O.; McBride, J.; Crisanti, A.; Toure, Y.; Bujard, H. *Infect. Immunol.* **1991**, *59*, 1319.
- (440) Hodder, A. N.; Crewther, P. E.; Anders, R. F. *Infect. Immunol.* **2001**, *69*, 3286.
- (441) Lee, E. A.; Flanagan, K. L.; Minigo, G.; Reece, W. H.; Bailey, R.; Pinder, M.; Hill, A. V.; Plebanski, M. *Eur. J. Immunol.* **2006**, *36*, 1168.
- (442) Good, M. F.; Kumar, S.; Miller, L. H. *Immunol. Today* **1988**, *9*, 351.
- (443) Good, M. F.; Zeving, Y.; Currier, J.; Bilsborough, J. *Parasite Immunol.* **1993**, *15*, 187.

CR068407V